JOURNAL OF GEOPHYSICAL RESEARCH, VOL. 86, NO. C8, PAGES 7210-7254, AUGUST 20, 1981

Tropospheric Chemistry: A Global Perspective

JENNIFER A. LOGAN, MICHAEL J. PRATHER, STEVEN C. WOFSY, AND MICHAEL B. MCELROY

Center for Earth Planetary Physics, Harvard University, Cambridge, Massachusetts 02138

A model for the photochemistry of the global troposphere constrained by observed concentrations of H_2O, O_3, CO, CH_4, NO, NO_2, and HNO_3 is presented. Data for NO and NO_2 are insufficient to define the global distribution of these gases but are nonetheless useful in limiting several of the more uncertain parameters of the model. Concentrations of OH, HO_2, H_2O_2, NO, NO_2, NO_3, N_2O_5, HNO_2, HO_2NO_2, CH_3O_2, CH_3OOH, CH_2O, and CH_3CCl_3 are calculated as functions of altitude, latitude, and season. Results imply that the source for nitrogen oxides in the remote troposphere is geographically dispersed and surprisingly small, less than 10^7 tons N yr^{-1}. Global sources for CO and CH_4 are 1.5×10^9 tons C yr^{-1} and 4.5×10^8 tons C yr^{-1}, respectively. Carbon monoxide is derived from combustion of fossil fuel (15%) and oxidation of atmospheric CH_4 (25%), with the balance from burning of vegetation and oxidation of biospheric hydrocarbons. Production of CO in the northern hemisphere exceeds that in the southern hemisphere by about a factor of 2. Industrial and agricultural activities provide approximately half the global source of CO. Oxidation of CO and CH_4 provides sources of tropospheric O_3 similar in magnitude to loss by in situ photochemistry. Observations of CH_3CCl_3 could offer an important check of the tropospheric model and results shown here suggest that computed concentrations of OH should be reliable within a factor of 2. A more definitive test requires better definition of release rates for CH_3CCl_3 and improved measurements for its distribution in the atmosphere.

1. INTRODUCTION

The hydroxyl radical plays an important role in the photochemistry of the troposphere. Reaction with OH provides the dominant path for removal of a variety of atmospheric species including CO, CH_4, C_2H_6, H_2, CH_3Cl, CH_3CCl_3, CH_3Br, H_2S, and SO_2.

The chemistry of tropospheric OH is complex. Hydroxyl is produced by reaction of $O(^1D)$ with H_2O [*Levy*, 1971, 1972], with $O(^1D)$ produced by photolysis of O_3 near 300 nm. In addition to the direct source, OH may be regenerated by a suite of reactions involving HO_2 and H_2O_2. Rates for these reactions vary appreciably in both time and space reflecting fluctuations in concentrations of species such as NO, CO, O_3, and H_2O. A comprehensive test of photochemical models for OH would require simultaneous measurement of these and a number of other species and has yet to be performed. The concentration of OH has been measured in selected environments by a number of investigators by using a variety of techniques [*Wang et. al.*, 1975; *Davis et al.*, 1976; *Perner et al.*, 1976; *Philen et al.*, 1978; *Campbell et al.*, 1979]. The measurements are difficult, however, and concentrations reported so far are subject to considerable uncertainty [*Selzer and Wang*, 1979; *Ortgies et al.*, 1980; *Davis et al.*, 1981*a*, *b*; *Wang et al.*, 1981].

Analysis of data for atmospheric CH_3CCl_3 (1,1,1-trichloroethane, commonly called methylchloroform) may provide the best current check on photochemical models. Methylchloroform is used extensively, and in increasing quantities, as a solvent. It is released to the atmosphere at a known rate [*Neely and Plonka*, 1978], and chemical industry provides the only established source. The concentration of the gas in the atmosphere has increased by more than a factor of 3 since it was first measured by Lovelock in 1972 [*Lovelock*, 1974]. Methylchloroform is removed from the atmosphere primarily by reaction with tropospheric OH. To the extent that the source is determined, measurements of atmospheric CH_3CCl_3 may be used to check calculations for the global distribution of OH. Preliminary studies [*Singh*, 1977; *Lovelock*, 1977] suggested that the concentration of OH was overestimated in early models [e.g., *Levy*, 1972; *Wofsy et al.*, 1972; *Crutzen*, 1974] by a factor between 2 and 5. We shall argue here that the discrepancies suggested by such comparisons may be attributed to a combination of factors: lack of a global model for the troposphere, inadequate information on the distribution of gases such as NO and NO_2, uncertainties in rates for key reactions, uncertainty in release rates for CH_3CCl_3, and inadequacy of the data for atmospheric CH_3CCl_3. A more comprehensive analysis is given below.

An acceptable model for OH must be consistent with knowledge of budgets for other gases, in particular CO. Reaction with OH is the primary removal mechanism for atmospheric CO. Thus, information on the distributions of OH and CO may be used to calculate the magnitude of the source required to maintain present concentrations of CO. Carbon monoxide is released to the atmosphere as a byproduct of combustion. It is formed also as an intermediate in the oxidation of CH_4 [*McConnell et al.*, 1971] and other hydrocarbons [*Wofsy et al.*, 1972; *Levy*, 1974], notably isoprene [*Zimmerman et al.*, 1978; *Logan et al.*, 1978]. As we shall see, rates for production of CO by automobiles and industry may be specified to within about a factor of 2. It is more difficult to quantify rates for production of CO associated with various agricultural practices. Fire is used extensively for land clearance in tropical agriculture and for maintenance of grassland in many regions of the world [*Spencer*, 1966; *Webster and Wilson*, 1967; *Watters*, 1971]. Rates for production of CO associated with oxidation of CH_4 and other hydrocarbons are uncertain, due in part to gaps in our understanding of atmospheric chemistry, in part to deficiency in our knowledge of strengths and distributions of relevant sources. It is important to obtain quantitative data on such sources, and studies of OH can play an important role.

Development of a comprehensive model for tropospheric OH is hampered particularly by lack of data for NO and NO_2. In the absence of such information we must rely on data for HNO_3 and predictions of the model for apportionment of species of odd nitrogen (NO, NO_2, NO_3, N_2O_5, HNO_2, HNO_3, $ClNO_3$, and HO_2NO_2). The analysis is constrained to reproduce the few measurements available for NO and NO_2 in

Paper number 1C0623.
0148-0227/81/001C-0623$01.00

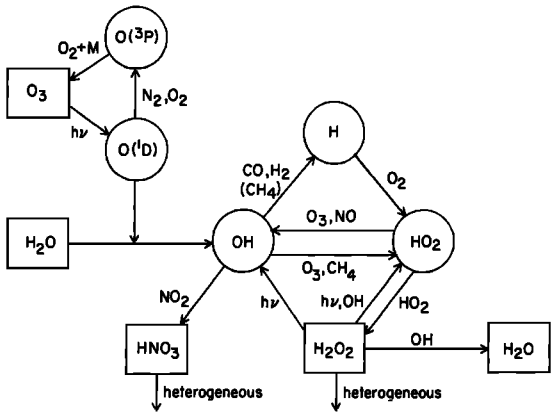

Fig. 1. Major chemical reactions affecting odd hydrogen (OH, H, HO_2, H_2O_2) in the troposphere.

clean air (~0.01–0.10 ppb), and leads to an estimate of 10 days for the average lifetime of HNO_3.

Tropospheric O_3 may be produced by in situ chemistry [*Chameides and Walker,* 1973; *Crutzen,* 1973; *Fishman et al.,* 1979] or by transfer from the stratosphere. The stratosphere provides a source of about 5×10^{10} molecules cm^{-2} s^{-1} averaged over the globe [*Danielson and Mohnen,* 1977; *Fabian and Pruchniewicz,* 1977; *Mahlman et al.,* 1980; *Gidel and Shapiro,* 1980]. In situ production arises from oxidation of CO and CH_4 and depends on the concentration of NO. Ozone is also consumed in the troposphere. Its loss by gas phase chemistry is independent of NO [*Fishman et al.,* 1979]. Our model finds that in situ sources and sinks for O_3 averaged over the globe are in approximate balance.

We begin with a discussion of tropospheric chemistry emphasizing areas of particular uncertainty. We follow with a review of observational data of special relevance to OH, notably the distributions of CO, CH_4, O_3, H_2O, HNO_3, NO, and NO_2. The atmospheric model is developed in section 4, with special attention to OH, O_3, and odd nitrogen. Implications for global budgets of CH_3CCl_3, CO, and CH_4 are discussed in section 5. Conclusions are given in section 6.

2. Chemistry

We shall be concerned here mainly with processes that affect the concentration of tropospheric OH. The chemistry of OH is linked directly to the chemistry of H, HO_2, and H_2O_2, as illustrated in Figure 1.

It is convenient to consider OH, H, HO_2, and H_2O_2 as a family, odd hydrogen. Major input to this family occurs through

$$h\nu + O_3 \rightarrow O(^1D) + O_2 \quad (1)$$

followed by

$$O(^1D) + H_2O \rightarrow OH + OH \quad (2)$$

The radical OH may react either with CO,

$$OH + CO \rightarrow H + CO_2 \quad (3)$$

or with CH_4,

$$OH + CH_4 \rightarrow H_2O + CH_3 \quad (4)$$

with (3) dominant, particularly in the northern hemisphere. Reaction (3) offers no net sink for odd hydrogen. The product H reacts with O_2 to form HO_2,

$$H + O_2 + M \rightarrow HO_2 + M \quad (5)$$

and HO_2 is removed either by

$$HO_2 + O_3 \rightarrow OH + 2O_2 \quad (6)$$

$$HO_2 + NO \rightarrow OH + NO_2 \quad (7)$$

or by

$$HO_2 + HO_2 \rightarrow H_2O_2 + O_2 \quad (8)$$

Hydrogen peroxide can be photolyzed,

$$h\nu + H_2O_2 \rightarrow OH + OH \quad (9)$$

It can react with OH,

$$OH + H_2O_2 \rightarrow H_2O + HO_2 \quad (10)$$

or it may be removed heterogeneously,

$$H_2O_2 \xrightarrow{\text{rain, aerosol}} \text{products} \quad (11)$$

Odd hydrogen is conserved in reactions (3) and in (5)–(9). Two molecules of odd hydrogen are lost in each of reactions (10) and (11). Reactions (10) and (11), together with

$$OH + NO_2 + M \rightarrow HNO_3 + M \quad (12)$$

and

$$HNO_3 \xrightarrow{\text{rain, aerosol}} \text{products} \quad (13)$$

constitute the dominant sinks for tropospheric odd H.

Table 1 summarizes kinetic data for reactions important in the chemistry of the troposphere. Absorption cross sections for ozone are well determined [*Griggs,* 1968] but quantum yields for production of $O(^1D)$ are uncertain. There is good agreement among several groups on the quantum yield between 300 and 325 nm, measured relative to the value at 300 nm [*Lin and DeMore,* 1973; *Moortgat and Kudszus,* 1978; *Brock and Watson,* 1980]. Absolute values for the quantum yield are available only for wavelengths shorter than 280 nm. Analyses of reaction products indicate a quantum yield of unity from 230 to 280 nm [*Amimoto et al.,* 1978; *Kajimoto and Cvetanovic,* 1979] while molecular beam studies [*Sparks et al.,* 1980; *Fairchild et al.,* 1978] give evidence for production of $O(^3P)$. The molecular beam data imply a quantum yield of about 0.9 for $O(^1D)$ at 266 and 274 nm. We adopted in the present model an absolute quantum yield of unity at 300 nm consistent with data presented in *Brock and Watson* [1980]. A quantum yield of 0.9 at 300 nm was recommended by the NASA panel for data evaluation [*NASA,* 1981]. The NASA result would provide a small (5–10%) reduction in calculated concentrations of HO_x.

Excited oxygen atoms react with H_2O (reaction (2)) or they may be quenched by O_2 and N_2,

$$O(^1D) + N_2 \rightarrow O(^3P) + N_2 \quad (14)$$

$$O(^1D) + O_2 \rightarrow O(^3P) + O_2 \quad (15)$$

The fraction of $O(^1D)$ atoms that react that H_2O is given by $k_2[H_2O]/(k_2[H_2O] + k_{14}[N_2] + k_{15}[O_2])$. Experimental determinations of k_2, k_{14}, and k_{15} by *Streit et al.* [1976] and *Amimoto et al.* [1979] give values for this ratio that agree within about 7%. Similar agreement is reported for k_2/k_{15} by *Streit et al.* [1976] and *Lee and Slanger* [1979] although results of Amimoto et al. are lower by 30%. It appears on the basis of these

comparisons that the results of *Heidner et al.* [1973] may be in error. We adopted values given by *Streit et al.* [1976] for k_2, k_{14}, and k_{15}.

The concentration of OH depends critically on rates for reactions (3) and (4). The rate constant for reaction with CO (reaction (3)) at 1 bar of air is about a factor of 2 larger than the value in the limit of low pressure [*Biermann et al.*, 1978]. The pressure effect was unexpected, and there may be other reactions of importance in tropospheric chemistry whose rate constants could have as yet unknown, although significant, variations with pressure and temperature. For example, the kinetics of reaction (8), the source for H_2O_2, are presently not well de-

TABLE 1. Kinetic Data

Number	Reaction	Rate expression[a]	References[a]
1	$O(^1D) + N_2 \rightarrow O(^3P) + N_2$	$2.0\text{–}11\ \exp(+107/T)$	
2	$O(^1D) + O_2 \rightarrow O(^3P) + O_2$	$2.9\text{–}11\ \exp(+67/T)$	
3	$O(^1D) + H_2O \rightarrow OH + OH$	2.3–10	
4	$O(^1D) + CH_4 \rightarrow OH + CH_3$	1.3–10	
5	$O(^1D) + CH_4 \rightarrow H_2 + H_2CO$	1.4–11	
6*a*	$O(^1D) + N_2O \rightarrow NO + NO$	6.2–11	
6*b*	$O(^1D) + N_2O \rightarrow N_2 + O_2$	4.8–11	
7	$O(^1D) + H_2 \rightarrow OH + H$	1.0–10	
8	$OH + CO \rightarrow CO_2 + H$	$1.35\text{–}13\ [1 + P\ (\text{atm})]$	
9	$OH + CH_4 \rightarrow CH_3 + H_2O$	$2.4\text{–}12\ \exp(-1710/T)$	
10	$OH + O_3 \rightarrow HO_2 + O_2$	$1.6\text{–}12\ \exp(-940/T)$	
11	$HO_2 + O_3 \rightarrow OH + 2O_2$	$1.1\text{–}14\ \exp(-580/T)$	
12	$HO_2 + NO \rightarrow OH + NO_2$	$4.3\text{–}12\ \exp(+200/T)$	
13	$HO_2 + NO_2 \rightarrow HNO_2 + O_2$	3.0–15	*Howard* [1977]
14	$HO_2 + HO_2 \rightarrow H_2O_2 + O_2$	$3.8\text{–}14\ \exp(1250/T) \times (1 + 2.5\text{–}18\ [H_2O])$	*Cox and Burrows* [1979], *Hamilton and Lii* [1977]
15	$OH + HO_2 \rightarrow H_2O + O$	4.0–11	
16	$O_3 + NO \rightarrow NO_2 + O_2$	$2.3\text{–}12\ \exp(-1450/T)$	
17	$O_3 + NO_2 \rightarrow O_2 + NO_3$	$1.2\text{–}13\ \exp(-2450/T)$	
18	$NO + NO_3 \rightarrow NO_2 + NO_2$	2.0–11	
19	$OH + H_2 \rightarrow H_2O + H$	$1.2\text{–}11\ \exp(-2200/T)$	
20	$OH + H_2O_2 \rightarrow H_2O + HO_2$	$2.9\text{–}12\ \exp(-164/T)$	*Keyser* [1980], *Sridharen et al.* [1980]
21	$OH + H_2CO \rightarrow H_2O + HCO$	1.0–11	
22	$OH + HNO_3 \rightarrow H_2O + NO_3$	8.5–14	
23	$OH + HNO_2 \rightarrow H_2O + NO_2$	6.6–12	*Cox et al.* [1976]
24	$OH + HO_2NO_2 \rightarrow H_2O + O_2 + NO_2$	5.0–13 (estimated)	
25	$OH + CH_3CCl_3 \rightarrow$ Products	$5.4\text{–}12\ \exp(-1820/T)$	*Jeong and Kaufman* [1980], *Kurylo et al.* [1980]
26	$CH_3OO + NO \rightarrow CH_3O + NO_2$	7.0–12	
27	$CH_3OO + HO_2 \rightarrow CH_3OOH + O_2$	6.0–12	
28	$CH_3OO + CH_3OO \rightarrow 2CH_3O + O_2$	4.6–13	*Baulch et al.* [1980]
29	$CH_3O + O_2 \rightarrow CH_2O + HO_2$	$5.0\text{–}13\ \exp(-2000/T)$	
30	$CH_3OOH + OH \rightarrow CH_3OO + H_2O$	$2.5\text{–}12\ \exp(-126/T)$ (estimated)	
31	$HO_2NO_2 + M \underset{k_r}{\overset{k_f}{\rightleftharpoons}} HO_2 + NO_2 + M$	$k_f = 1.7 + 28\ \exp(-11977/T) \cdot k_r$	*Uselman* [1978]
32	$N_2O_5 + M \underset{k_r}{\overset{k_f}{\rightleftharpoons}} NO_2 + NO_3 + M$	$k_f = 8.4 + 26\ \exp(-11178/T) \cdot k_r$	*Graham and Johnston* [1978]

Number	Reaction	k_0^{300}	n	k_∞^{300}	m
	Termolecular Processes[b]				
33	$O + O_2 + M \rightarrow O_3 + M$	6.2–34	2.0	—	—
34	$H + O_2 + M \rightarrow HO_2 + M$	5.5–32	1.4	—	—
35	$OH + NO + M \rightarrow HNO_2 + M$	6.7–31	3.3	3.0–11	1.0
36	$OH + NO_2 + M \rightarrow HNO_3 + M$	2.6–30	2.9	2.4–11	1.3
37	$HO_2 + NO_2 + M \rightarrow HO_2NO_2 + M$	2.1–31	3.0[c]	6.5–12	2.0
38	$NO_2 + NO_3 + M \rightarrow N_2O_5 + M$	1.4–30	2.8	9.0–13	−0.7
39[d]	$CH_3OO + NO_2 + M \rightarrow CH_3OONO_2 + M$				
	Photolytic Processes				
40	$O_3 + h\nu \rightarrow O_2 + O$				
41	$NO_2 + h\nu \rightarrow NO + O$				
42	$NO_3 + h\nu \rightarrow NO + O_2$ $\rightarrow NO_2 + O$				
43	$N_2O_5 + h\nu \rightarrow NO_2 + NO_3$				
44	$HNO_2 + h\nu \rightarrow OH + NO$				
45	$HNO_3 + h\nu \rightarrow OH + NO_2$				
46	$HO_2NO_2 + h\nu \rightarrow OH + NO_3$				
47	$H_2O_2 + h\nu \rightarrow OH + OH$				
48	$H_2CO + h\nu \rightarrow H + HCO$ $\rightarrow H_2 + CO$				
49	$CH_3OOH + h\nu \rightarrow CH_3O + OH$				

TABLE 1. (continued)

Number	Reaction	Rate Expression	Altitude
		Heterogeneous Processes	
50	Precipitation scavenging (H_2O_2, HNO_2, HNO_3, HO_2NO_2, H_2CO, CH_3OOH)	2.31–6 2.31–6 exp(1.6–0.4z) (units: s^{-1})	0–4 km 4–12 km
51	H_2O_2 + aerosol → loss[e]	sticking probability $\phi = 0.0$	

[a] Units: s^{-1} for unimolecular processes; $cm^3\ s^{-1}$ for bimolecular processes; $cm^6\ s^{-1}$ for termolecular processes. The notation 1.0–11 is intended to be read as 1.0×10^{-11} Rate constants and cross sections are taken from *NASA* [1979] unless otherwise indicated.

[b] $k = \{k_0[M]/(1 + k_0[M]/k_\infty)\}\ 0.6^{(1+[\log_{10}\{k_0[M]/k_\infty\}]^2)^{-1}}$; $k_0 = k_0^{300}(T/300)^{-n}$; $k_\infty = k_\infty^{300}(T/300)^{-m}$.

[c] Estimated.

[d] The rate for reaction (39) is somewhat slower than that for reaction (26), and methyl peroxynitrate is thought to be the product [*Niki et al.*, 1978*a*; *Cox and Tyndall*, 1980; *Sander and Watson*, 1980]. Analogous adducts (HO_2NO_2, PAN) undergo thermal decomposition in the lower troposphere, but may be thermally stable in the upper troposphere [*Graham et al.*, 1977; *Uselman et al.*, 1978; *Cox and Roffey*, 1977]. Kinetic data are currently unavailable for the reverse of (39), and CH_3OONO_2 was not included in the present model for CH_4 oxidation.

[e] $k(z) = \phi\bar{v}(z)A(z)$ (units: s^{-1})
ϕ = sticking probability; $\bar{v}(z) = (kT/2\pi m)^{1/2}$
$A(z)$ = surface area of aerosols ($4\pi r^2$)
= 4.0–7 exp (−z/1.2 km) + 4.0–8 (maritime)
= 2.0–6 exp (−z/1.2 km) + 4.0–8 (continental).

fined. The reaction is independent of pressure from 25 to 760 torr and appears to have a large negative activation energy. The rate appears to be directly proportional to pressure at low pressures, and the temperature dependence may be much weaker there than at high pressure [*Cox and Burrows*, 1979; *Thrush and Wilkinson*, 1979]. The rate may be enhanced by the presence of water vapor at high pressures [*Hamilton and Lii*, 1977]. It is clear that (8) proceeds by a complex mechanism, and rate measurements are needed for conditions of pressure and humidity typical of the atmosphere.

Reaction of OH with H_2O_2 (reaction (10)) is an important sink for odd hydrogen in the troposphere. Recent studies find that the rate for this reaction is almost independent of temperature [*Keyser*, 1980; *Sridharan et al.*, 1980], in contrast to earlier work, which suggested a significant activation energy (~1.5 kcal $mole^{-1}$, see *Hampson and Garvin* [1978]). The new measurements imply that k_{10} at 230 K is about 4 times larger than recommended recently by *NASA* [1979].

Reaction (4) initiates a complex sequence of transformations in which carbon is oxidized, ultimately to CO and CO_2, as shown schematically in Figure 2. Kinetic parameters for reactions shown in Figure 2 are given in Table 1. Reaction (4) is followed by

$$CH_3 + O_2 + M \rightarrow CH_3O_2 + M \qquad (16)$$

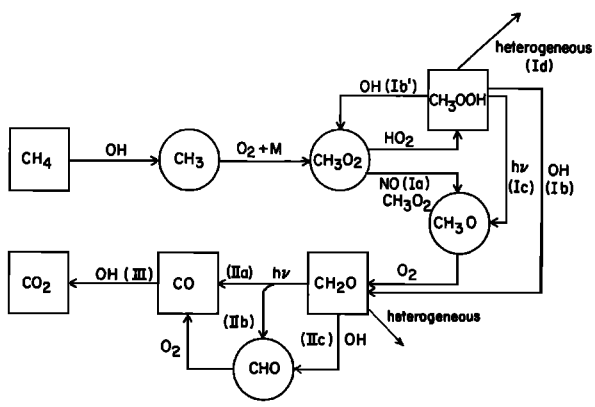

Fig. 2. The atmospheric oxidation of methane.

with CH_3O_2 removed by

$$CH_3O_2 + NO \rightarrow CH_3O + NO_2 \qquad (17)$$

$$CH_3O_2 + HO_2 \rightarrow CH_3OOH + O_2 \qquad (18a)$$

$$\rightarrow CH_3O + OH + O_2 \qquad (18b)$$

and

$$CH_3O_2 + CH_3O_2 \rightarrow \text{products} \qquad (19)$$

The rate constant for (17) is similar to that for the analogous reaction (7) (see Table 1). Work by *Cox and Tyndall* [1980] suggests that k_{18} may be comparable to k_{17} and that the reaction could have a negative activation energy similar to that exhibited by (8). The rate for (18) is independent of water vapor concentration, although the CH_3O_2 radical appears to form a complex with H_2O [*Kan and Calvert*, 1979]. The rate constant for (19) is considerably smaller than values reported for (17) and (18) [*Parkes*, 1977]. It would appear that reactions (17) and (18) should represent major paths for removal of CH_3O_2 in the troposphere (see Figure 16).

The yield of CO from oxidation of methane could be less than unity if significant quantities of stable intermediates (e.g., CH_3OOH or CH_2O were removed heterogeneously. Hydroperoxides undergo acid-catalyzed and sometimes base-catalyzed decomposition [*Hiatt*, 1971]. Consequently, CH_3OOH might be destroyed by reactions on aerosols or in droplets. Likely decomposition products include formaldehyde and perhaps methanol [*Niki et al.*, 1978*a*]. These products could be removed by rain, but they could be vaporized also from the aerosol surface and oxidized in the atmosphere to CO (see also Appendix 1).

Photolysis of CH_2O is more rapid than that of CH_3OOH [*Bass et al.*, 1980; *Molina and Arguello*, 1979]. Heterogeneous reactions are consequently less important for CH_2O than for CH_3OOH. The low concentrations of CH_2O measured in aerosols and rainwater [*Klippel and Warneck*, 1978, 1980; *Zafiriou et al.*, 1980; *Thompson*, 1980] at remote locations are consistent with the view that loss of formaldehyde by heterogeneous processes is negligible relative to loss by photochemical reactions.

TABLE 2. Major Pathways for CH_4 Oxidation

Path	Reaction	Effect on Odd-O[a]	Effect on OH	Effect on HO_2[a]	Effect on Odd-H
Ia	$CH_4 + OH \rightarrow CH_3 + H_2O$ $CH_3 + O_2 + M \rightarrow CH_3O_2 + M$ $CH_3O_2 + NO \rightarrow CH_3O + NO_2$ $CH_3O + O_2 \rightarrow HO_2 + CH_2O$				
	net: $CH_4 + OH + NO + 2O_2 \rightarrow CH_2O + NO_2 + HO_2 + H_2O$	+1	−1	+1	0
Ib	$CH_4 + OH \rightarrow CH_3 + H_2O$ $CH_3 + O_2 + M \rightarrow CH_3O_2 + M$ $CH_3O_2 + HO_2 \rightarrow CH_3OOH + O_2$ $CH_3OOH + OH \rightarrow CH_2OOH + H_2O$ $CH_2OOH + M \rightarrow CH_2O + OH + M$				
	net: $CH_4 + OH + HO_2 \rightarrow CH_2O + 2H_2O$	0	−1	−1	−2
Ib′	$CH_3O_2 + HO_2 \rightarrow CH_3OOH + O_2$ $CH_3OOH + OH \rightarrow CH_3OO + H_2O$				
	net: $OH + HO_2 \rightarrow H_2O + O_2$	0	−1	−1	−2
Ic	$CH_4 + OH \rightarrow CH_3 + H_2O$ $CH_3 + O_2 + M \rightarrow CH_3O_2 + M$ $CH_3O_2 + HO_2 \rightarrow CH_3OOH + O_2$ $CH_3OOH + h\nu \rightarrow CH_3O + OH$ $CH_3O + O_2 \rightarrow CH_2O + HO_2$				
	net: $CH_4 + O_2 + h\nu \rightarrow CH_2O + H_2O$	0	0	0	0
Id	$CH_4 + OH \rightarrow CH_3 + H_2O$ $CH_3 + O_2 + M \rightarrow CH_3O_2 + M$ $CH_3O_2 + HO_2 \rightarrow CH_3OOH + O_2$ $CH_3OOH \rightarrow$ heterogeneous loss				
	net: $CH_4 + OH + HO_2 \rightarrow H_2O +$ products	0	−1	−1	−2
IIa	$CH_2O + h\nu \rightarrow H_2 + CO$	0	0	0	0
IIb	$CH_2O + h\nu \rightarrow H + CHO$ $H + O_2 + M \rightarrow HO_2 + M$ $CHO + O_2 \rightarrow HO_2 + CO$				
	net: $CH_2O + 2O_2 + h\nu \rightarrow 2HO_2 + CO$	0	0	+2	+2
IIc	$CH_2O + OH \rightarrow H_2O + CHO$ $CHO + O_2 \rightarrow HO_2 + CO$				
	net: $CH_2O + OH + O_2 \rightarrow HO_2 + H_2O + CO$	0	−1	+1	0
III	$CO + OH \rightarrow CO_2 + H$ $H + O_2 + M \rightarrow HO_2 + M$				
	net: $CO + O_2 + OH \rightarrow CO_2 + HO_2$	0	−1	+1	0

Average branching ratios IIa : IIb : IIc ≃ 1.5 : 1 : 1.5.
[a] Production of odd oxygen may result also from reaction of HO_2 with NO.

Rainout of CH_3OOH and CH_2O was parameterized in the present model according to the loss profile given in Table 1. Mean rates for heterogenous removal were chosen to be consistent with observations of species such as ^{210}Pb and ^{210}Po formed from decay of ^{222}Rn [*Junge*, 1963; *Moore et al.*, 1973]. The yield of CO from methane oxidation calculated in this manner is 78%. The yield is lowered to 50% if we assume efficient loss of CH_3OOH on aerosols (see Appendix 1). The maximum rate for heterogeneous loss of CH_3OOH is controlled by (17) and (18). At most, 56% of the global methane flux could be removed heterogeneously with concentrations of NO adopted below.

Table 2 summarizes net reactions for the methane oxidation scheme and specifies the effect of each pathway on odd hydrogen. Oxidation of CH_4 could provide either a source or a sink for odd H, depending on relative rates for (17) and (18). It is likely to represent a source for odd H if NO were abundant. It could introduce a sink of comparable magnitude if NO were low. The source of odd H is dominated however by (2) over most of the troposphere with methane reactions accounting for approximately 20% of the net sink. Photolysis of CH_2O is the major source of odd H in the upper troposphere (~10 km).

The chemistry of odd H may be simplified if we neglect the influence of methane oxidation and assume that the concentration of NO is less than 200 ppt. Loss of odd hydrogen under these conditions proceeds mainly by reaction of OH with H_2O_2 and by heterogeneous removal of H_2O_2. The concentration of HO_2 is given by

$$[HO_2] = \left\{\frac{(J_9 + k_{10}[OH] + k_{11})\, k_2[O(^1D)][H_2O]}{k_8(k_{10}[OH] + k_{11})}\right\}^{1/2} \quad (20)$$

where $[X]$ denotes the number density of X and k_i, J_i represent

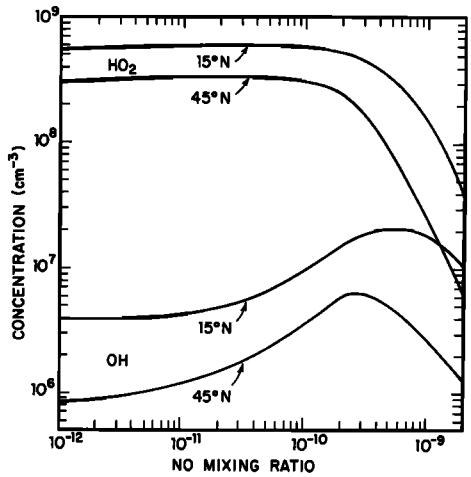

Fig. 3. Concentrations of OH and HO_2 as a function of the NO mixing ratio. Noon values at the surface are shown for equinoctial conditions at 15°N and 45°N. Nitric acid is calculated from the one-dimensional diffusion model described later in the text and in Appendix 2. The model allows for separate flow of HNO_3 and $(NO+NO_2)$. The deposition velocity of HNO_3 is taken to be 0.5 cm s^{-1}. Other model parameters are taken from the standard model (see Table 4).

rate constants for reaction i. The concentration of OH is given by

$$[OH] = \frac{2k_2[O(^1D)][H_2O] + [HO_2]\{k_6[O_3] + k_7[NO]\} + 2J_9[H_2O_2]}{k_3[CO] + k_4[CH_4]} \quad (21)$$

The second and third terms in the numerator of (21) reflect reactions that generate OH by cycling odd hydrogen. Reaction (9) can provide a source for OH in the upper troposphere comparable to production by (2).

As we shall see, production of OH in lower regions of the tropical troposphere occurs mainly by (2) with smaller contributions from (6), (7), and (9). Contributions from (6) and (7) grow in importance with latitude reflecting an increase in concentrations of NO and O_3, together with a decrease in insolation and in concentrations of H_2O (see Figure 15). Cycling of odd H by reaction with NO (reaction (7)) is more important than cycling by reaction with O_3 (reaction (6)) if $[NO]/[O_3]$ exceeds 2×10^{-4}. Reaction (7) is more important than (6) in the tropics if NO exceeds 4 ppt. A higher concentration of NO, about 8 ppt, is required to ensure dominance of (7) at higher latitudes.

Variations of HO_2 and OH with NO are shown for surface air at several latitudes in Figure 3. Concentrations of HO_2 are insensitive to NO for values less than 200 ppt, a result that follows from (20) and (21). The concentration of OH is independent of NO for NO below about 10 ppt and is an increasing function of NO between 10 and 500 ppt [cf. *Weinstock et al.*, 1980; *Hameed et al.*, 1979; *Fishman et al.*, 1979]. The concentration of OH decreases as NO increases above 1 ppb, behavior that reflects the increasing importance of reaction (13) as a sink for odd hydrogen.

Reactions that affect odd H can also influence the budget of tropospheric O_3 [*Crutzen*, 1973; *Chameides and Walker*, 1973; *Fishman et al.*, 1979]. It is useful in this context to define a family of species undergoing rapid reactions leading to formation or removal of O_3. We identify this family, odd oxygen, with $O(^1D)$, $O(^3P)$, NO_2, and O_3. Ozone is formed by

$$O(^3P) + O_2 + M \rightarrow O_3 + M \quad (22)$$

and is removed mainly by photolysis

$$h\nu + O_3 \rightarrow O(^1D) + O_2 \quad (1a)$$

$$h\nu + O_3 \rightarrow O(^3P) + O_2 \quad (1b)$$

The metastable $O(^1D)$ is quenched by O_2 and N_2 (reactions (14) and (15)) though, as seen earlier, it can react with H_2O (reaction (2)). Nitric oxide reacts with O_3 to form NO_2,

$$NO + O_3 \rightarrow NO_2 + O_2 \quad (23)$$

Nitrogen dioxide is removed mainly by photolysis

$$h\nu + NO_2 \rightarrow O(^3P) + NO \quad (24)$$

Ozone lost in (23) is reconstituted by (24) and (22), and the cyclic nature of the chemistry is illustrated in Figure 4. Individual members of the odd oxygen family, $O(^1D)$, $O(^3P)$, and NO_2 are transformed to O_3 in the troposphere on time scales of 2×10^{-5} s, 2×10^{-5} s, and 2×10^2 s, respectively.

Odd oxygen is conserved in reactions (1), (14), (15), and (22)–(24). It is formed in the troposphere by reactions of NO with HO_2 and CH_3O_2 (reactions (7) and (17)). It is removed by reaction of $O(^1D)$ with H_2O, by reaction of O_3 with HO_2 and with OH, by formation of nitrates from NO_2 and by heterogeneous reactions of O_3 and NO_2 at the earth's surface.

The chemistry shown in Figures 1, 2, and 4 leads to net consumption of odd oxygen at low concentrations of NO. Reaction (2) is the dominant sink for tropospheric odd O in the tropics while rates for removal of odd O by (2) and (6) are comparable at mid-latitudes. The time for removal of the total column of tropospheric O_3 by (2) and (6) ranges from 21 days in the tropics to about 75 days at a latitude of 45°. Loss of odd oxygen by (2) and (6) is balanced by production in (7) and (17) for concentrations of NO near 30 ppt [cf. *Fishman et al.*, 1979]. Homogeneous reactions provide a net source for tropospheric O_3 if NO exceeds 30 ppt.

Production of O_3 in the troposphere is limited on a global scale by supply of CO, CH_4, and other hydrocarbons. One molecule of O_3 may be formed for each molecule of CO consumed by (3). The yield of O_3 from oxidation of CH_4 could be as large as 3.5 per molecule of CH_4, as may be seen from Table 2 and Figure 2. The yield from oxidation of other hydrocarbons depends on details of the oxidation path and could be much higher than that for CH_4. According to present knowledge, CH_4 is formed by anaerobic metabolism and released to the atmosphere at an average rate of about 1.5×10^{11} molecules cm^{-2} s^{-1} [*Wofsy et al.*, 1972; *Ehhalt and Schmidt*, 1978]. As we shall see, production of CO by sources other than oxidation of CH_4 provide about 2.5×10^{11} molecules CO cm^{-2} s^{-1}. The potential yield of O_3 from oxidation of CO and CH_4 could be as large as 8×10^{11} molecules cm^{-2} s^{-1} if an adequate supply of NO were available. This source would suffice to double the concentration of tropospheric O_3 in about 2 weeks.

3. Observations

As is discussed above, the distribution of tropospheric OH depends on H_2O, O_3, CH_4, CO, NO, and NO_2. All of these species, with the exception of CH_4, show significant variation with latitude, altitude, and time. Variations of H_2O are deter-

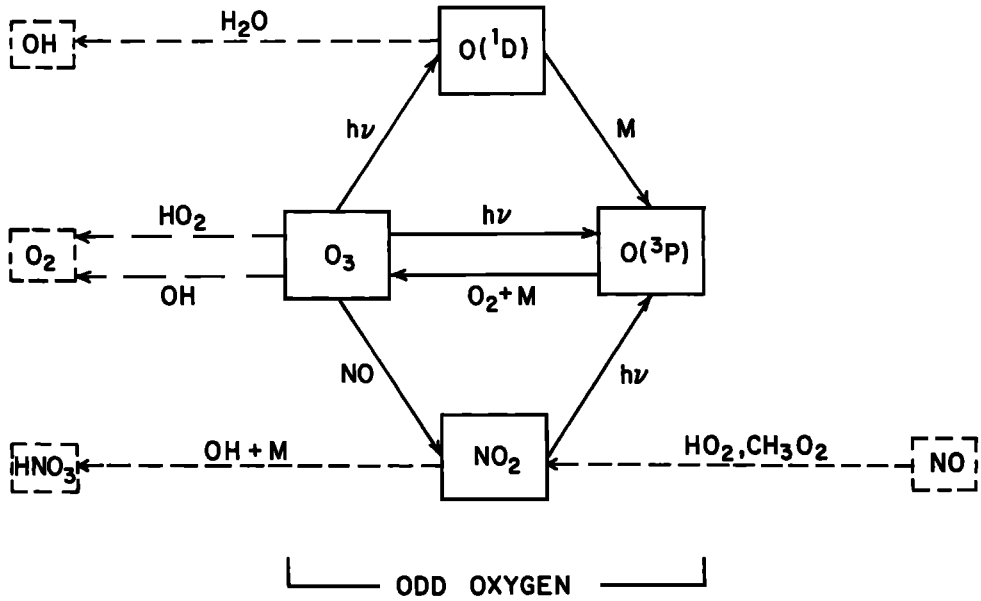

Fig. 4. Major chemical reactions affecting odd oxygen (O_3; $O(^3P)$, $O(^1D)$, NO_2) in the troposphere. Air molecules acting as third bodies are denoted by 'M' (N_2, O_2, Ar, H_2O).

mined mainly by physical processes. Ozone is affected by both chemistry and transport. Carbon monoxide, NO and NO_2 are influenced by physical and chemical processes in the atmosphere and by biogenic and anthropogenic sources at the ground. We begin with a review of observational data for H_2O.

The concentration of OH is proportional to the concentration of H_2O raised to a power, which varies between 0.5 and 1.0. The concentration of H_2O is quite variable, with largest fluctuations above about 3 km, where concentrations may change over short distances and times by factors as large as 10^2 [*Mastenbrook,* 1966, 1968, also private communication, 1980). Figure 5 shows a number of profiles measured over Washington, D. C., and over Trinidad. It includes results from a statistical analysis of summer and winter data acquired over a period of about 10 years. Note that values for the mean concentration of H_2O are consistently higher than are values for the median, reflecting the occasional presence of exceedingly high concentrations of H_2O. Concentrations of H_2O shown in Figure 5 are somewhat lower than climatological means given by A. H. Oort (private communication, 1979). This comparison underscores the difficulty of defining average concentrations for OH. Mastenbrook's measurements provide the only source of data for the upper troposphere. His measurements are limited however to cloud-free conditions at three stations. Oort used a larger data base from the radiosonde network [*Oort and Rasmusson,* 1971]. It is known, however, that the radiosonde results are inaccurate at low humidities [cf. *Routhier and Davis,* 1980]. Profiles adopted for present purposes are given in Figure 6. They were derived below 6 km from latitudinal and seasonal averages provided by A. H. Oort (private communication, 1979); above 6 km they are based on Mastenbrook's measurements at Washington, D. C. (38.5°N) and at Trinidad (10°N). We estimate that uncertainties in the distribution of H_2O could lead to errors as large as 15% in values calculated for the mean concentration of OH.

Data from the North American Ozonesonde Network give a valuable record of O_3 below 30 km for the period 1963–1969 [*Hering and Borden,* 1964, 1967, 1975; *Chatfield and Harrison,* 1977*a*]. Most of the early measurements, between 1963 and 1966, were made with Regener chemiluminescent sondes, and it appears that concentrations obtained for the troposphere in this manner may be too small by about 30%. Sources of experimental error are discussed by *Chatfield and Harrison* [1977*b*] and by *Wilcox* [1978], who conclude that the Brewer-Mast electrochemical sonde favored in the later measurements should be more reliable than the chemiluminescent method used before 1966. The more recent observations are limited to six stations, in contrast to the 13 stations included earlier. Only one mid-latitude station, Bedford, Massachusetts (42.5°N), was operated during both observational periods. Six years of data for tropospheric ozone, obtained with the more reliable electrochemical technique, are available for two mid-latitude stations in Europe [*Dütsch and Ling,* 1973; *Attmanspacher and Hartmannsgruber,* 1976].

Ozone profiles selected for the northern hemisphere were derived from measurements made with the electrochemical technique and are given in Figure 7. The mid-latitude profiles were obtained by averaging measurements from four stations: Wallops Island, Virginia (37.5°N); Bedford, Massachusetts (42.5°N) [*Chatfield and Harrison,* 1977*a*]; Payerne, Switzerland (47°N) [*Dütsch and Ling,* 1973]; and Hohenpeissenberg, Federal Republic of Germany (48°N) [*Attmanspacher and Hartmannsgruber,* 1976]. Measurements from Panama (9°N) [*Chatfield and Harrison,* 1977*a*] are assumed typical for conditions in the tropics.

Measurements are sparse for ozone in the southern hemisphere. A long record is available for one mid-latitude station, Aspendale, Australia (38°S). Profiles for O_3 were measured at this site with the electrochemical technique at weekly intervals for 8 years [*Pittock,* 1977]. The data show little seasonal variation below 3 km, in contrast to data from mid-latitudes in the northern hemisphere. Ozone is about 40% lower in summer at 2 km at Aspendale than at Wallops Island (37.5°N), as shown in Figure 8 (A. B. Pittock, private communication, 1980). Comparison of Figures 7 and 8 indicated that mid-latitude ozone is similar for the two hemispheres in autumn and winter.

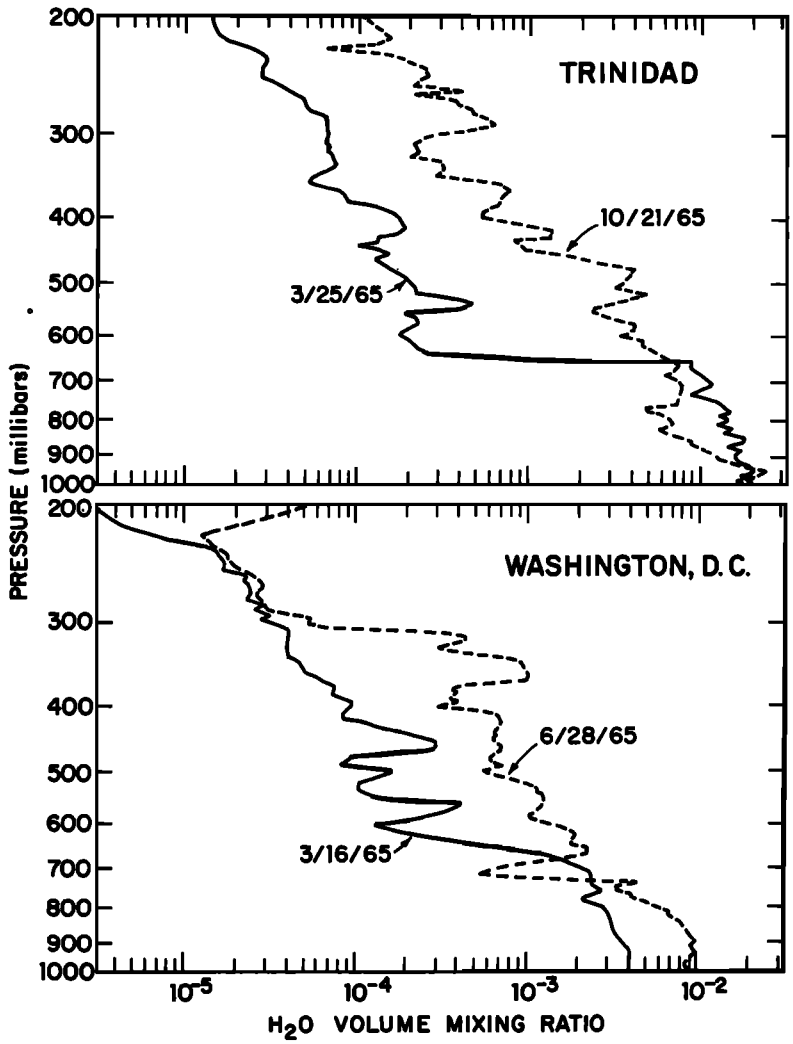

Fig. 5a. Individual profiles of water vapor over Trinidad and Washington, D. C. The measurements are from *Mastenbrook* [1966].

Very few profiles have been reported for O_3 in the southern tropics. *Fishman et al.* [1979] analyzed 31 profiles from Canton Island (2°S) and 10 from La Paz (16°S). These were obtained by using the less reliable chemiluminescent technique. A comparison of measurements made with the chemiluminescent method indicates that ozone is about 35% lower at 2 km at southern tropical stations than at Panama (see Figure 8). Interhemispheric asymmetry is indicated also by data acquired over the Pacific Ocean [*Routhier et al.*, 1980]. Figure 8 illustrates differences between results obtained by the two measurement techniques at Panama. It is obvious that north/south comparisons must be based on data acquired with a single observational method.

The ozone data are sparse, and it is difficult to separate true hemispheric differences from variations with longitude, or with oceanic, coastal or inland environments. It should be noted in particular that the sea-level stations between 35°–45°N are all located in North America, while the single mid-latitude station for the southern hemisphere is on the south coast of Australia, a less polluted environment than that of the northern stations. Urban pollution may lead to elevated concentrations of ozone in the lower troposphere of the eastern United States and Europe, particularly in the summer.

The data base allows us little choice but to assume that measurements at Aspendale are representative of ozone at southern mid-latitudes. The mean profile for ozone in the southern tropics is based on the chemiluminescent technique and must be corrected to account as far as possible for errors resulting from use of this method. The corrected profile, shown in Figure 8, was obtained by scaling the Canton Island and La Paz results by the ratio of concentrations measured, using the electrochemical technique at Panama to results derived with the chemiluminescent method at the same location (approximately 0.8). This ratio is available only above 2 km, and ozone at ground level in the southern tropics was taken equal to the mean value for Samoa, 14°S [*Oltmans*, 1981]. Resulting profiles are consistent with measurements by *Routhier et al.* [1980].

The concentration of O_3 is variable near the surface and may be very low at times, at least over the tropical ocean. Figure 7 shows mixing ratios for O_3 in the range 12–18 ppb near the surface at Panama, similar to concentrations observed at Samoa (14°S) [*Oltmans*, 1981]. Mixing ratios as low as 1–5 ppb have been reported for the tropical South Pacific [*Routhier et al.*, 1980], though values as high as 30 ppb were observed by *Rasmussen et al.* [1976]. The data for tropospheric O_3 are obviously sparse, and information is particularly lacking for the marine environment. We believe that uncertainties

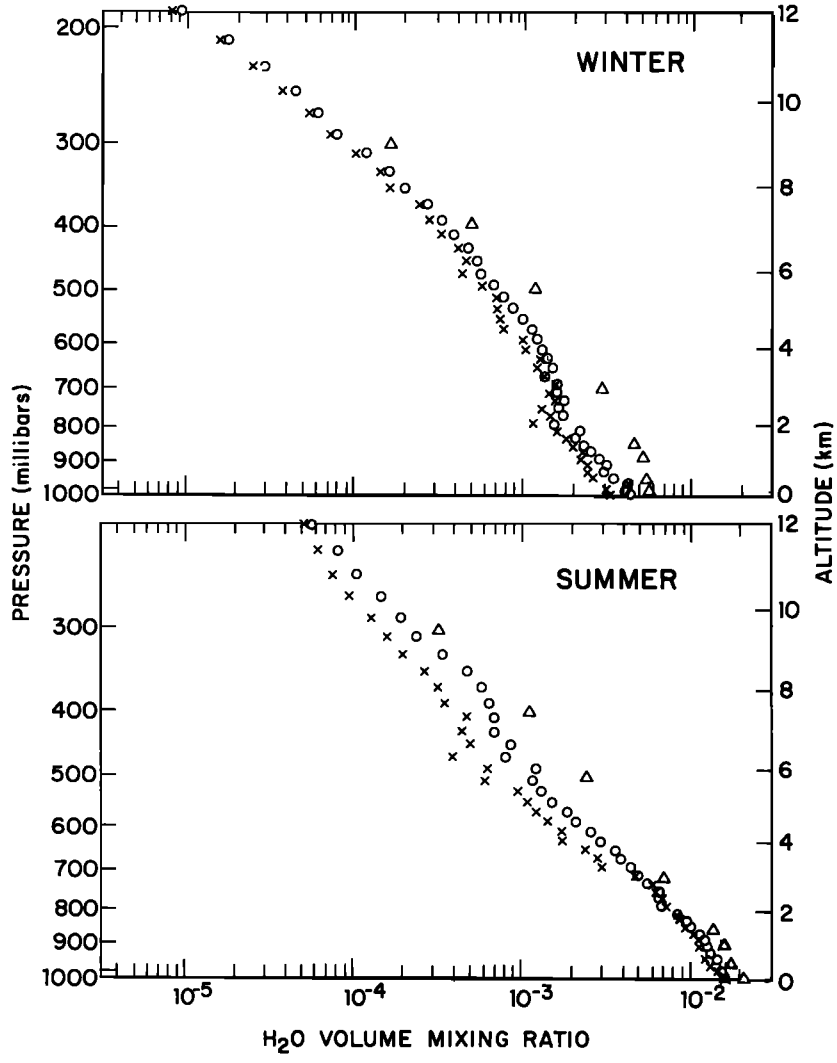

Fig. 5*b*. Averaged profiles of water vapor over Washington, D. C., in summer and winter. The open circles show the mean values and the crosses show the median values of the water vapor mixing ratio. The profiles represent data from about 50 balloon ascents made between 1965 and 1976. [*Mastenbrook*, 1968; H. J. Mastenbrook, private communication, 1980]. The triangles show mean values of the water vapor mixing ratio, from the radiosonde network, at 37.5°N, 75°W (A. H. Oort, private communication, 1979). The altitude scale on the right is taken from the *U.S. Standard Atmosphere Supplements* [1966], 45°N.

in the distribution of O_3 are comparable to those for H_2O and are likely to have similar impact on calculations for the distribution of OH.

The rate for production of odd hydrogen is sensitive to the overhead column of ozone. The seasonal and latitudinal distribution of the total ozone column was taken from *Dütsch* [1974], whose results agree with *Gebhart et al.* [1970] within 10%. Both studies used data from the global Dobson network. Comparison of ground-based measurements of total ozone with satellite observations shows similar agreement except at high latitudes (>50°) [*Prior and Oza*, 1978]. *Angell and Korshover* [1978] concluded that global ozone may vary temporally by as much as 10%. Their analysis suggests that errors in the absolute calibration of the Dobson network are of similar magnitude. A 10% error in the ozone column would be reflected by a 10% error in the global mean concentration of OH.

A summary of observations for tropospheric CO is given in Figure 9 and in Table 3. These data were selected from observations in the clean troposphere. Most of the measurements were taken over the ocean, either from ships or aircraft. The data shown in Figure 9 for northern mid-latitudes were derived exclusively from measurements over the North Atlantic and may be affected by transport from strong sources on the North American continent. The influence of sources is apparent in vertical soundings over Europe that show considerable variability, as evident in Figure 10. It appears that the northern hemisphere contains approximately 1.5–2 times as much CO as the southern hemisphere. The concentration of CO in surface air is significantly higher than at altitude, at least for the northern hemisphere.

Measurements at Mauna Loa Observatory in Hawaii (19.5°N) [*Seiler et al.*, 1976] and at Cape Meares, Oregon (R. A. Rasmussen et al., private communication, 1980) indicate that CO may vary seasonally by about a factor of 2, with concentrations highest in winter, lowest in summer. The behavior at these sites might reflect relatively localized meteorological conditions. At Mauna Loa, for example, prevailing winds are

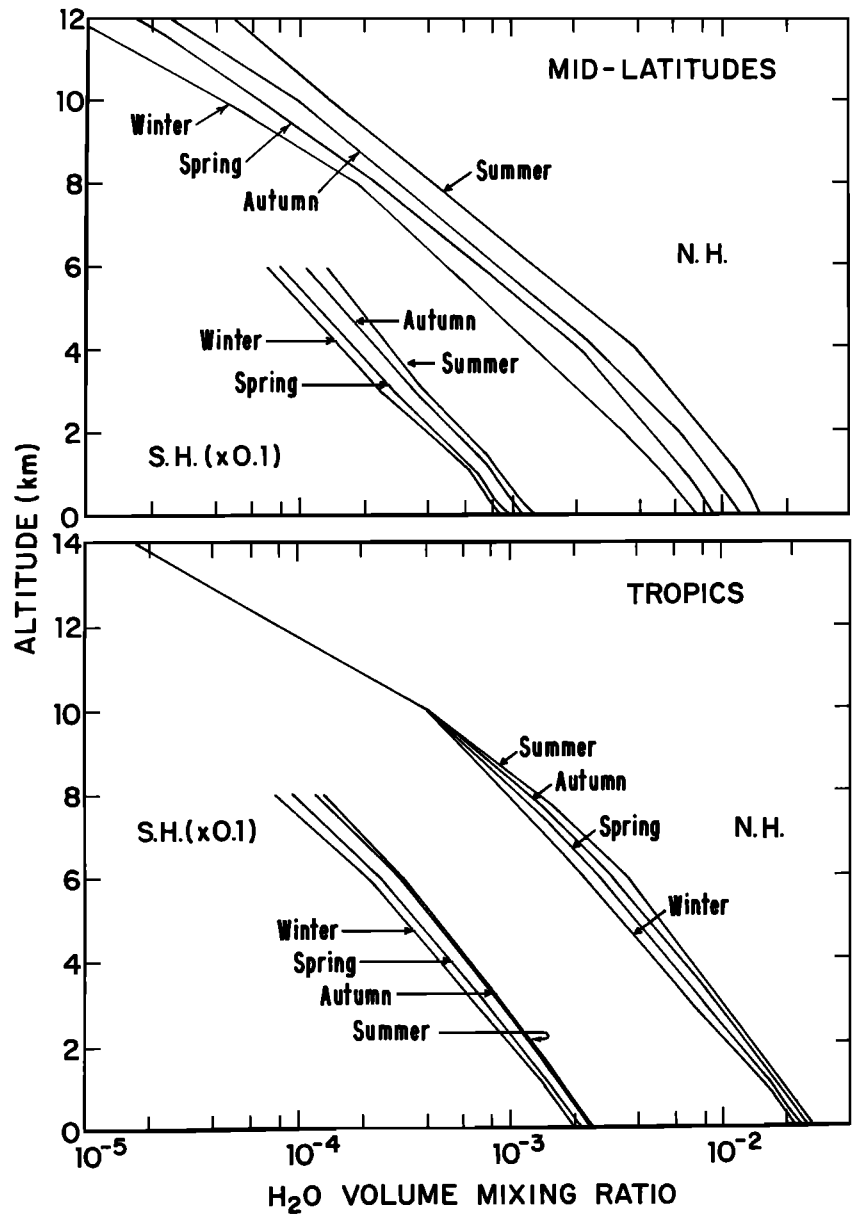

Fig. 6. Altitude profiles of water vapor in the northern and southern hemispheres. For altitudes below 6 km the profiles are derived from seasonal data for every 10° in latitude, for the years 1968–1973 (A. H. Oort, private communication, 1979). Above 6 km the profiles are taken from the measurements of H. J. Mastenbrook (private communication, 1980) at Washington, D. C. (38.5°N; ~100 soundings) and Trinidad (10°N; ~15 soundings).

from the northeast and are comparatively steady in summer. Conditions are more variable in winter with frequent storms, which would enhance exchange of air with higher latitudes, thus raising ambient concentrations of CO. On the other hand, variations in CO could reflect a seasonal dependence either of the source or of the loss, (reaction (2)). *Stevens et al.* [1972] reported an annual cycle for CO in rural Illinois (43°N). Concentrations of CO were generally lowest in summer, although there were large fluctuations associated with local sources of pollution. The seasonal variation of ^{14}CO has been measured in Europe, and there, also a minimum was observed in summer [*Volz et al.*, 1981]. Further data will be required to identify and quantify seasonal or other temporal variability in CO. It appears that the global budgets for CH_4 and CH_3CCl_3 are insensitive to possible seasonal variations in CO (see Table 7).

The distribution shown in Figure 11 for CO was constructed on the basis of information in Figures 9 and 10. There is appreciable uncertainty, perhaps 20–30%, in the distribution of CO. The uncertainty may be attributed in part to the inhomogeneity of northern hemispheric CO, in part to inadequate definition of temporal variability, and in part to possible errors in the determination of absolute concentrations. We estimate that uncertainties in the distribution of CO could lead to uncertainty of about 15% in calculated values for OH. Inference regarding the magnitude of the net sink for CO is relatively insensitive to uncertainties in concentrations assumed for CO. Calculated concentrations of OH and CO tend to be inversely related since reaction with CO represents the major sink for tropospheric OH.

The latitudinal distribution of CH_4 was derived from measurements of *Seiler et al.* [1978], *Fabian et al.* [1979], *Ehhalt*

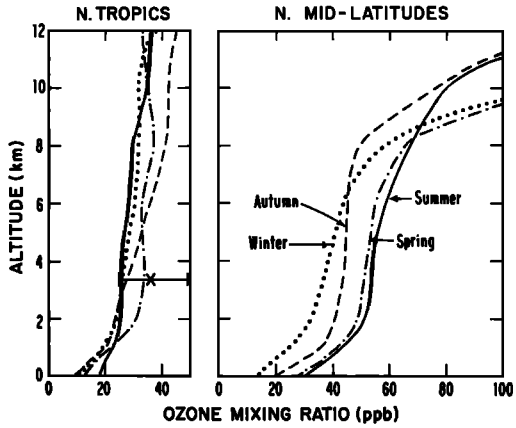

Fig. 7. Altitude profiles for ozone in the northern hemisphere. The tropical profiles are from Panama, 9°N. The cross indicates the mean and the bar indicates the range of values for ozone at Mauna Loa, Hawaii, 19.5°N, 3.4 km [*Oltmans*, 1981]. The mid-latitude profiles are an average of data obtained at four mid-latitude stations as described in the text.

[1978], *Heidt and Ehhalt* [1980], and *Heidt et al.* [1980]. Mixing ratios for CH_4 were taken as 1.7 and 1.6 ppmv for the northern and southern hemispheres, respectively. The mixing ratio of H_2 was taken as 0.55 ppmv [*Schmidt*, 1978].

The largest uncertainty in our model of tropospheric chemistry may be attributed to lack of data for NO and NO_2. Information on the distribution of NO is available for the clean troposphere at only a few locations and times. The sparseness of the data reflects the difficulty in measuring concentrations of NO lower than about 0.5 ppb, and it is clear that ambient concentrations of NO are often much smaller than this. Measurements for surface continental air are available for Colorado and Wyoming. Mixing ratios are sometimes lower than 20 ppt, though often higher than 1 ppb [*Drummond*, 1977; *Bush et al.*, 1979; *Kelly et al.*, 1980]. High values are associated with advection of urban pollutants. The concentration of NO in air over cities is often as large as 10 ppb [*Spicer*, 1977]. The data from Colorado and Wyoming suggest that concentrations of NO near the ground at clean continental sites should lie in the range 20–100 ppt.

We expect sources of NO in the marine environment to be much smaller than those over land. The anthropogenic influence is minimal, and rates for emission of fixed nitrogen are small [*Zafiriou and True*, 1979, *Tsunogai*, 1971; *Georgii and Gravenhorst*, 1977]. *McFarland et al.* [1979] found concentrations of NO of about 4 ppt in surface air over the midtropical Pacific. *Schiff et al.* [1979] reported mixing ratios for NO of 30–40 pptv both in and above the boundary layer over the Pacific Ocean, with slightly higher values (40–60 pptv) in clean air over North America. They emphasized, however, that their values represent upper limits. (An NO signal, presumably spurious, corresponding to about one half the daytime value was observed after sunset.) *Kley et al.* [1980] reported concentrations of ($NO + NO_2$) in the range 40–200 pptv at 7 km above Wyoming in December. *Roy et al.* [1980] observed 100–150 pptv NO in summer at 8 km over Australia (34°S) with 130–230 pptv at 10 km.

Optical measurements by *Noxon* [1978] near sunrise and sunset show that the integrated column of tropospheric NO_2 is typically less than 5×10^{14} molecules cm^{-2}. If NO_2 were distributed uniformly throughout the troposphere, this result would correspond to concentrations of NO_2 less than about 25 ppt and would imply daytime average mixing ratios of NO smaller than 10 ppt. Somewhat higher values of NO could be accommodated by Noxon's observations if NO and NO_2 were located primarily in the upper troposphere. The colder temperatures at these levels would allow a larger ratio NO/NO_2.

Measurements of HNO_3 provide a useful guide to distributions of NO and NO_2. *Huebert and Lazrus* [1978, 1980] found concentrations of HNO_3 nearly uniform with latitude in the middle troposphere with a median value of about 100 ppt and a range of <30–280 ppt. About 30% of observations over the ocean fell below their detection limit (~30 ppt). Concentrations of HNO_3 were somewhat lower in the marine boundary layer, about 60 ppt at ~1 km [*Huebert and Lazrus*, 1980], 15–70 ppt near the ocean surface [*Huebert*, 1980]. The surface measurements were made aboard ship at the same time that *McFarland et al.* [1979] observed NO concentrations of 4 ppt. *Kelly et al.* [1980] observed low concentrations of HNO_3 (<100 ppt) in unpolluted surface air in Colorado. The observations of HNO_3 are consistent with the view that the gas is removed rapidly from the boundary layer [*Huebert and Lazrus*, 1980; *Kelly et al.*, 1980].

(It is possible that pernitric acid (HO_2NO_2) may contribute to the acidic nitrate observed by *Huebert and Lazrus* [1978, 1980]. The chemistry of HO_2NO_2 is not accurately known for atmospheric conditions. If we adopt the kinetic parameters recommended in *NASA* [1979, 1981] and the results of *Molina and Molina* [1980] for the absorption cross sections of HO_2NO_2, we would calculate that 30–50% of the observed acidic nitrate could be in the form of HO_2NO_2 in the upper

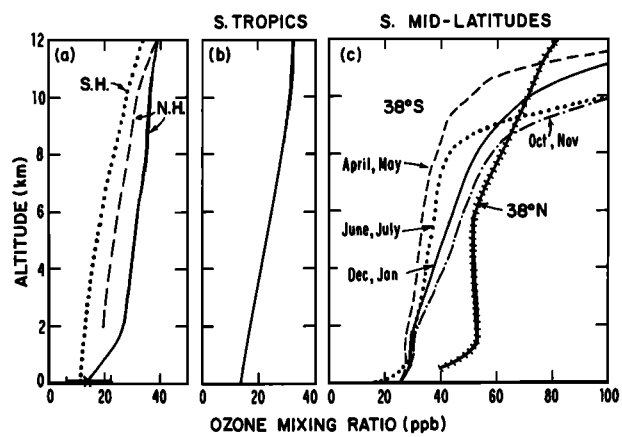

Fig. 8. Altitude profiles for ozone in the southern hemisphere. (*a*) The southern hemisphere tropical profile (dotted line) derived by *Fishman et al.* [1979]. The profile represents 41 soundings at 2°S and 16°S, measured during 1963–1965 with chemiluminescent sondes. The northern hemisphere data are yearly averages from Panama and are derived from 73 soundings measured in 1963–1964 with chemiluminescent sondes (dashed line) [*Hering and Borden*, 1967] and 43 soundings measured in 1966–1969 with electrochemical sondes (solid line) [*Chatfield and Harrison*, 1977*a*]. The cross indicates the mean and the bar indicates the range of values for surface ozone at Samoa, 14°S [*Oltmans*, 1981]. (*b*) The annual mean 15°S profile derived from the profiles in Figure 8*a* as described in the text. (*c*) The averages of 284 soundings as Aspendale, 38°S (A. B. Pittock, private communication, 1980); dashed-dotted line, October–November; solid line, December–January; dashed line, April–May; dotted line, June–July. These profiles were used in the calculations for spring, summer, autumn, and winter, respectively. The summer profile for Wallops Island (38°N) is also shown (hatched line) [*Chatfield and Harrison*, 1977*a*].

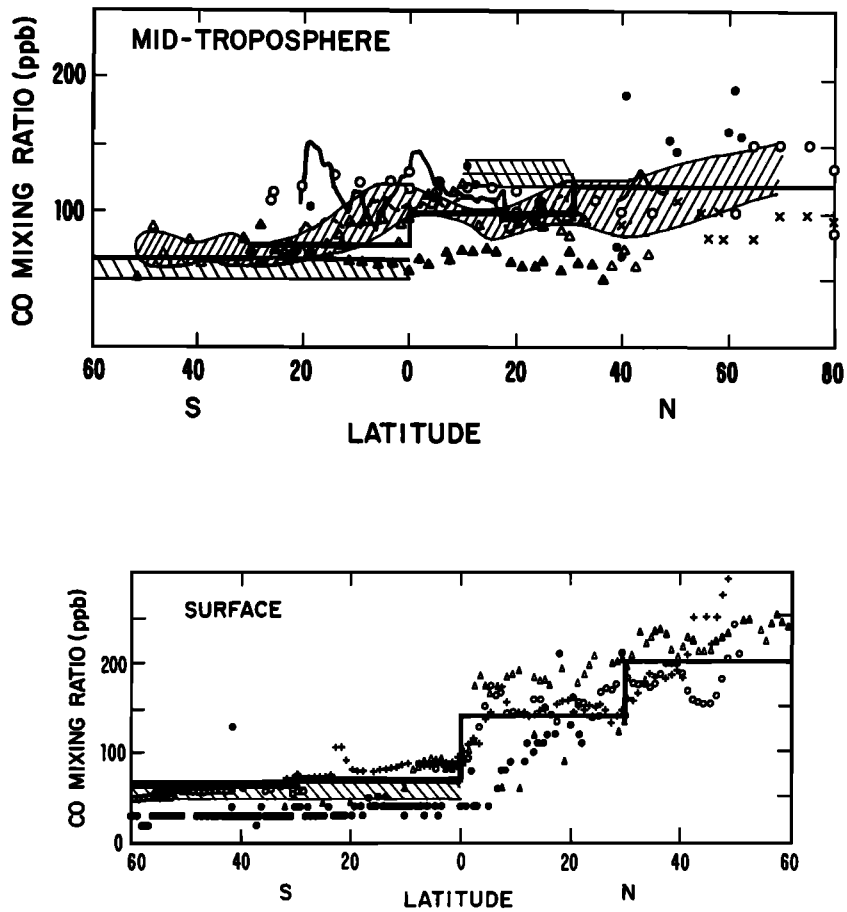

Fig. 9. Observational data for carbon monoxide near the surface and in the midtroposphere. The symbols are explained in Table 3. The heavy lines show the values for CO used in the model.

troposphere (see Figure 14). It is possible also that HO_2NO_2 may affect the response of the chemiluminescent instrument used to observe NO.)

Conversion of NO and NO_2 to HNO_3 proceeds through (7), (17), and (23) followed by (12), with a time constant of about a day. In contrast, 2–4 weeks are required to convert HNO_3 back to (NO + NO_2). Nitric acid is a soluble gas, and it may be removed by heterogeneous processes such as rainout, washout, or loss to aerosols within a few days [*Junge*, 1963; *Levine and Schwartz*, 1981]. The concentration of HNO_3 would be determined in this case by balance between (12) and (13). If heterogeneous processes are unimportant, NO, NO_2, and HNO_3 would tend to a photostationary state, and the data for HNO_3 would imply concentrations of NO in summer

TABLE 3. Observational Data for Carbon Monoxide

Reference	Date	Latitude	Location	Symbol
		Surface Measurements		
Robinson and Robbins [1969]	Nov.-Dec. 1967	37°N–37°S	Pacific	solid triangle
Seiler and Schmidt [1974]	April–May 1969	60°N–10°S	Atlantic	open triangle
Seiler and Schmidt [1974]	Nov. 1971	50°N–30°S	Atlantic	plus
Seiler and Schmidt [1974]	March 1972	50°N–60°S	Atlantic	open circle
Wilkniss et al. [1973]	Nov.–Dec. 1972	30°N–77°S	Pacific	solid circle
Heidt et al. [1980]	May 1978	30°N–60°S	Pacific	left-leaning hatching
		Midtroposphere Measurements		
Junge et al. [1971]	Jan.–April 1968	80°N–40°N	Pacific	cross
Junge et al. [1971]	Nov. 1968	85°N–26°S	Atlantic	open circle
Seiler and Schmidt [1974]	Nov. 1971	50°N–20°S	Atlantic	solid line
Seiler and Schmidt [1974]	March 1972	30°N–20°S	Atlantic	dashed line
Seiler [1976]	July–Aug. 1974	65°N–56°S	east and west American Coasts	solid circle/right-leaning hatching
Pratt and Falconer [1979]	Oct. 1977	45°N–53°S	Atlantic	open triangle
		36°N–32°S	Pacific	solid triangle
Heidt et al. [1980]	May 1978	30°N–60°S	Pacific	left-leaning cross hatching

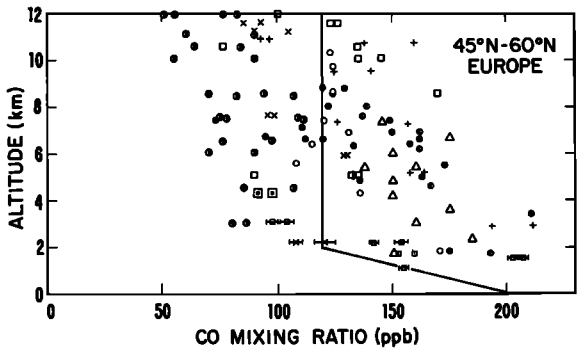

Fig. 10. Tropospheric profiles for CO. The individual symbols indicate data from separate flights over Europe and are from *Seiler et al.* [1978] and *Fabian et al.* [1979]. Also shown are results from one flight over the eastern United States at 45°N in January (open triangle, *Reichle and Condon* [1979]). The solid line indicates the profile used in the model at northern mid-latitudes.

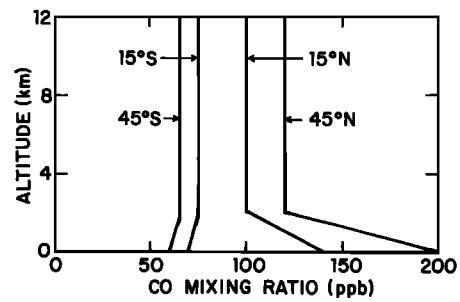

Fig. 11. Tropospheric profiles for CO. These profiles are derived from the measurements in Figures 9 and 10 and are used in the model calculations.

much smaller than was measured by *Schiff et al.* [1979] and *Roy et al.* [1980]. A role for heterogeneous loss is indicated further by observations of a relatively large fraction of nitrate in particulate form in the remote troposphere [*Huebert and Lazrus,* 1978, 1980].

We adopted an empirical model designed to fit the available observations for NO, NO_2, and HNO_3. Calculated values for OH were used to estimate the rate for (12) and heterogeneous loss was parameterized as shown in Table 1. One-dimensional diffusion calculations, constrained to give observed concentrations of HNO_3, were carried out for various latitudes and seasons (see Appendix 2). The model assumed that loss of HNO_3 was balanced in part by input from the stratosphere (~5%) and in part by production of NO and NO_2 in the troposphere (~95%). The loss frequency for HNO_3 was taken independent of latitude and season. The sources of (NO + NO_2) must be similarly uniform. With these assumptions, concentrations of (NO + NO_2) vary inversely with OH (see Figure 12). Model profiles for HNO_3, NO, and NO_2 are shown in Figure 12.

The model indicates 5–20 ppt NO in the lower troposphere at noon and implies a column abundance for NO_2 near twilight of about 3–7 × 10^{14} cm^{-2}. Concentrations calculated for NO and NO_2 are directly proportional to the rate adopted for

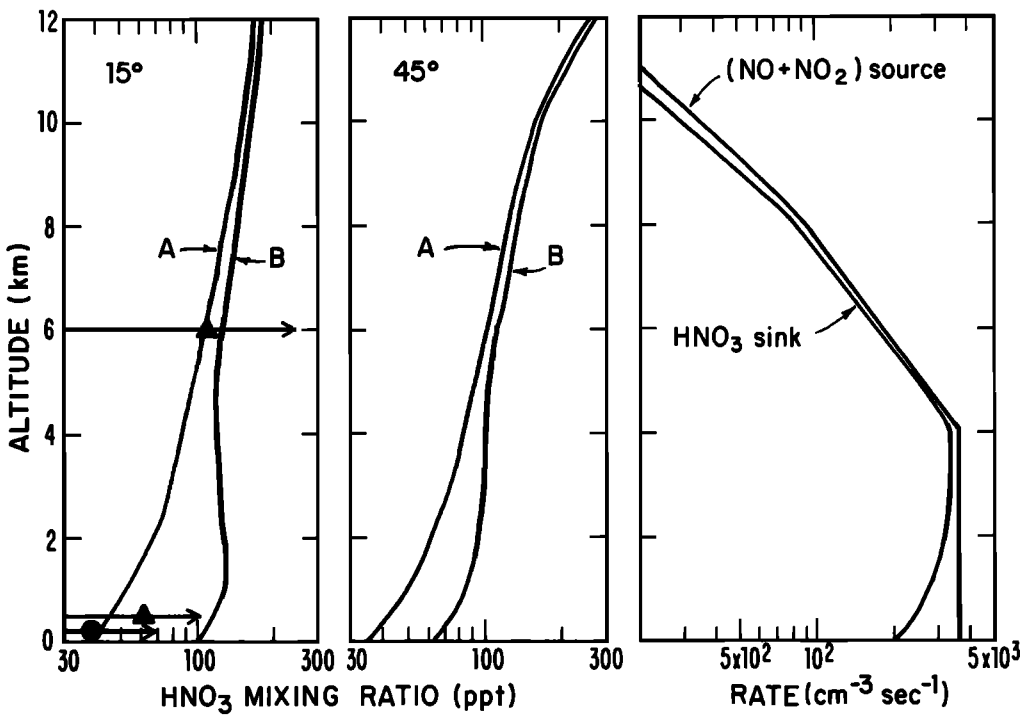

Fig. 12*a*. Calculated altitude profiles for nitric acid. Results are shown for the following conditions. (1) The stratospheric input of odd N is 1.4 × 10^8 molecules cm^{-2} s^{-1}. (2) The column production rate of (NO + NO_2) is 3 × 10^9 molecules cm^{-2} s^{-1} and is distributed with altitude as shown in the right-hand panel. (3) Rainout of nitric acid is included, with an effective tropospheric lifetime of about 10 days (see Table 1). The corresponding loss rate for HNO_3 at 15°N is shown in the right-hand panel; results for 45°N are similar. (4) The deposition velocity for HNO_3 is 0.5 cm s^{-1}. (5) In model A, the surface flux of (NO + NO_2) is set equal to zero; in model B, the mixing ratio of (NO + NO_2) at the surface is prescribed at 100 pptv. All results shown are for equinox and global mean cloud cover. Results for cloud-free conditions and for other seasons are almost identical. Other model parameters are given in Table 4. The symbols show median concentrations of acidic nitrate: solid triangle *Huebert and Lazrus* [1980]; solid circle, *Huebert* [1980].

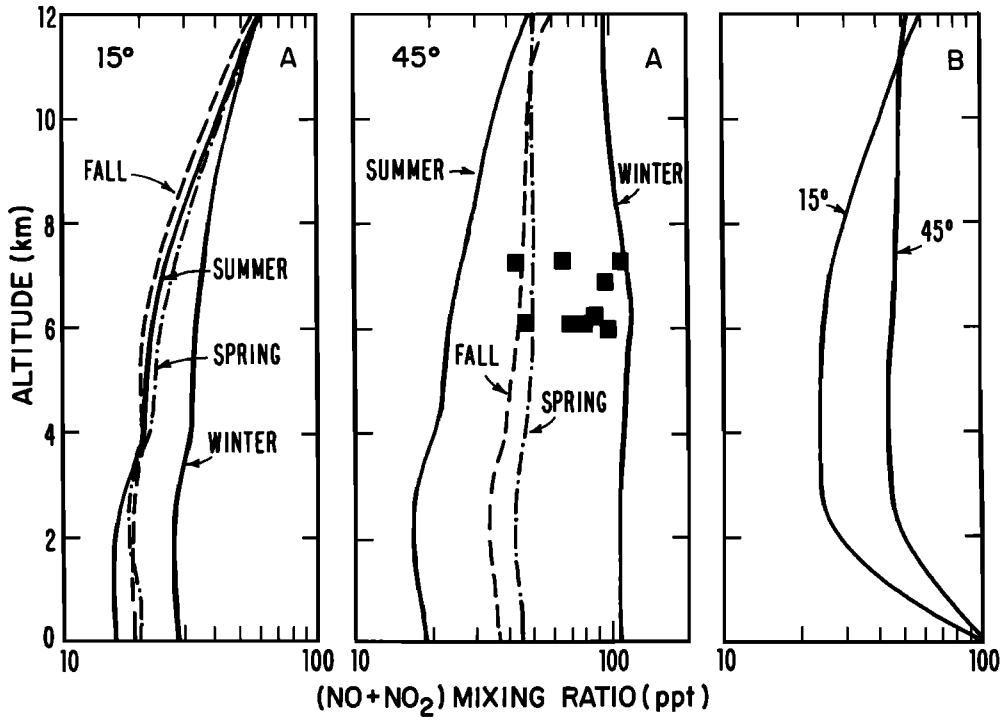

Fig. 12*b*. Altitude profiles for (NO + NO_2). The left and center panels show seasonal results for model A described above. The right-hand panel shows results for model B at equinox. These calculations include the effects of clouds. The symbols show the measurements of *Kley et al.* [1980].

heterogeneous removal of HNO_3 and are sensitive to the vertical distribution assumed for the source of (NO + NO_2). The relatively large concentrations of HNO_3 observed in the middle troposphere suggest a globally distributed source for odd nitrogen. The model implies that the source should be about 10^7 tons N yr^{-1}, which may be compared with the flux of odd N from the stratosphere, calculated to be about 5×10^5 tons N yr^{-1}.

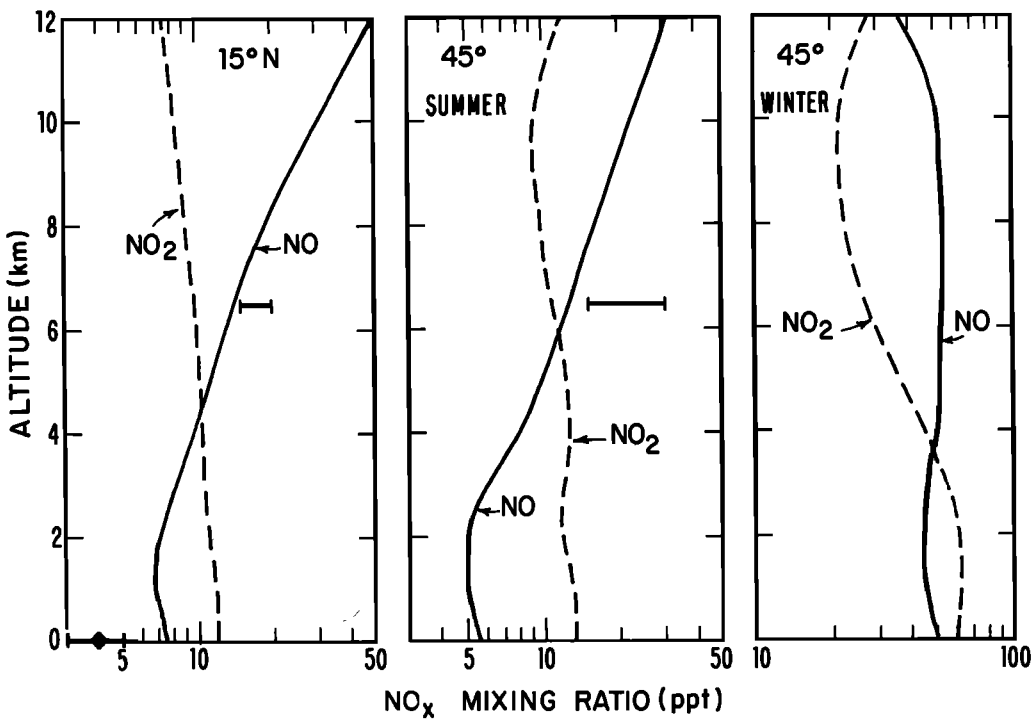

Fig. 12*c*. Altitude profiles for NO and NO_2. Concentrations are noontime values, under cloud-free conditions. The results are from model A and are shown for 15°N at equinox and for 45°N in summer and winter. The bars show the range of daytime concentrations of NO, derived from the upper limits given by *Schiff et al.* [1979]. Their limits have been divided by 2 to account for the observed nighttime signal. Noontime concentrations for NO reported by *McFarland et al.* [1979] are shown by the diamond.

Levy et al. [1980] suggested that nitrogen oxides from the stratosphere could provide a dominant source for odd nitrogen in the upper troposphere. Heterogeneous removal should be slow at these altitudes, as indicated by studies of nuclear bomb debris and natural radionuclides (e.g., Be^7) [*Junge,* 1963; *Bleichrodt,* 1978]. The three-dimensional general circulation model used by *Levy et al.* [1980] incorporated wet removal processes parameterized to reproduce the behavior of tracers in the upper troposphere [*Mahlman and Moxim,* 1978].

The role of stratospheric odd N in the middle and lower troposphere is less clear. *Levy et al.* [1980] argue that stratospheric input could contribute significantly to the abundance of tropospheric odd N in marine locations far from continental sources, even below 8 km. It is difficult to reconcile this view with the high concentrations of NO reported in the midtroposphere [*Schiff et al.,* 1979; *Roy et al.,* 1980] as discussed above, but the fragmentary data base precludes a definitive discussion.

Kley et al. [1981] and *Liu et al.* [1980] give global distributions for ($NO + NO_2$) derived from a one-dimensional 'eddy-diffusion' model used in conjunction with the tracer distributions of *Levy et al.* [1980]. The assumption underlying their calculations (stratospheric source only) is quite different from that adopted here. Our approach invokes a distributed tropospheric source. The resulting profiles for ($NO + NO_2$) in the two models are nonetheless quite similar. In particular, both models indicate concentrations of ($NO + NO_2$) sufficiently low as to imply that OH should be insensitive to NO (see Figures 3 and 24*b*).

Suggestions for in situ sources of nitrogen oxides in the remote troposphere include lightning [*Noxon,* 1976], decomposition of PAN [*Crutzen,* 1979], and oxidation of NH_3 [*McConnell,* 1973]. Estimates for production by lightning range from 4 to 90×10^6 tons N per year [*Tuck,* 1976; *Noxon,* 1978; *Chameides,* 1979; *Dawson,* 1980; *Hill et al.,* 1980], more than enough to supply the required source. The source must be relatively constant with latitude, however, to account for the observed distribution of HNO_3, and the lightning mechanism may fail to satisfy this constraint [*Orville and Spencer,* 1979]. It seems unlikely that peroxyacetyl nitrate or similar compounds should be the precursors for nitrogen oxides observed over the South Pacific, since these species are relatively short lived [*Cox and Roffey,* 1977; *Hendry and Kenley,* 1979; *Winer et al.,* 1977] and are thought to originate on land.

Oxidation of ammonia could contribute in remote areas and might satisfy the need for a distributed source. Oxidation is initiated by reaction with OH [*McConnell,* 1973; *Stuhl,* 1973].

$$OH + NH_3 \rightarrow NH_2 + H_2O \quad (25)$$

The fate of NH_2 is unclear. Recent laboratory studies indicate that NH_2 does not react with O_2, but it may react rapidly with NO, NO_2, and O_3 [*Lesclaux and Demissey,* 1977; *Hancock et al.,* 1977; *Kurasawa and Lesclaux,* 1979, 1980],

$$NH_2 + NO \rightarrow \text{products } (N_2, N_2O) \quad (26)$$

$$NH_2 + NO_2 \rightarrow \text{products } (N_2, N_2O) \quad (27)$$

$$NH_2 + O_3 \rightarrow \text{products (NH, HNO, NO)} \quad (28)$$

Reaction (28) would lead to production of NO and NO_2, while odd nitrogen is removed by (26) and (27). The kinetic data [*Kurasawa and Lesclaux,* 1980] imply that oxidation of ammonia should represent a source for oxides of nitrogen when the concentration of ($NO + NO_2$) is less than about 60 ppt. Oxidation of NH_3 could provide a sink for nitrogen oxides at concentrations of ($NO + NO_2$) above 60 ppt.

There are few observations of NH_3 in the remote troposphere. *Tsunagai* [1971] observed concentrations between 0.1 and 1 ppb in surface air over the Pacific Ocean, and *Georgii and Gravenhorst* [1977] reported similar values for the central Atlantic. J. D. Tjepkema and coworkers (private communication, 1981) found low values in Massachusetts (~0.1 ppb). Concentrations at high southern latitudes are also about 0.1 ppb [*Ayers and Gras,* 1980]. Values between 0.1 and 1 ppb would imply a source of nitrogen oxides from (25) in the range $1\text{–}10 \times 10^6$ tons N yr^{-1}, and would suggest that production from NH_3 could be comparable to or larger than input from the stratosphere.

The higher concentrations of ($NO + NO_2$) observed in the continental boundary layer may be derived from a variety of sources at the ground. Combustion of fossil fuel accounts for emissions of 2×10^7 tons N yr^{-1} of ($NO + NO_2$) [*Soderlund and Svensson,* 1976] and biomass burning might provide additional sources as large as 5×10^7 tons N yr^{-1} [*Crutzen et al.,* 1979]. *Galbally and Roy* [1978] observed fluxes of NO from soils in Australia, which they attributed to chemical reactions of NO_2^- in the soil. They speculated that this mechanism could provide 10^7 tons N yr^{-1}, widely dispersed over land areas. We may note in this context that soil microorganisms (ammonium oxidizers) appear to generate similar quantities of NO and N_2O [*Goreau et al.,* 1980; F. Lipschultz and others, private communication, 1981). Our data indicate that soil microorganisms may account for the emissions observed by *Galbally and Roy* [1978]. The associated source of NO would be similar to the source for N_2O (~10^7 tons N yr^{-1}). Model B (see Appendix 2) attempts to simulate the influence of terrestrial sources with a relatively high mixing ratio for ($NO + NO_2$), 0.1 ppb, at the ground in continental areas. Such sources have only slight influence above 2 km owing to rapid removal of NO_2 and HNO_3 in the boundary layer.

The major uncertainty in our model for tropospheric odd nitrogen derives from inadequate definition of mechanisms and rates for heterogeneous processes that remove soluble and reactive gases from the atmosphere. These processes may affect the distribution of H_2O_2, a key species in the odd hydrogen family. There is evident need for research to quantify rates for heterogeneous reactions.

4. MODEL

Most of the results presented here were obtained by solving time-dependent continuity equations as described in Appendix 2. The chemical model is discussed in section 2; kinetic data and model parameters are summarized in Tables 1 and 4, respectively. Rates for photolytic processes were allowed to vary diurnally with insolation. Calculations were carried out for cloud-free conditions, for full cloud cover, and for insolation intended to simulate the climatological mean distribution of clouds as discussed in Appendix 3. Results showing the diurnal variation of HO_x and odd nitrogen in the absence of clouds are given in Figures 13 and 14 for two altitudes, 0 and 6 km, for latitudes of 15°N and 45°N, for equinoctial conditions. Computations used the standard model summarized in Table 4.

As might be expected, concentrations of OH and HO_2 respond rapidly to insolation, reaching maximum values at

TABLE 4. Standard Model

Chemical Species	Distribution
H_2O	Figure 6
O_3	Figures 7, 8*b*, 8*c*
CO	Figure 11
HNO_3	Figure 12*a*, model A
$NO + NO_2$	Figure 12*b*, model A
CH_4	1.7 ppmv (NH); 1.6 ppmv (SH)
H_2	0.55 ppmv
O_3 column	*Dütsch* [1974]
Model Parameter	**Notes**
Model atmosphere (*T*, *M*)	*U.S. Standard Atmosphere Supplements* [1966]
Kinetic data	Table 1 (without HO_2NO_2 chemistry)
Aerosol loss of H_2O_2	None
Ground albedo	0.1
Aerosol absorption	0.1 at 3100 Å
Vertical diffusion coefficient	1×10^5 cm^{-2} s^{-1}

noon. The concentration of OH drops rapidly near sunset as rates for (2), (7), and (9) become negligible. At night, HO_2 and OH are cycled by (3), (5), and (6) and by the methane oxidation chain. Concentrations of OH and HO_2 decline slowly during the night owing to formation of H_2O_2 (reaction (8)) and CH_3OOH (reaction (18*a*)).

Figure 13 includes values calculated for the diurnally averaged concentration of OH. The mean value for the concentration of OH over the sunlit portion of the day is equal to approximately 0.5 times the value at noon. The diurnal mean value for OH may be estimated, therefore, with adequate accuracy from knowledge of the noontime result if one were to account for the number of hours of sunlight.

The relative abundances of NO and NO_2 are determined primarily by (7), (17), (23), and (24). Nitric oxide is converted to NO_2 by reaction with O_3, HO_2, and CH_3O_2. Abundances of NO and NO_2, as shown in Figures 13 and 14, are comparable during the day, with NO_2 dominant at night. The rate for oxidation of NO by reaction with HO_2 and CH_3O_2 is similar to the rate for oxidation by O_3. One might expect additional oxidation near the ground owing to reaction with RO_2,

$$NO + RO_2 \rightarrow NO_2 + RO \qquad (29)$$

where R denotes an organic radical (R = C_2H_5, CH_3CO, etc.) formed by oxidation of higher hydrocarbons.

The increase in NO_2 immediately after sunrise results from rapid photolysis of NO_3. Measured concentrations of NO_3 in continental air at night are significantly lower than values predicted by photochemical models [*Platt et al.*, 1980; *Noxon et al.*, 1980]. Observations of NO_2 near sunrise might provide clues to help solve this puzzle.

Rates for production and loss of OH are shown as functions of altitude and latitude in Figure 15. Results apply to noon at equinox under cloud-free conditions. As is discussed earlier, cycling of HO_2 to OH is more important at high latitudes and altitudes, and at high concentrations of NO, while direct production of OH from (2) dominates in the tropics (cf. Figures 6, 7, and 12).

Rates for loss of HO_2 and CH_3O_2, averaged over a 24-hour day, are shown in Figure 16. Reaction with HO_2 is an important sink for CH_3O_2, especially in the tropics, and significant concentrations of CH_3OOH are produced. Oxidation of methane provides a net sink for odd hydrogen in the lower troposphere and a net source in the upper troposphere.

Rates for production and loss of odd hydrogen and odd oxygen, averaged over a 24-hour day, are shown in Figure 17. Loss of odd oxygen is most important in the boundary layer below 2 km, while production of odd oxygen is distributed throughout the troposphere. As discussed earlier, the balance between photochemical sources and sinks for O_3 is regulated by NO. In situ chemistry (i.e., the net balance of local sources and sinks) provides net global production for O_3 of magnitude 8×10^{10} molecules cm^{-2} s^{-1}. Rates for production and loss of odd oxygen are nearly equal in the northern hemisphere, both at mid-latitudes and in the tropics, as shown in Table 5. Photochemical production exceeds loss by about 40% in the southern hemisphere, a result of the lower concentrations assumed for ozone in the south (see Figures 7 and 8). Photochemical sources and sinks of odd oxygen would balance if NO concentrations in Figure 12 were reduced by about 30% for the southern hemisphere or if southern hemispheric ozone were assumed to be similar to that in the north. Net production of ozone is much larger in model B than in model A, a reflection of the higher concentrations of NO in the boundary layer of model B. If relatively high values for $NO + NO_2$ (>100 ppt) were in fact typical of the continental boundary layer, in situ photochemistry could dominate the tropospheric ozone budget at latitudes with large land areas, such as northern mid-latitudes [cf. *Fishman and Seiler*, 1980]. The net chemical source of ozone in the troposphere (8×10^{10} molecules cm^{-2} s^{-1}) is comparable to the flux of ozone from the stratosphere [*Danielson and Mohnen*, 1977; *Fabian and Pruchniewicz*, 1977; *Mahlman et al.*, 1980; *Gidel and Shapiro*, 1980]. If NO concentrations were 10 times lower than values assumed in the standard model, ozone would be consumed by photochemistry in the troposphere at a rate in excess (>4 times) of supply from the stratosphere.

The lifetime for odd hydrogen is about 2 days near the ground, increasing to ~8 days in the upper troposphere. Heterogeneous loss of H_2O_2 (reaction (11)) and reaction of OH with H_2O_2 (reaction (10)) provide the major sinks for odd H. Reaction (10) dominates loss of odd H in the upper troposphere and also in the lower tropical troposphere, while (11) dominates in the lower troposphere at mid-latitudes. The rate for gas phase removal of odd H exceeds the rate for heterogeneous removal over most of the troposphere. The OH distribution is consequently insensitive to the rate assumed for heterogeneous loss (see also Figure 24*c*).

Meridional cross sections for OH, HO_2, H_2O_2, CH_3O_2, CH_3OOH, and CH_2O are given for summer and winter in Figures 18–23. These contours are appropriate for cloud-free conditions at noon. Calculated concentrations of CH_2O are in good agreement with recent measurements of formaldehyde in clean air [*Platt et al.*, 1979; *Platt and Perner*, 1980; *Zafiriou et al.*, 1980; *Lowe et al.*, 1980; *Neitzert and Seiler*, 1981]. It is probable that concentrations of CH_3OOH, H_2O_2, and CH_2O may be quite variable in the planetary boundary layer where heterogeneous reactions provide important paths for removal. Earlier studies suggested that OH should be lower on average in the northern hemisphere than in the southern hemisphere, due to the higher levels of CO in the north [*Wofsy*, 1976; *Sze*, 1977]. In the present model, however, ozone concentrations are taken to be larger in the northern hemisphere than in the south. This asymmetry leads to enhanced production of HO_x in the north offsetting effects of elevated CO. Thus OH is (some-

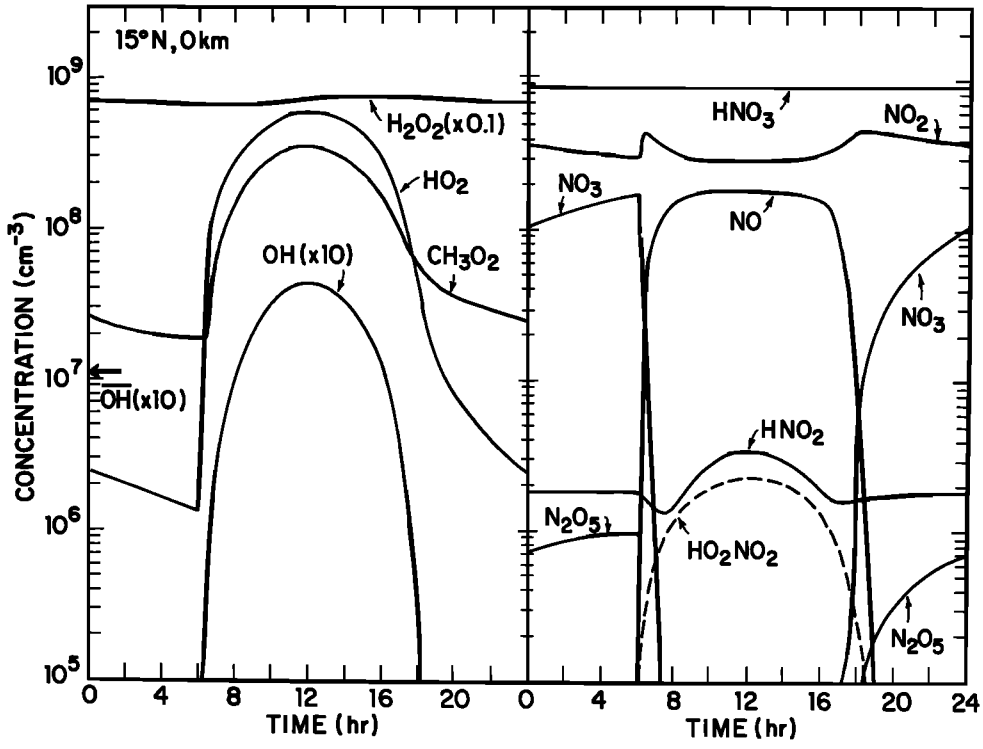

Fig. 13*a*

Fig. 13. Diurnal variations of HO_x and nitrogen oxides in the tropics and at mid-latitudes. Results are given for cloud-free equinoctial conditions at the surface and at 6 km. The solid lines are derived from the standard model described in Table 4, which does not include the chemistry of peroxynitric acid. The diurnally averaged concentration of OH is indicated by the arrow.

what fortuitously) nearly symmetric about the equator [*Fishman and Crutzen*, 1978] while concentrations of HO_2 and H_2O_2 are larger in the north than in the south.

Sensitivity of OH to various parameters of the model is shown in Figure 24. The concentration of OH could vary significantly in response to H_2O. Curve A of Figure 24*a* was obtained with a profile for H_2O measured at Trinidad, (3/25/65 in Figure 5). A distribution of OH with altitude similar to that

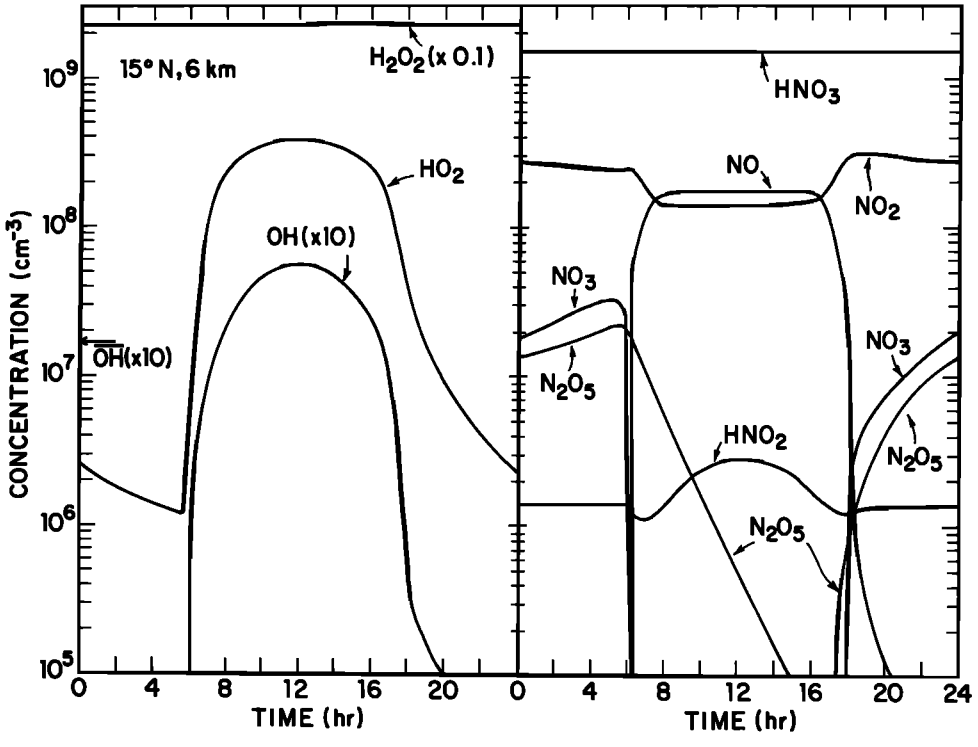

Fig. 13*b*

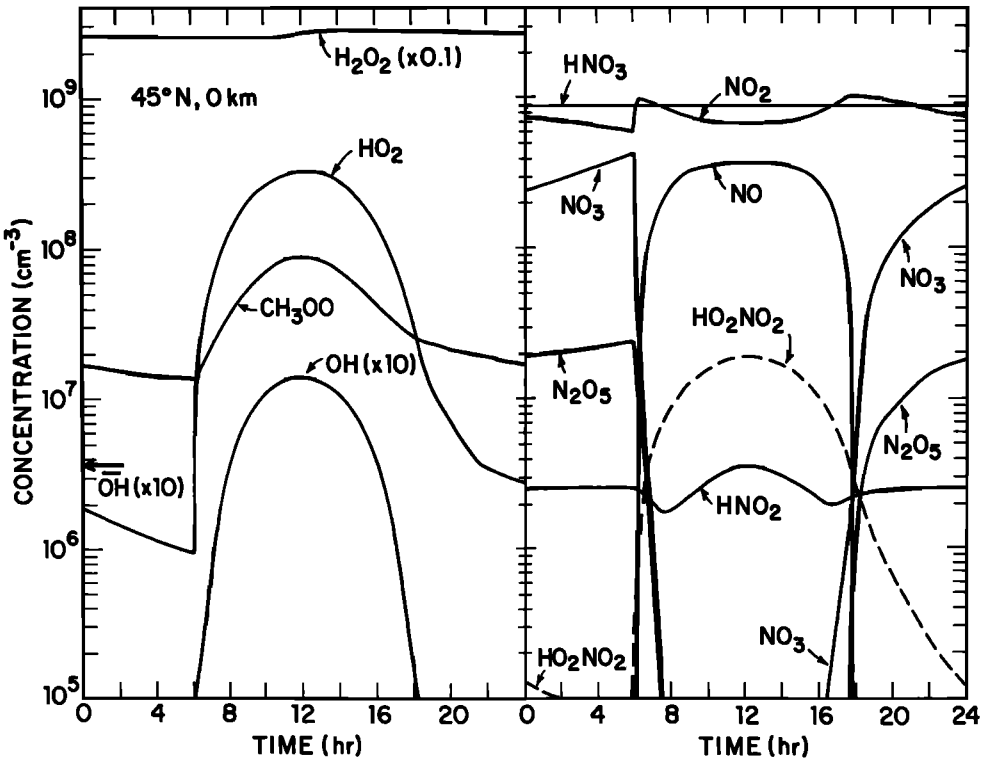

Fig. 13*c*

exhibited by curve A has been reported by *Davis et al.* [1978]. Curve B (the standard model) exhibits a slight maximum at about 2 km reflecting the local maximum in ozone (see Figure 7).

The dependence of OH on NO is illustrated in Figure 24*b*. Curve A was obtained with the standard model for (NO + NO_2). Curves B and C adopt 3 times and 1/3 as much (NO + NO_2), respectively. The range of results shown in Figure 24*b* emphasizes the need for better measurements of global distributions for NO and NO_2.

Figure 24*c* shows profiles for OH obtained with a variety of models for heterogeneous loss of H_2O_2. Model A neglects heterogeneous processes in their entirety, while model B allows for rainout (wet removal) of H_2O_2. Model C shows the effect

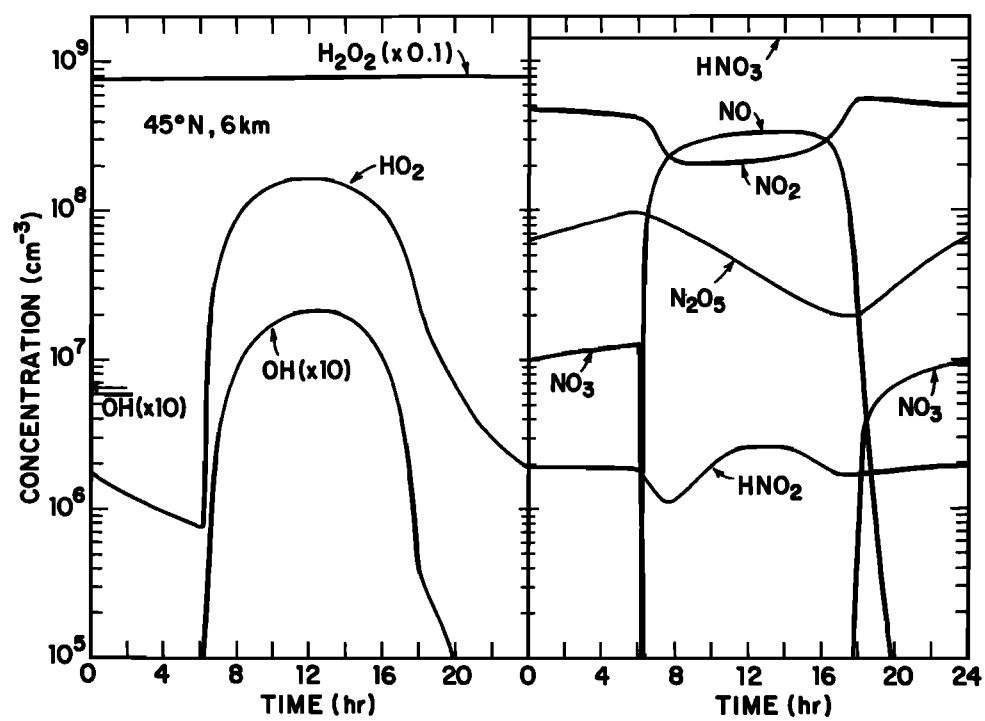

Fig. 13*d*

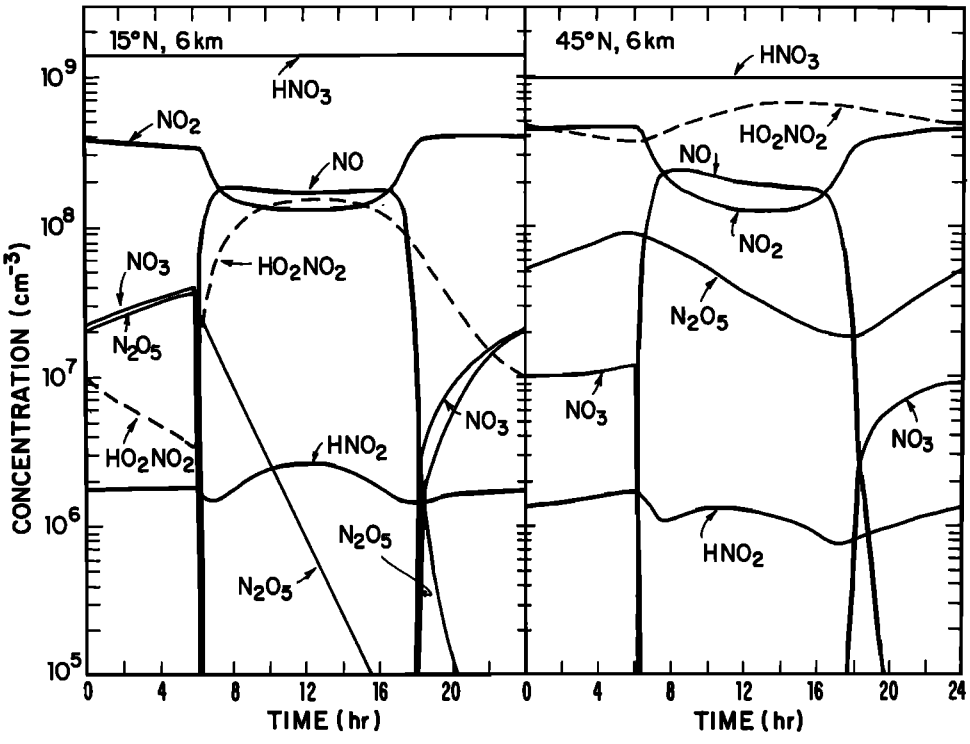

Fig. 14. Diurnal variations of nitrogen oxides at 6 km in the tropics and at mid-latitudes. Results are given for cloud-free, equinoctial conditions. The calculations use the standard model of Table 4 and, in addition, include the chemistry of HO_2NO_2. The concentration of HO_2NO_2 at the ground is shown by the dashed line in Figure 13. Concentrations of other species at the ground are changed by less than 10% by the inclusion of HO_2NO_2 chemistry in the model.

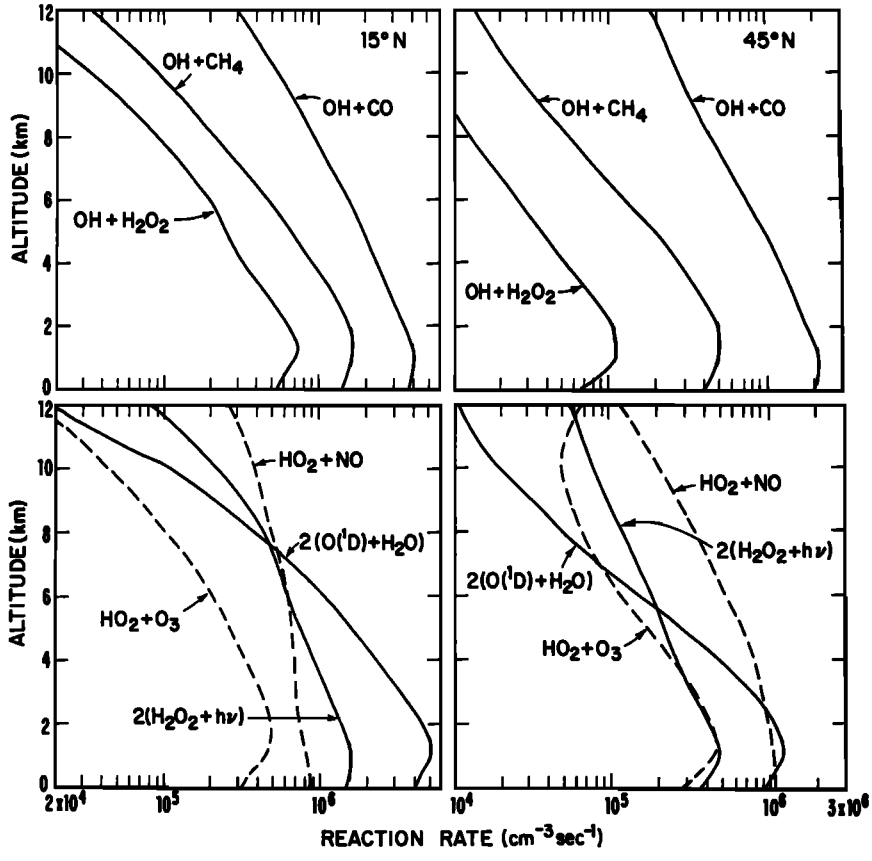

Fig. 15. Noontime rates for production and loss of OH (bottom and top panels, respectively). Results are given for cloud-free, equinoctial conditions and calculated for the standard model described in Table 4.

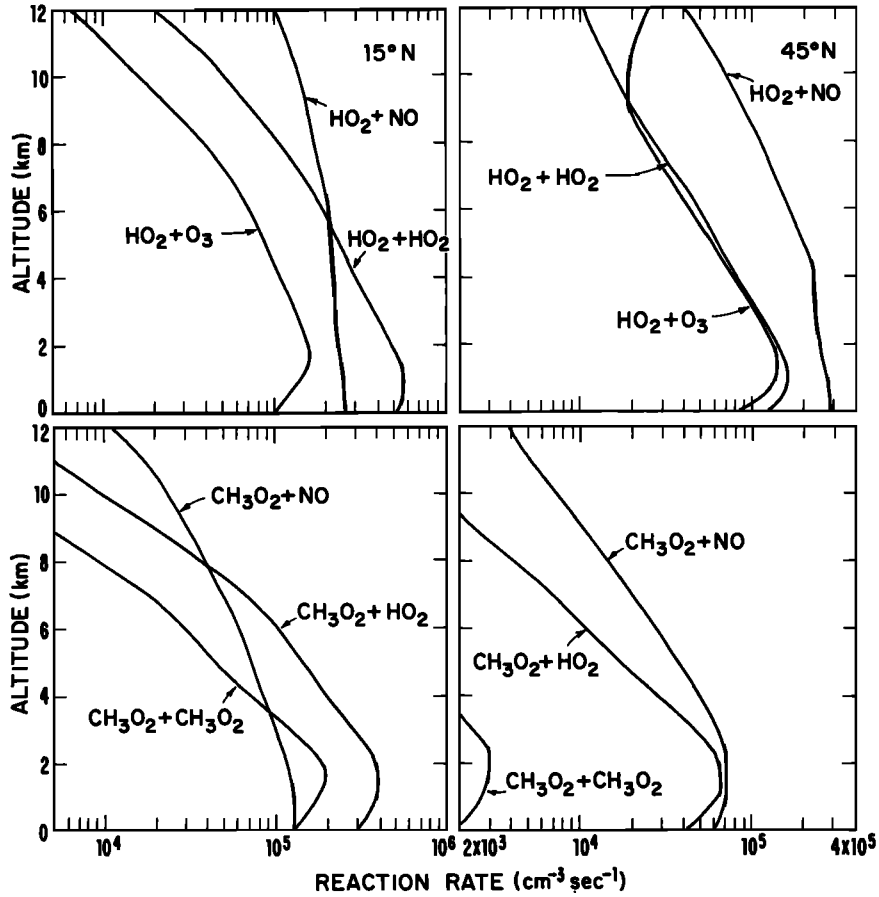

Fig. 16. Diurnally averaged rates for loss of HO_2 and RO_2. Results are given for cloud-free, equinoctial conditions and are calculated for the standard model described in Table 4.

of efficient removal of H_2O_2 by aerosols. Model C1 assumes a probability of 8×10^{-4} for H_2O_2 to stick on the surface of an aerosol, a value observed by *Baldwin and Golden* [1979] for attachment of H_2O_2 to a surface of sulfuric acid. Model C2 adopts a much larger probability for attachment, 3×10^{-2}, based on the sticking probability observed for attachment of water vapor to a water droplet [*Chodes et al.*, 1974]. Models C1 and C2 assumed rapid destruction of H_2O_2 after incorporation in the aerosol, which implies lifetimes for H_2O_2 in the particulate phase of less than 10 and 0.3 s, respectively. Evidently, the OH profiles of models A and C1 differ insignificantly from those of model B in which aerosol processes were excluded. The assumptions of model C2 result in reduction of calculated concentrations for OH by 20% near the ground, by 40% in the upper troposphere. As discussed in Appendix 1, it is unlikely that aerosol processes could destroy H_2O_2 in the clean troposphere as rapidly as assumed in model C2. This conclusion is based on consideration of the physical and chemical properties of atmospheric aerosols and aqueous H_2O_2.

The concentration of OH should respond to changes in the intensity of ultraviolet radiation, influenced by the presence of clouds and aerosols, as shown in Figure 24*d*. Effects of clouds and aerosols on the radiation field are discussed in detail in Appendix 3. On average, absorption of radiation by aerosols leads to significant reduction in OH, while aerosol scattering has relatively little effect. The concentration of OH would decrease by about 20% at the ground if we assumed absorption by aerosols corresponding to a mean optical depth of 0.1 (see Appendix 3). Incorporation of clouds in the model further reduces OH by about 20% at the ground while producing a small increase above the clouds.

5. Budgets

We turn our attention now to consideration of sources and sinks for CH_3CCl_3 and CO. According to present understanding, the source of atmospheric CH_3CCl_3 may be attributed primarily to industrial activity, specifically the widespread and growing use of CH_3CCl_3 as a solvent. The magnitude of the release rate has been estimated by *Neely and Plonka* [1978], and we expect that about 95% of the release occurs in the northern hemisphere. The gas is removed by reaction with OH,

$$OH + CH_3CCl_3 \rightarrow H_2O + CH_2CCl_3 \qquad (30)$$

Recent laboratory studies by *Kurylo et al.* [1979] and *Jeong and Kaufman* [1979] appear to resolve earlier discrepancies in our knowledge of the rate constant for (30). Therefore, measurement of the concentration of CH_3CCl_3 may be used to check the accuracy of models for OH.

We shall argue that the concentration of OH may be estimated within a factor of 2 for mean conditions in the tropical troposphere. The discussion that follows explores implications of this analysis for attempts to quantify the budget of CO. As we shall see, estimates for the rate at which CO is removed from the atmosphere by reaction with OH may be used to place valuable constraints on the magnitude of several possible sources for CO.

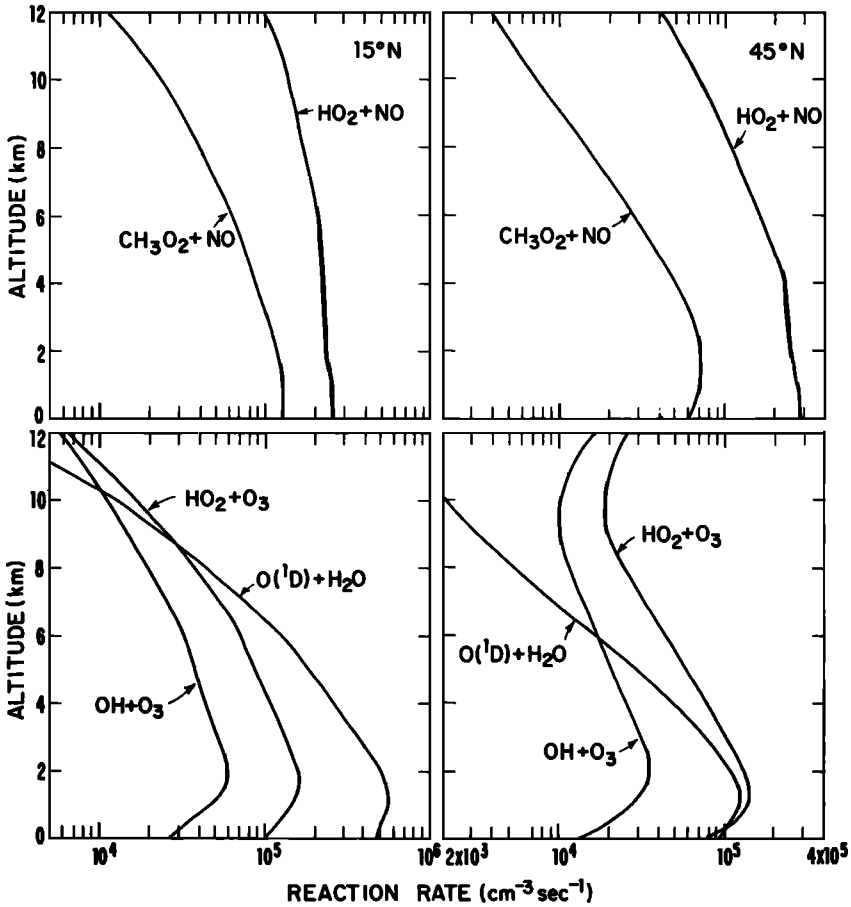

Fig. 17*a*. Diurnally averaged rates for production and loss of odd oxygen (top and bottom panels, respectively).

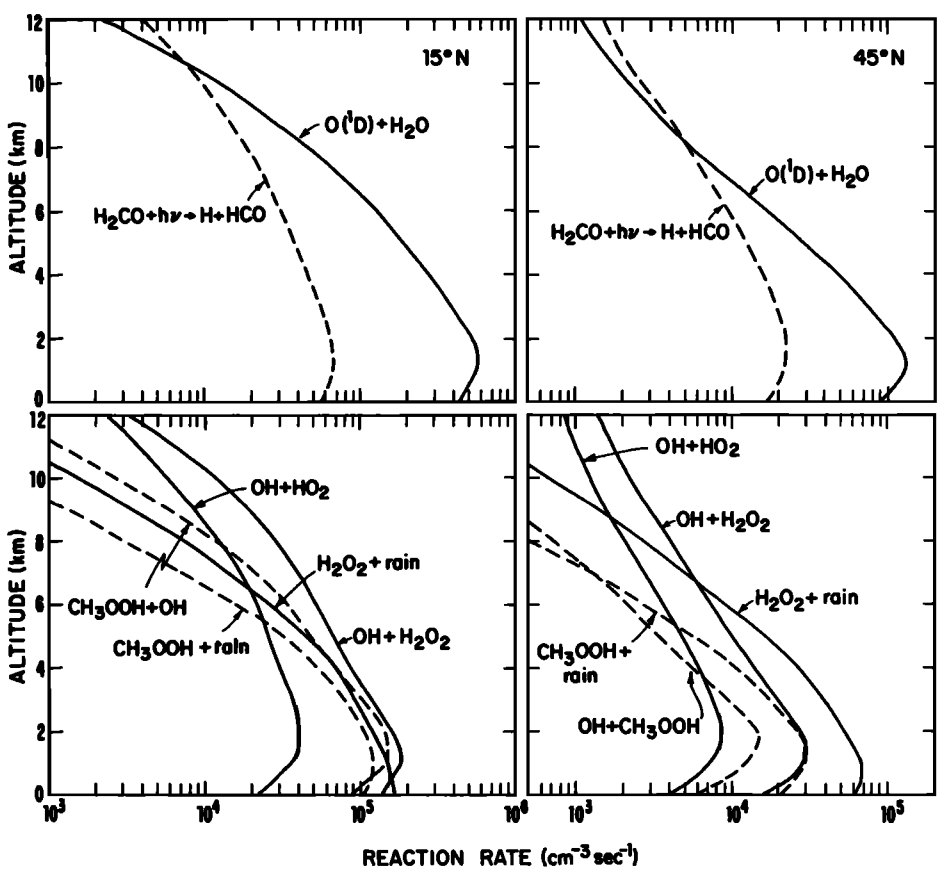

Fig. 17*b*. Diurnally averaged rates for production and loss of odd hydrogen. Results are given for cloud-free, equinoctial conditions and are calculated for the standard model described in Table 4. The net effect of each methane oxidation pathway on odd-H is given in Table 2.

TABLE 5. Photochemical Production and Loss of Odd-Oxygen

Model A	45°N	15°N	15°S	45°S	Mean
Production (odd-O)[a]	2.1	3.5	3.4	2.1	2.8
Loss (odd-O)[b]	1.9	3.4	2.4	1.3	2.2
(Production-Loss)	0.19	0.11	1.0	0.86	0.54
Model B					
Production (odd-O)	2.6	4.8	4.7	2.7	3.7
Loss (odd-O)	1.9	3.4	2.5	1.3	2.3
(Production-Loss)	0.70	1.3	2.2	1.4	1.4
Global Model[c]					
Production (odd-O)	2.3	3.9	3.7	2.2	3.0
Loss (odd-O)	1.9	3.4	2.4	1.3	2.2
(Production-Loss)	0.45	0.46	1.3	0.94	0.78

Odd oxygen is defined as (O_3 + $O(^3P)$ + $O(^1D)$ + NO_2). Rates are given in units of 10^{11} molecules cm^{-2} s^{-1}. The profiles for (NO + NO_2) for models A and B are given in Figure 12*b*. The calculations assumed global mean cloud cover, and the results have been seasonally averaged.

[a] The major sources for odd-O are reactions (7) and (17).

[b] The major sinks for odd odd-O are reactions (2), (6), and OH + O_3.

[c] The global model represents an average of models A and B weighted by the areas of the oceans and continents, respectively.

Concentrations of CH_3CCl_3 were obtained as functions of time and latitude by using a simple parameterized model for transport. The troposphere was divided into four latitude zones of equal area with boundaries at 30°N, 0°, and 30°S. Mixing ratios of CH_3CCl_3 were assumed uniform in each zone. Rates for exchange between zones were obtained by application of the model to data for CF_2Cl_2 and $CFCl_3$. Parameters of the exchange model are given in Table 6. Results for CF_2Cl_2, $CFCl_3$, and CH_3CCl_3 are shown in Figures 25 and 26.

Concentrations of OH were calculated as functions of altitude and time as described earlier (see Table 4 and Appendix 2). Each latitude zone was subdivided into land and ocean compartments, and it was assumed that concentrations of (NO + NO_2) over oceans and continents were given by curves A and B of Figure 12*b*, respectively. Concentrations of OH were obtained for each latitude zone by suitably averaging land and ocean areas. Calculations were performed for climatological mean cloud cover as discussed in Appendix 3. Results in Figure 27*b* reflect an average over diurnal, seasonal, and cloud-related changes in insolation.

The model predicts concentrations for CH_3CCl_3 in reasonable accord with observation, as shown in Figure 26. There

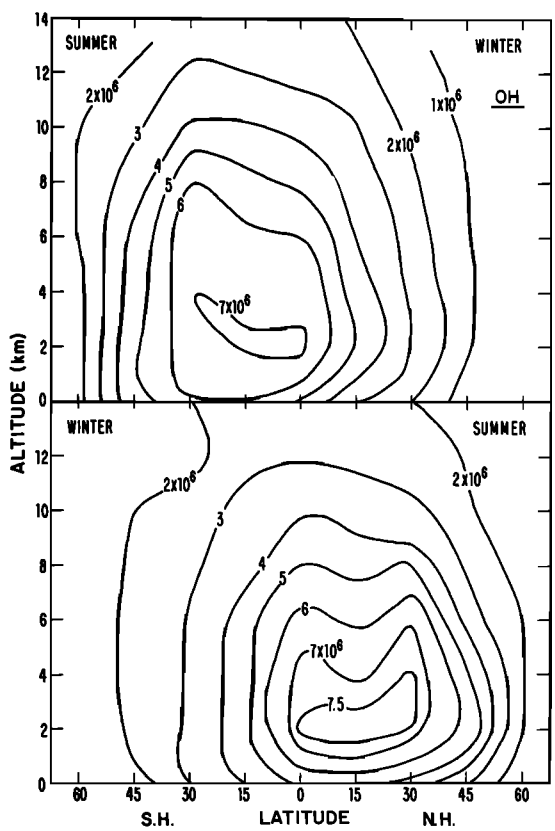

Fig. 18. Concentration of OH at noon as a function of latitude, altitude, and season. Results are given for cloud-free conditions and are calculated for the standard model of Table 4.

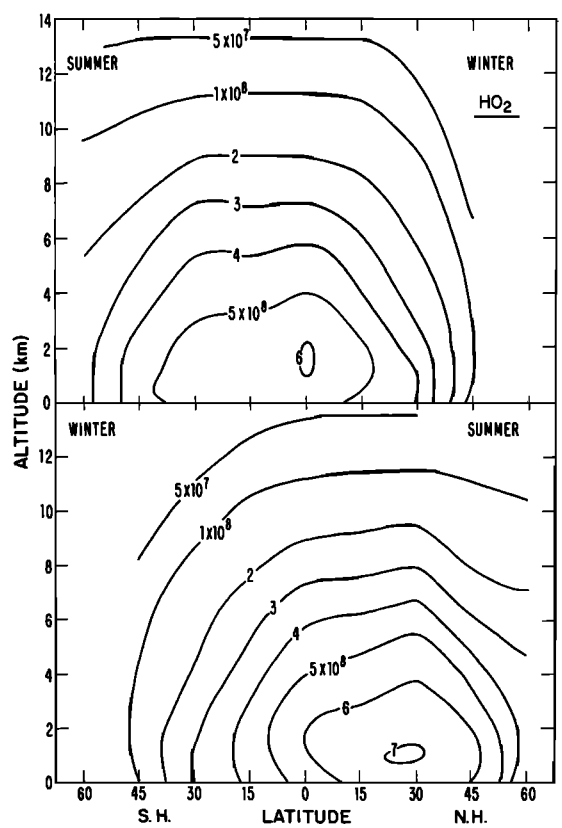

Fig. 19. Concentration of HO_2 at noon as a function of latitude, altitude, and season. Results are given for cloud-free conditions and are calculated for the standard model of Table 4.

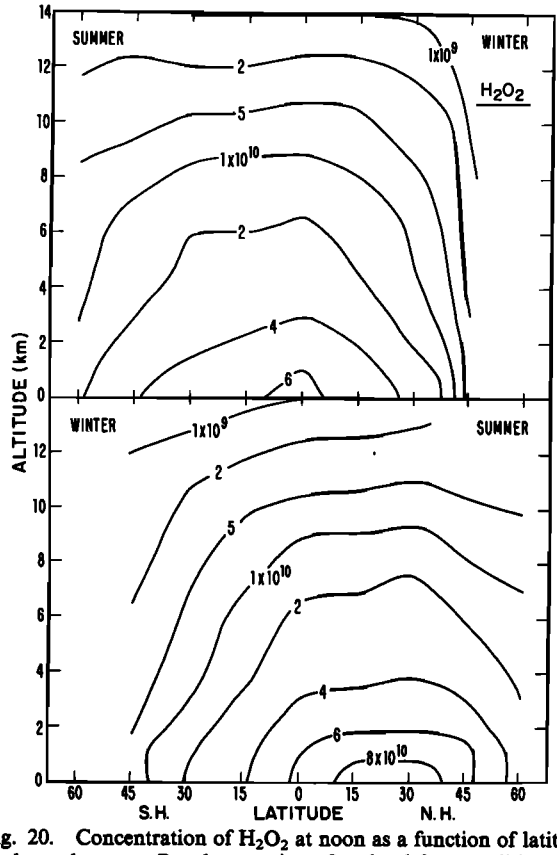

Fig. 20. Concentration of H_2O_2 at noon as a function of latitude, altitude, and season. Results are given for cloud-free conditions and are calculated for the standard model of Table 4.

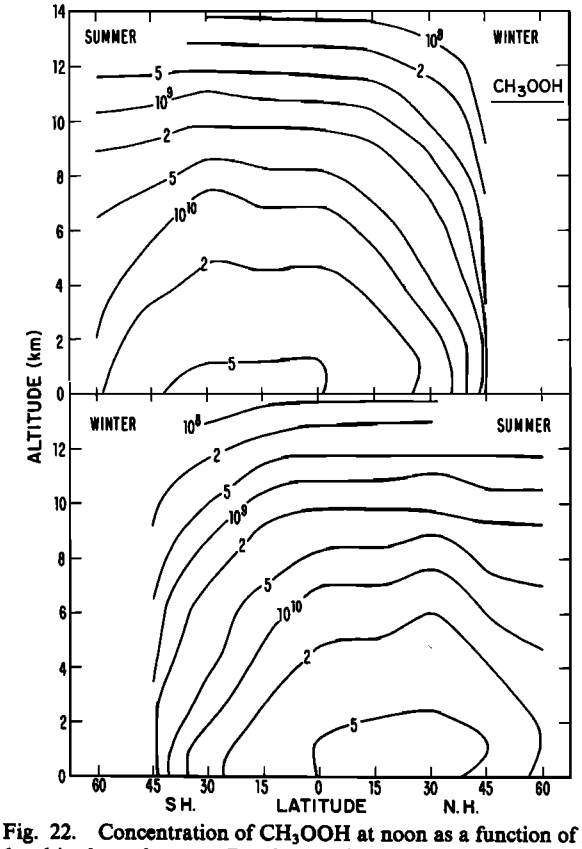

Fig. 22. Concentration of CH_3OOH at noon as a function of latitude, altitude, and season. Results are given for cloud-free conditions and are calculated for the standard model of Table 4.

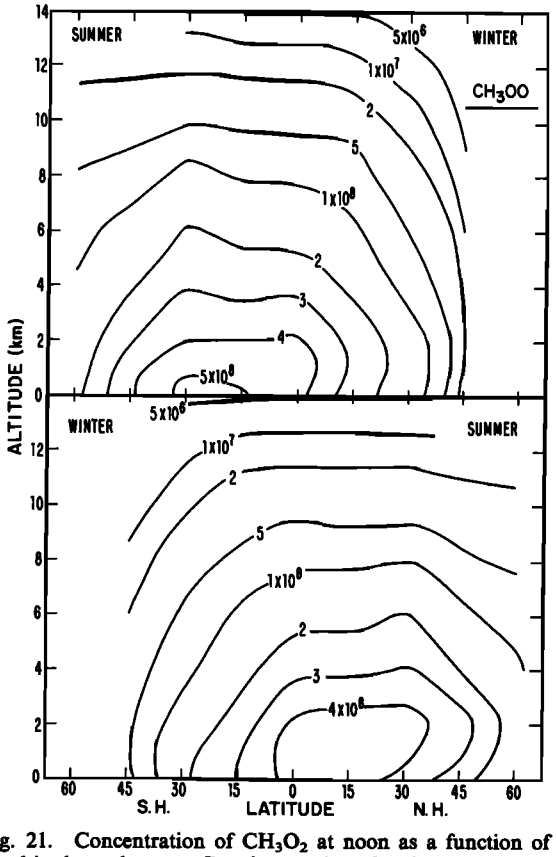

Fig. 21. Concentration of CH_3O_2 at noon as a function of latitude, altitude, and season. Results are given for cloud-free conditions and are calculated for the standard model of Table 4.

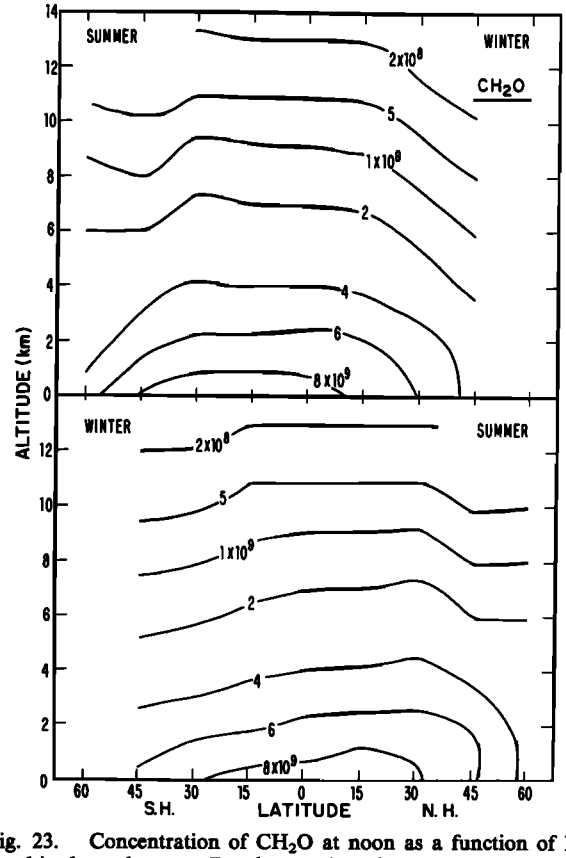

Fig. 23. Concentration of CH_2O at noon as a function of latitude, altitude, and season. Results are given for cloud-free conditions and are calculated for the standard model of Table 4.

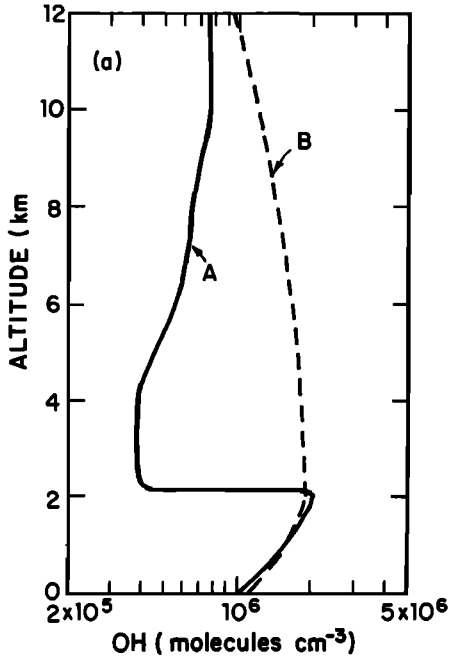

Fig. 24a. Altitude profiles for diurnally averaged OH. Results are given for cloud-free, equinoctial conditions. Model parameters are those for the standard model described in Table 4, unless otherwise specified. Curve A: The water vapor profile is taken from Figure 5 (Trinidad, March 25, 1965). Curve B: Standard water vapor profile for spring, 15°N.

are systematic discrepancies, however. We show, for comparison, concentrations of CH_3CCl_3 that would apply in the limit of an infinite tropospheric lifetime and also results that would obtain if concentrations of OH were increased or decreased by a factor of 2. Evidently, concentrations of OH lower than values of the standard model would provide a better fit to the recent observational data.

Results shown in Figure 26 must be interpreted with caution. The accuracy of the observational data is uncertain owing to difficulties in calibration and sampling. The magnitude of the calibration problem may be gauged from a comparison of measurements by *Lovelock* [1977] and *Rasmussen et al.* [1981] or from results of the laboratory intercalibration exercise conducted by Rasmussen [*Rasmussen*, 1978; *NASA*, 1979]. Concentrations measured by Rasmussen are higher than values measured by Lovelock by about 20%. Discrepancies of similar magnitude were observed during an intercalibration exercise involving several laboratories. Further, samples from the North American continent or Europe could be influenced by proximity to sources. It is possible, therefore, that hemispheric mean values for CH_3CCl_3 may be somewhat lower than implied by the data in Figure 26.

The model results rely on release rates for CH_3CCl_3 provided by *Neely and Plonka* [1978], and it is difficult to ascertain the accuracy of these data. The quality of the data base differs from that for CF_2Cl_2 and $CFCl_3$. The study of chlorofluorocarbons was based on a survey of manufacturers and included estimates for sources in Eastern Bloc countries

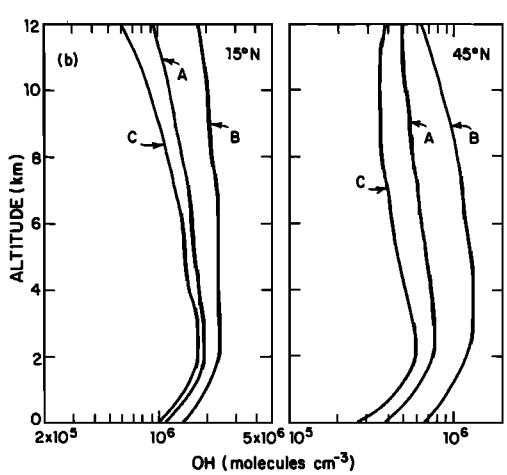

Fig. 24b. Same as Figure 24a except curve A: The (NO + NO_2) profile is taken from model A, Figure 12. Curve B: The (NO + NO_2) concentrations of model A are multiplied by a factor of 3. Curve C: The (NO + NO_2) concentrations of model A are decreased by a factor of 3.

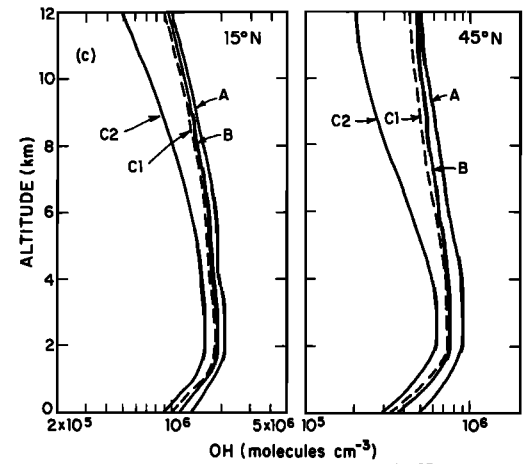

Fig. 24c. Same as Figure 24a except curve A: Heterogeneous loss of H_2O_2 is omitted. Curve B: Rainout of H_2O_2 is included (see Table 1). The rainout rate corresponds to an effective tropospheric lifetime of about 10 days. Curve C1: Aerosol loss of H_2O_2 is included, using the parameterization given in Table 1. A sticking probability of 8×10^{-4} for H_2O_2 on the surface of an aerosol is adopted. Curve C2: Same as Curve C1, with a sticking probability of 3×10^{-2}.

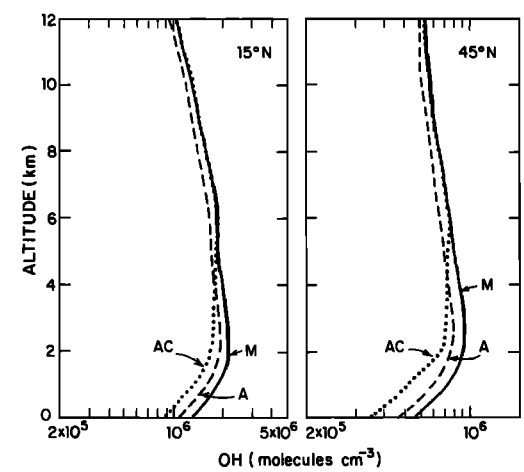

Fig. 24d. Altitude profiles for diurnally averaged OH. Results are shown for cloud-free conditions with molecular scattering only (M), for cloud-free conditions with aerosol absorption (A) and molecular scattering, and for global mean cloud cover with aerosol absorption and molecular scattering (AC). The aerosol absorption (0.1) and altitude distribution are given in Tables 1 and 4 and the cloud model is described in Table A2. Results are shown for equinoctial conditions. Calculations used the standard model of Table 4 with the exception of the parameters given above.

[*McCarthy et al.*, 1977]. The tabulation for CH_3CCl_3 uses estimates for western sales outside of the United States in the absence of specific data from individual manufacturers. It does not account for use in Eastern Bloc countries (H. Farber, Dow Chemical, private communication, 1981). An underestimate in release rates by as little as 25% would bring the standard model into good agreement with some of the recent observations. The uncertainty in release data would appear to allow this possibility.

Difficulties associated with the use of atmospheric measurements to verify or adjust models are illustrated also by Figure 25. The data for $CFCl_3$ indicate a relatively abrupt rise in the concentration of this gas in the southern hemisphere over a period of about a year in 1976. The magnitude of the rise would imply a hemispheric source of magnitude 4×10^5 tons yr^{-1}, which may be compared with estimates for global production of 3.2×10^5 tons yr^{-1} [*Bauer*, 1979]. It is possible that the discrepancies in Figure 25 could be explained if one were to invoke a relatively abrupt increase in the rate for interhemispheric exchange, with exchange assumed to be quite slow before 1976. It seems more likely, however, that problems in Figure 25, and some of the difficulties in Figure 26, reflect sampling errors and the absence of continuous and consistent calibration.

Exchange rates in Table 6 were obtained from a comparison of the model with observations for CF_2Cl_2 and $CFCl_3$ made subsequent to 1976. The model provides a good fit to interhemispheric gradients derived from upper tropospheric measurements by *Goldan et al.* [1980] and surface measurements by *Singh et al.* [1979] and by *Rowland et al.* [1980] as shown in Figure 28. The north/south gradient for CH_3CCl_3 depends on concentrations of OH as well as on parameters describing exchange. There is sufficient scatter in the observations to preclude accurate experimental definition of the gradient. The data in Figure 28 (lower panel) are of limited use therefore as a test of the model for OH.

The model indicates that methylchloroform is removed from the atmosphere mainly in the tropical troposphere, a point illustrated in Figure 29. Thus, model results in Figure 26 are particularly sensitive to values of OH in the tropics, a region that accounts for approximately 70% of the global sink. Approximately 50% of the global sink occurs over the tropical ocean, and it is important to emphasize the lack of observational data in this regime for trace gases such as H_2O, O_3, and NO.

Table 7 gives estimates for the effect of uncertainties in concentrations of CO, O_3, H_2O, and NO, on globally averaged rates for removal of CH_3CCl_3. Concentrations of NO in the standard model are sufficiently low that reaction(7), which cycles odd hydrogen, is of minor importance in the tropics (see Figure 15.).The rate for removal of CH_3CCl_3 is insensitive consequently to a decrease in NO. A uniform increase in NO would lead to significant increase in OH (cf. Figures 3 and 24*b*) with obvious effects for CH_3CCl_3. However, an increase in NO in the continental boundary layer (model B) has only a modest effect on the average rate for removal of CH_3CCl_3.

Assumption of an efficient aerosol loss process for H_2O_2 could reduce the removal rate for CH_3CCl_3 by as much as 20% and would improve agreement between model and observa-

TABLE 6. Exchange Parameters for Troposphere Box Model

Latitude Box	Mass, 10^{20} gm	Mass Exchange[a] Rate(10^{20} gm yr^{-1})	Mass Exchange[a,b] to Stratosphere (10^{20} gm yr^{-1})
90°–30°N	10.6	80	0
30°N–0°	12.1	20	V
0°–30°S	12.1	80	V
30°–90°S	10.6		0

[a] Mass flux of tracer = mass exchange rate × mass mixing ratio.
[b] Return of tracer from the stratosphere is neglected. For CH_3CCl_3, $V = 0.56$; $CFCl_3$, $V = 0.39$; CF_2Cl_2, $V = 0.19$. Fluxes of these compounds to the stratosphere were determined by application of a one-dimensional stratospheric model [see *Logan et al.*, 1978].

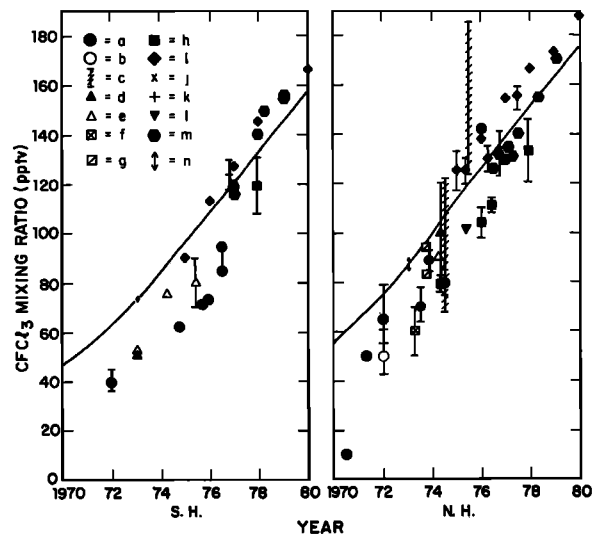

Fig. 25*a*

Fig 25. Measurements of $CFCl_3$ and CF_2Cl_2 in the northern and southern hemispheres as a function of time. Each symbol represents data from a different group of investigators—a: (30°–90°); b: (0–30°), c: *Lovelock* [1971, 1972, 1974], *Lovelock et al.* [1973], *Pack et al.* [1977], *NASA* [1979]; d: (30°–90°); e: (0–30°) *Wilkness et al.* [1973, 1975*a*, *b*, 1978]; f: *Zafonte et al.* [1975], *Hester et al.* [1975]; g: *Heidt et al.* [1975]; h: *Singh et al.* [1977*a b*, 1979]; i: *Grimsrud and Rasmussen* [1975], *Robinson et al.* [1976], *Cronn et al.* [1977], *Pierotti et al.* [1978], *Rasmussen et al.* [1981]; j: *Fraser and Pearman* [1978]; k: *Tyson et al.* [1978]; l: *Krey et al.* [1977]; m: *Goldan et al.* [1980]. The solid lines show results of the model calculations, which used the mass exchange parameters given in Table 6 and the $CFCl_3$ and CF_2Cl_2 release rates given by *Bauer* [1979]. We assumed that 90% of the release takes place in the northern hemisphere. Model results are mean hemispheric values. The arrows (n) show the range of concentrations from the model for mid-latitudes and the tropics.

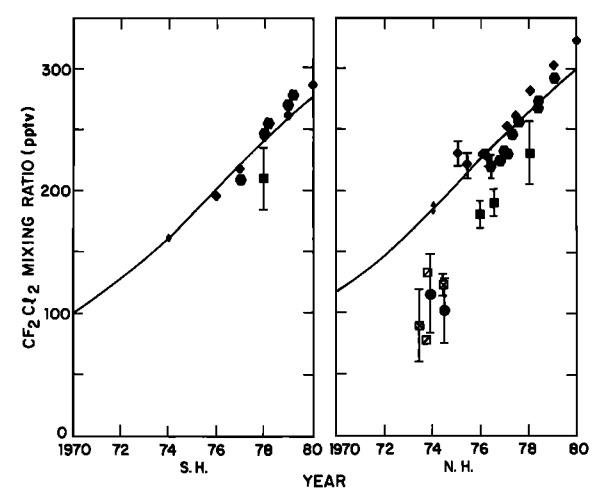

Fig. 25*b*

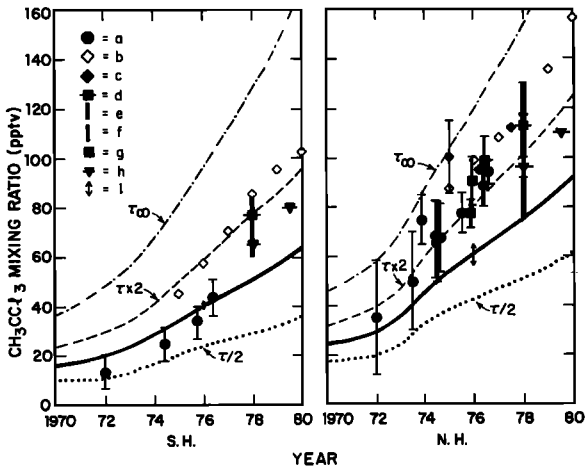

Fig. 26. Measurements of CH_3CCl_3 in the northern and southern hemispheres as a function of time. Each symbol represents data from a different group of investigators—a: *Lovelock* [1974, 1977]; b: *Rasmussen et al.* [1981]; c: *Grimsrud and Rasmussen* [1975], *Cronn et al.* [1977], *Pierotti et al.* [1978]; d: (hemispheric mean); e: (range, 0–30°); f: (range, 30°–60°), *Singh et al.* [1979]; g: *Singh et al.* [1977*a*, *b*]; h: (1978, mid-latitude mean; 1979, hemispheric mean) *Rowland et al.* [1980]. Model calculations used the mass exchange parameters given in Table 6 and the release rate for CH_3CCl_3 given by *Neely and Plonka* [1978]. We assumed that 95% of the release takes place in the northern hemisphere. Model results are mean hemispheric values. The arrows (i) show the range of concentrations from the model for mid-latitudes and the tropics. The solid lines give the results of the standard model (OH profiles from Figure 27*b*). In each latitude zone a mean OH profile is derived from marine and continental profiles, weighted by the appropriate area in each zone. The dashed curves show results in which OH concentrations from the standard model are multiplied by 0.5 while the dotted curves are for OH concentrations multiplied by 2. The dot-dash curves show results for an infinite tropospheric lifetime for CH_3CCl_3 (OH concentration = 0).

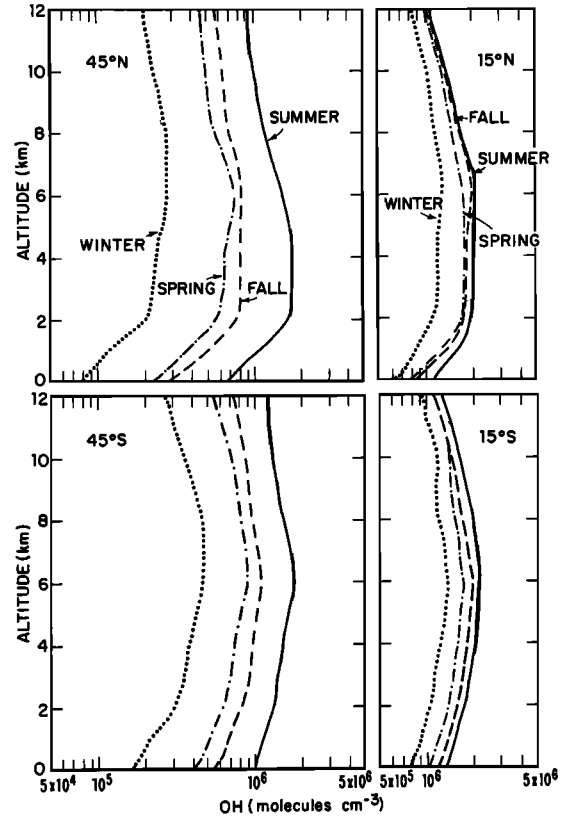

Fig. 27*a*. Altitude profiles for diurnally averaged OH as a function of latitude and season. Results are given for global mean cloud cover (see Table 6) and for the standard model of Table 4. These calculations adopt the NO_x concentrations of model A, Figure 12 (assumed to be representative of marine air).

tions. It is difficult, however, as is discussed in Appendix 1, to envision a mechanism by which aerosols would efficiently destroy peroxide in the remote troposphere.

The standard model omitted possible removal of OH by hydrocarbons other than CH_4. Omission of reactions with saturated hydrocarbons such as C_2H_6 is probably justified owing to the low concentration of these gases in the atmosphere. The mixing ratio for C_2H_6 is about 1 ppb [*Robinson*, 1978; *Singh et al.*, 1979; *Cronn and Robinson*, 1979]. Although the rate constant for OH + C_2H_6 is larger than that for OH + CH_4 by about a factor of 30 [*Atkinson et al.*, 1979], the difference in rate constants is not sufficiently large to offset the difference in concentrations. Similar arguments may be used to exclude the possibility of significant OH loss by reaction with other alkanes and with acetylene [*Robinson*, 1978; *Cronn and Robinson*, 1979; *Atkinson et al.*, 1979; *Chameides and Cicerone*, 1978]. Removal of OH by C_2H_4 in the boundary layer could be comparable to removal by CH_4 if the mixing ratio for C_2H_4 were about 1 ppb [*Atkinson et al.*, 1979]. Preliminary observational data for C_2H_4 in clean air suggest that concentrations are generally lower than 0.5 ppb [*Rudolph et al.*, 1979; *Rasmussen and Khalil*, 1980].

Limited data are available for isoprene and terpenes. Isoprene is a major component of the volatile emissions of many species of land plants, and concentrations as high as 2 ppb have been observed in forests [*Sanadze*, 1963; *Rasmussen*, 1970; *Robinson*, 1978]. Concentrations of terpenes appear to lie in the range 10 ppt to 1 ppb [*Holdren et al.*, 1979]. This suggests that reaction with unsaturated hydrocarbons could be important for OH, at least under some conditions. Isoprene could be removed also by reaction with O_3, although laboratory data are lacking. Studies of analogous reactions involving butenes, pentenes [*Japar et al.*, 1974] and terpenes [*Ripperton et al.*, 1972; *Grimsrud et al.*, 1975] indicate that the relevant rate constant could be as large as 5×10^{-16} cm^3 s^{-1}. Rates for removal of isoprene by O_3 and OH would be comparable if

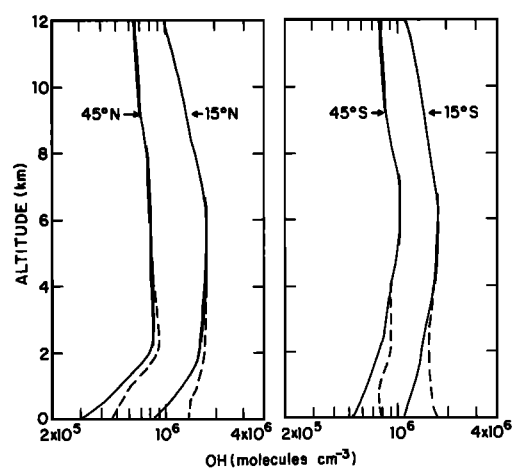

Fig. 27*b*. Altitude profiles for OH averaged over an annual cycle. Annual averages of the seasonal profiles of Figure 27*a* are shown by the solid lines. Annual averages of seasonal OH profiles based on model B of Figure 12 are shown by the dashed lines. (Model B includes higher concentrations for (NO + NO_2) near the surface than does Model A and is assumed to be representative of continental air.)

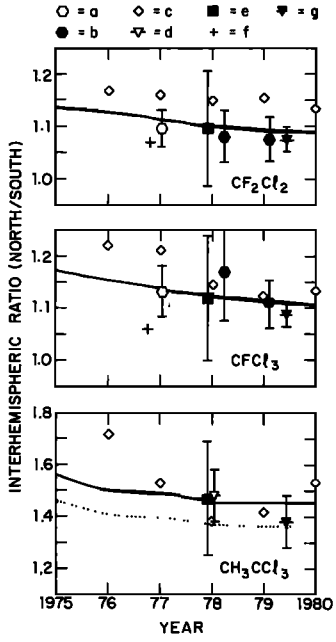

Fig. 28. Ratio of the concentrations in the northern hemisphere to those in the southern hemisphere to those in the southern hemisphere for CF_2Cl_2, $CFCl_3$, and CH_3Cl_3. The symbols are a: 41°N/5°S; b: 41°N/(5°S+78°S), upper troposphere, *Goldan et al.* [1980]; c: Pacific N.W./Antarctica, at the surface, *Rasmussen et al.* [1981]; d: N. mid-latitudes/S. mid-latitudes, surface, *Rowland et al.* [1980]; interhemispheric means e, at the surface, *Singh et al.* [1979]; f: upper troposphere, *Tyson et al.* [1978]; g, at the surface, *Rowland et al.* [1980]. Note that true hemispheric mean values were not determined in many cases. Error bars are omitted where estimates could not be made. The solid line shows the results of the standard model. The dotted line shows a calculation in which OH concentrations of the standard model have been divided by 1.5.

the isoprene $+O_3$ rate constant were of order 10^{-16} cm^3 s^{-1}. The standard model does not account for possible removal of OH by either isoprene or terpenes. Present uncertainties are such as to preclude quantitative analysis. Observational studies are needed to define better the distribution of reactive hydrocarbons, and there is an additional need for laboratory work to characterize mechanisms for decomposition in the atmosphere. *Zimmerman et al.* [1978] estimate a global source for isoprene of about 3.5×10^8 tons C yr^{-1}, subject to an uncertainty of about a factor of 3. If we were to assume that each molecule of isoprene could remove one molecule of OH, isoprene could account for an increase in the lifetime for CH_3CCl_3 of about 5%. Reaction of OH with degradation products of isoprene could have a larger effect on OH. The source strength for terpenes could be similar to isoprene [*Went*, 1960; *Rasmussen*, 1972; *Zimmerman et al.*, 1978] with similar effect on CH_3CCl_3. It is apparent that concentrations of OH could be substantially reduced near strong sources of isoprene and terpenes.

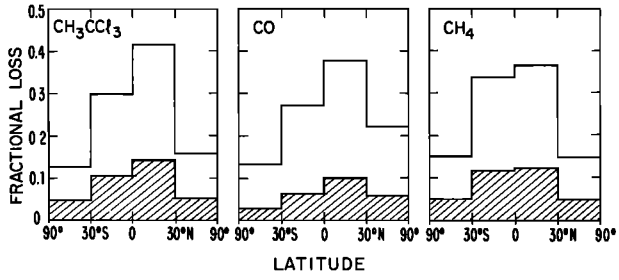

Fig. 29. Latitudinal distribution of the atmospheric loss for CH_3CCl_3, CO, and CH_4. The upper lines represent the fraction of the global loss rate which occurs in each of the four latitude zones; the cross-hatched region represents the loss in the lowest 2 km.

TABLE 7. Sensitivity of the Loss Rate for CH_3CCl_3 to Parameters of the Model

Parameter	Relative Loss Rate for CH_3CCl_3[a]
Standard model	1.00
Model B[b]	1.10
$(NO + NO_2)$ profile × 0.1	0.79
$(NO + NO_2)$ profile × 10	2.41
H_2O profile × 0.7	0.84
H_2O profile × 1.3	1.14
CO profile × 0.7	1.13
CO profile × 1.3	0.90
Seasonal variation in CO[c]	1.03
O_3 profile × 0.5	0.77
O_3 profile × 1.5	1.15
Total ozone column[d] × 0.8	1.26
Total ozone column × 1.2	0.81
Efficient aerosol loss for H_2O_2[e]	0.81
No clouds, no aerosols[f]	1.23

[a] The global loss rate for CH_3CCl_3 by reaction (30) is given, normalized to the loss rate of the standard model (see Table 4). Global mean cloud cover was included in the calculations. The standard model uses model A for $(NO + NO_2)$ as given in Figure 12*b*.

[b] Model B uses the profiles for $(NO + NO_2)$ in the right-hand panel of Figure 12*b*.

[c] The mean profiles for CO in Figure 11 were used for spring and fall. Summer profiles for CO were derived by decreasing the annual mean profiles by 30% at mid-latitudes and 20% in the tropics. Winter profiles were derived by increasing the mean profiles by the same amounts.

[d] The ozone profile in the troposphere was not changed.

[e] A sticking probability of 0.03 was used. It is assumed that peroxide is destroyed instantaneously after adsorption.

[f] Cloud cover and aerosols were omitted from the calculation; the surface albedo was 0.1.

It would appear that globally averaged concentrations of OH much higher than results of the model may be excluded on the basis of the comparison with observations of CH_3CCl_3 shown in Figure 26. Adjustment of calculated concentrations of OH downward by a factor of 1.5 would provide a satisfactory fit to the measurements by *Lovelock* [1977] and by *Rowland et al.* [1980]. Changes in the standard model to accommodate much lower concentrations of OH would require an improbable alignment of uncertainties in our knowledge of the concentration and distribution of relevant trace gases, with a similar bias in our choice of kinetic data. In what follows we assume that mean concentrations of OH determined here are reliable within about a factor of 2. The magnitude and distribution of the sink for CO should be determined therefore with corresponding accuracy.

Carbon monoxide is removed mainly by reaction with OH [*Levy*, 1971; *Weinstock*, 1969] with a small additional sink owing to biological activity in soil. The standard model implies photochemical sinks for CO in the northern and southern hemispheres of 1.9×10^9 tons CO yr^{-1} and 1.3×10^9 tons CO yr^{-1}, respectively. Measurements by *Liebl and Seiler* [1976] indicate deposition velocities for CO over soils in the range of 0.02–0.07 cm s^{-1}. If we were to adopt a median value of 0.04 cm s^{-1} as implied by their observations and were to use data for CO given in Figure 11, we would calculate a sink for CO of magnitude 2.5×10^8 tons yr^{-1} owing to uptake by soils. We estimate, from consideration of available land area, that ap-

TABLE 8. Global CO Budget (10^{12} gm CO yr^{-1})

	Total	Northern Hemisphere	Southern Hemisphere
Sources			
Fossil fuel use	450 (400–1000)	425	25
Oxidation of anthropogenic hydrocarbons	90 (0–180)	85	5
Oxidation of natural hydrocarbons	560 (280–1200)	380	180
Emissions by plants	130 (50–200)	90	40
Wood used as fuel	51 (25–150)	33	17
Forest wild fires	25 (10–50)	22	3
Forest clearing	380 (200–800)	260	120
Savanna burning	200 (100–400)	100	100
Ocean	40 (20–80)	13	27
CH_4 oxidation	810 (400–1000)	405	405
Total	2740 (1500–4000)	1820	920
Sinks			
Soil uptake	250	210	40
Photochemistry	3170 (1600–4000)	1890	1280
Total	3420	2100	1320

proximately 80% of this sink should occur in the northern hemisphere. Our estimate for the magnitude of the biological soil sink is similar to values given by *Liebl and Seiler* [1976] and *Seiler* [1976].

As was noted earlier, the CO content of the northern hemisphere is significantly larger than that of the southern hemisphere, 2.9×10^8 tons as compared to 1.7×10^8 tons. Exchange of air between hemispheres should lead to net transfer of CO from north to south. We estimate, using rates for mass exchange given in Table 6, that air motions should provide an effective source of 1.2×10^8 tons CO yr^{-1} to the southern hemisphere with correponding removal from the northern hemisphere. A similar flux of CO (±10%) is derived from the model of *Newell et al.* [1974] for mass exchange between the hemispheres. According to Newell's model, most of the transport of CO from north to south takes place in the upper troposphere. Estimates for exchange quoted here, combined with values given earlier for the photochemical and biological sinks, indicate a global source for CO of about 3.4×10^9 tons yr^{-1} of which approximately two thirds (2.3×10^9 tons yr^{-1}) should occur in the northern hemisphere.

The source of CO associated with oxidation of CH_4 may be taken as relatively well known. Both CO and CH_4 are removed by reaction with OH. Thus the fractional contribution of CH_4 to the total source of CO may be calculated with some confidence. The estimate is insensitive to details of the chemical model for OH, depending primarily on the yield for CO from oxidation of CH_4. The oxidation scheme discussed earlier implies a yield of about 80%, and suggests that CH_4 oxidation accounts for 25% of global production of CO. As is indicated in Table 8, our analysis implies a source for CO owing to oxidation of CH_4 of magnitude 8.0×10^8 tons yr^{-1}, distributed evenly between hemispheres.

The source of CO due to combustion of fossil fuel could be comparable to that from oxidation of CH_4. Combustion gave rise to a source of CO_2 of magnitude 4.6×10^9 tons C in 1976 [*United Nations*, 1978*a*]. The source was divided more or less equally between North America, Europe, and the rest of the world. Liquid fuel accounted for 44% of the net source of CO_2; solid fuel and natural gas represented 41% and 15%, respectively, as summarized in Table 9.

Use patterns for various forms of fossil fuel are displayed

TABLE 9. Fuel Consumption Patterns, 1976 (10^6 tons carbon)

	Solid fuel	Liquid fuel	Gas	Total
North America[a]	399	670	328	1397
Europe[b]	804	740	251	1795
Western Europe	276	467	101	
Rest of the World	684	600	91	1375
Totals	1887	2010	670	4567

These values were compiled from statistics for energy use published by the *United Nations* [1978*a*]. The U.N. gives energy consumption in units of metric tons of coal equivalent (MTCE), which is defined as 7000 calories per gram (1 MTCE = 1 metric ton coal = 0.64 metric tons liquid fuel = 7.51×10^2 m^3 natural gas). The U.N. has taken into account the percentages of carbon in different grades of coal and lignite, and solid fuel is taken to be 70% carbon. The carbon content of liquid fuel is 84% and that of natural gas 0.536 gm l^{-1} [*Keeling*, 1973].

[a] North America includes the United States and Canada.

[b] The values for Europe include 80% of fuel use in the U.S.S.R. [*Lydolph*, 1970].

TABLE 10. Fuel Use Patterns

	United States	Europe
Hard coal		
Energy conversion	0.69	0.45
Coke ovens	0.16	0.36
Industry	0.13	0.10
Residential	0.02	0.09
Lignite[a]		
Energy conversion	0.93	0.84
Coke ovens		0.09
Industry	0.07	0.05
Residential		0.02
Natural and Manufactured Gas		
Energy conversion	0.33	0.34
Industrial	0.39	0.40
Commercial	0.09	0.05
Residential	0.19	0.21
Oil		
Energy conversion	0.14	0.17
Industrial		
Residual fuel oil	0.03	0.20
Diesel	0.014	0.045
Liquified gases	0.036	0.01
Residential	0.20	0.28
Road transport		
Gasoline	0.44	0.16
Diesel	0.05	0.065
Trains	0.02	0.02
Air transport	0.07	0.03
Agriculture		0.02

The values shown are the fraction of fuel used in each category for the different fossil fuels. These figures were compiled from statistics for the U.S. and western European countries published by the *Organization for Economic Cooperation and Development* [1976] for the years 1973–1975. Limited statistics available for Eastern Europe [*United Nations,* 1974] suggest that similar values apply throughout Europe. In all other countries an average of 18% of liquid fuel used is gasoline [United Nations, 1976*a*, 1978*a*] and this value was used for the 'Rest of the World' category in deriving the results in Table 10. It should be noted that among those countries for which little statistical data could be found, China is the largest user of coal, accounting for about half the total, and Japan is the largest user of liquid fuel, accounting for about 30% of the total.

[a] Europe uses about 90% of all lignite.

for the United States and Europe in Table 10. Emission factors, defined as the amount of CO produced per unit of fuel consumed, are given in Table 11, while Table 12 summarizes amounts of CO released during manufacture of various industrial commodities. Automobiles account for about 50% of the source of CO from fossil fuel, with approximately equal contributions from North America, Europe, and the rest of the world, as indicated in Table 13. North America consumes 2.5 times as much gasoline as Europe. The similarity of CO source strengths given for the two continents in Table 13 reflects a view that emission control measures are more effective in North America. The data on which this conclusion is based are summarized in Table 14. Our estimate for the total of CO emissions from burning of fossil fuel is similar to earlier estimates by *Jaffe* [1973] and *Seiler* [1974].

The source of CO due to use of coal in residential heating is surprisingly large. Most of this source arises outside of the United States. We used emission factors reported by *Welzel and Davids* [1978] for the Federal Republic of Germany (F.R.G.). Emission factors for the United States are much lower [*U.S. Environmental Protection Agency,* 1977]. The source of CO due to residential use of coal in North America would be small, however, even if we were to adopt emission factors appropriate for Germany. The source of CO from residential use of coal in Germany is comparable with that from automobiles [*Welzel and Davids,* 1978], while automobiles are clearly dominant for the United States.

The sum of CO emissions from the various industrial activities included in Table 12 is relatively large. It may be important to point out that the emission factors used here reflect industrial practices in the United States [*U.S. Environmental Protection Agency,* 1977]. Data for other industrial economies are obviously needed. Production of steel could represent a major source if substantial quantities of CO produced during manufacture were allowed to vent to the atmosphere. One might note that the United States accounts for only 17% of total steel production. The remainder is widely distributed, with the U.S.S.R., Japan, F.R.G., and China contributing 21%, 16%, 6%, and 4%, respectively [*United Nations,* 1978*b*].

Table 8 shows an estimate of 9.0×10^7 tons CO due to atmospheric oxidation of industrial hydrocarbons. These hydro-

TABLE 11. Emission Factors for CO

Fossil Fuel Combustion	United States[a]	Germany[b]
	kg ton^{-1}	
Hard coal		
Utility boilers	0.5–1.0	0.4
Coke ovens	0.6	
Industrial boilers	0.5–1.0	4.0
Residential units	5–45	293
Lignite		
Utility boilers	1.0	
Coke ovens	1.0	
Industrial boilers	1.0	
Residential units	45	137
	kg 10^6 m^{-3}	
Natural gas		
Utility boilers	272	39
Utility turbines	1842	
Industrial boilers	272	78
Commercial and residential boilers	320	2730
	kg 10^3 l^{-1}	
Oil		
Utility boilers[c]	0.63–63	0.12
Utility turbines	1.85	
Industrial boilers[c]	0.63–63	0.4
Industrial gasoline internal combustion engines	472	
Industrial diesel internal combustion engines	12.2	
Liquified petroleum gas	0.18–0.24	
Residential boilers[c]	0.63–63	3.7
Transportation		
Road transport		
Gasoline[d]	180–360	244
Diesel		30
Trains	16	26

[a] Emission factors for the United States were taken from *U.S. Environmental Protection Agency* [1977], *Salveson et al.* [1978], and *DeAngelis and Reznik* [1979]. The low values for utility and industrial boilers and for oil and gas-fired residential boilers have been confirmed recently by field measurements [*Barrett et al.*, 1973; *Cato et al.*, 1976, *Crawford et al.*, 1978].

[b] Emission factors are given for West Germany by *Welzel and Davids* [1978].

[c] For oil-fired boilers, emissions may increase by a factor of 10–100 if the unit is improperly operated or not well maintained. For this reason a value of 6.3 kg 10^3 l^{-1} was used in deriving the results in Table 10.

[d] Derivation of these emission factors is given in Table 14.

TABLE 12. Industrial Sources of CO

Process	Emission Factor[a] (kg/ton of Product)	Total Production[b] (tons)	CO Production (10^6 tons)
Pig iron production	80	5.1×10^8	42
Steel production	69.5	6.7×10^8	47
Catalytic cracking of crude oil[c]	39.2 kg 10^3 l^{-1}	3.47×10^{11}	13.6
Carbon black production	2000	3.9×10^6	7.8
Ammonia production	100	4.4×10^7	4.4
Pig iron, foundry	72.5	2.5×10^7	1.8
Miscellaneous industrial processes[d]			12
Total			130

[a] Emission factors were taken from *U.S. Environmental Protection Agency* [1977] and *Kemp and Dykema* [1978] and are typical of current industrial practices in the United States.
[b] Production rates were taken from the Yearbook of Industrial Statistics, 1976 [*United Nations,* 1978*b*].
[c] About 12% of crude oil is catalytically cracked [*International Petroleum Encyclopedia,* 1979]. The production rate is given in liters.
[d] Estimated to be about a factor of 3 larger than the U.S. source [*U.S. Environmental Protection Agency,* 1976, 1978*b*].

carbons are associated in part with emission from automobiles, about 45%, and in part with evaporation of fuels and solvents, about 40%. Emission data for the United States [*U.S. Environmental Protection Agency,* 1976, 1978*b*] and information in Tables 9 and 10 were used to estimate the magnitude of the global source of anthropogenic hydrocarbons. We assumed that 50% of carbon in volatile hydrocarbons was converted photochemically to CO.

The sources discussed so far are relatively well defined. They contribute, according to our estimates, 9.1×10^8 tons CO yr^{-1} in the northern hemisphere and 4.4×10^8 tons CO yr^{-1} in the southern hemisphere, less than half of the estimated net source in each hemisphere. It remains to account for additional production of about 1.4×10^9 and 7.6×10^8 tons CO yr^{-1} in the northern and southern hemispheres, respectively. Possible sources include the oceans, combustion of wood for fuel, wild forest fires, burning of vegetation in land clearance for agriculture, emission by plants, and oxidation of natural hydrocarbons. Observations by *Linnenbom et al.* [1973] and *Seiler* [1974] suggest that the marine biosphere should represent at most a small source for CO as shown in Table 8. According to United Nations statistics [*Food and Agricultural Organization,* 1979], 8.5×10^8 tons of wood are used annually as fuel. Wood is the major source of energy for about 1.5 billion people [*Eckholm,* 1979] with use averaging between 0.1 and 2 tons per capita per year [*Openshaw,* 1974; *Revelle and Munk,* 1978]. In different countries, between 6 and 40% of wood fuel is converted to charcoal prior to combustion [*Openshaw,* 1974; *Arnold and Jongma,* 1978]. The emission factor for wood (60 kg CO per ton of wood) is appropriate for combustion in an open fire [*U.S. Environmental Protection Agency,* 1977]. Insufficient data exist for emission associated with the manufacture and combustion of charcoal. Accordingly, we used an emission factor similar to that for wood fuel. The source for CO given in Table 8 could be uncertain to at least a factor of 3. Our estimate of the uncertainty assumes that the United Nations survey is reliable within about a factor of 2 and that emission factors could be different from values adopted here by about 50%.

The estimate for production of CO in wild forest fires reflects a product of three factors: the area of forests burned per year, the quantity of fuel consumed per unit area, and the production of CO per unit of fuel. Relatively accurate data are available for forests in the United States, Canada, and Austra-

TABLE 13. CO Emissions (10^6 tons yr^{-1})

	Europe	North America	Rest of the World	Total
Combustion				
Coal	24	1	23	48
Lignite	3	—	—	3
Gas	0.3	0.2	0.1	0.6
Oil	4.6	2.2	3.7	11
Total Combustion	32	3.4	27	62
Transportation[a]	71	94	66	233
Sub total	103	97	93	295
Industrial Processes	46	36	48	130
Waste Disposal[b]	6	3	11	20
Total	155	137	152	445

These estimates are derived from the statistics for fossil fuel consumption, fuel use patterns, and emission factors, given in Tables 9, 10, 11, 12, and 14. Emission factors for the United States were used except for two categories. Residential use of coal is discussed in the text. For the transportation source of CO, we used the emission factors derived in Table 14 for gasoline and the German emission factor for diesel vehicles. The uncertainty in the transportation source is considered to be about 30% and in all other sources about a factor of 2.
[a] The total includes a source of CO from aviation of 1.6×10^6 tons. (A. Broderick, private communication, 1980).
[b] Estimate, based on limited data for the United States [*U.S. Environmental Protection Agency,* 1977] and world population figures.

TABLE 14. Emission Factors for Gasoline

	North America	Western Europe	Rest of the World
U.S. Environmental Protection Agency average vehicle emission factor for year	1976	1974[a]	1970[b]
Urban traffic, CO emission rate (gm km^{-1})[c]	51.1	55.3	60.3
Highway/rural traffic, CO emission rate (gm km^{-1})[d]	18.1	20.1	25.2
Fuel economy (km l^{-1})[e]	5.2	8.4	8.4
Emission factor (kg 10^3 l^{-1})[f]	180	320	360

[a]Vehicle exhaust emission standards were implemented earlier and are stricter in the United States as compared with the European economic community [*U.S. Environmental Protection Agency*, 1978*a*; *Simanaitis*, 1977; *Becker et al.*, 1976]. This estimate for Western Europe is based on the assumption that mean emission rates (in gm CO km^{-1}) are similar to those in the United States 2 years previously. It is difficult to compare directly emission rates for different countries because they are based on different test procedures [*Simanaitis*, 1977].

[b]It is assumed that mean emission rates outside North America and Western Europe are similar to those in the United States prior to regulation of exhaust emission.

[c]These emission rates are appropriate for a speed of 31.5 km $hour^{-1}$ and an ambient temperature of 10°C for the year given in the row above and are taken from *U.S. Environmental Protection Agency* [1978*a*]. These values include an average over the age distribution of vehicles in the United States, the distances traveled by different types of vehicles (cars, trucks, etc.), and typical percentages of hot and cold starts. The value for 1976 includes a minor component for diesel vehicles, while the values for 1974 and 1970 are appropriate for gasoline-powered vehicles only.

[d]These rates are for an average speed of 72 km $hour^{-1}$ with no cold starts [*U.S. Environmental Protection Agency*, 1978*a*].

[e]The values for North America are taken from fuel economy figures for all vehicles for 1976 and 1977 [*U.S. Department of Transportation*, 1977] in the United States. For elsewhere, fuel economy was derived from statistics for Europe given in *United Nations* 1973, 1976*b* for 1971–1975.

[f]In the United States, approximately equal distances are driven in rural and urban areas [*U.S. Department of Transportation*, 1977]. The emission rates for rural and urban traffic were averaged in deriving the final emission factors. These factors may be compared with limited estimates for countries other than the United States. In Germany, where exhaust emissions are checked annually, a mean value of 244kg 10^3 l^{-1} was used by Welzel and Davids [1978] in their compilation of national CO emissions. *Becker et al.* [1976] quote the results of a Swedish survey of 500 European cars, around 1970, which gave a mean emission rate of 50 gm km^{-1}. A recent British report [*Apling et al.*, 1cs] gives an emission factor of 300 kg 10^3 l^{-1}.

lia, regions containing approximately 25% of the world's forests [*Persson*, 1974]. About 0.4% of the forested area of these countries is affected annually by fire [*U.S. Environmental Protection Agnecy*, 1977; *Yamate*, 1975]. Approximately 30 tons of fuel are consumed for each hectare burnt in North America, with a somewhat smaller value associated with tropical fires according to *Yamate* [1975]. The estimate in Table 8 assumes that 100 kg of CO are produced per ton of fuel, a compromise between values of 70 and 130 kg CO ton^{-1} quoted by the *U.S. Environmental Protection Agency* [1977] and by *Crutzen et al.* [1979], respectively. We estimate that the corresponding source in Table 8 could be uncertain to at least a factor of 3. Year to year fluctuations in the area of forests burned in the United States between 1963 and 1972 are as large as 0.4% of the total forest area [*Yamate*, 1975]. Data are sparse for the tropics, while direct measurements are available only recently for production of CO in wild forest fires [*Crutzen et al.*, 1979].

Table 8 includes estimates for the source of CO due to burning of forest and grassland for purposes of agriculture. Fire plays a central role in the shifting cultivation characteristic of agriculture over large areas of the tropics, especially in Africa [*Nye and Greenland*, 1960; *Gourou*, 1966; *Webster and Wilson*, 1967; *Watters*, 1971; *Ruthenberg*, 1976]. It is difficult, however, to obtain quantitative data on either the amount or nature (grass, forest) of land cleared annually in different regions or on the number of people engaged in shifting cultivation [*Sommer* 1976; *Food and Agricultural Organization*, 1957]. *Spencer* [1966] estimates that about 1.4×10^{11} m^2 of tropical forest are cleared annually in south east Asia by 10^7 families. His value for the area of land cleared per person per year (0.28 ha) is somewhat larger than values given for other parts of the world, 0.05–0.25 ha $person^{-1}$ $year^{-1}$ [*Nye and Greenland*, 1960; *Wilbert*, 1961; *Gourou*, 1966; *Watters*, 1971; *Ruthenberg*, 1976]. If we were to use a median value of 0.15 ha $person^{-1}$ $year^{-1}$, combined with published data for the size of agricultural populations in Africa and Latin America [*Food and Agricultural Organization*, 1977] and maps, which show the extent of shifting cultivation [*Whittlesey*, 1937; *Grigg*, 1974], it would be possible to estimate the area of land involved in shifting agriculture for different geographical regions. A summary of demographic information used in these estimates is given in Table 15.

It appears that the fraction of the total agricultural population using these techniques is largest for Africa. We assume for present purposes that the number of people involved in shifting cultivation in Africa, Latin America, and Asia are 1.5×10^8, 2×10^7, and 5×10^7, respectively. Our analysis suggests that the total area of cropland cleared annually in tropical forests could be as large as 2.4×10^{11} m^2, with perhaps an additional 1.6×10^{11} m^2 obtained from clearing of woodland and savanna in Africa (see Table 16).

Burning of savanna to maintain grassland for grazing involves large areas, perhaps half that shown for total pasture in Table 17. It appears that as much as 5×10^{12} m^2 of grassland could be consumed annually by fire.

Our estimate for the area of cropland derived from tropical forest is consistent with statistical data for the total area of harvested land [*Food and Agricultural Organization*, 1978]. If we were to assume that land in shifting cultivation would be allowed to return to forest in about 2 years, we may estimate

TABLE 15. Agricultural Populations in the Tropics, 1976

Region	10^6 Persons
Africa	
All countries[a]	225
Population in the region of shifting cultivation[b]	150
Population in the tropical forest region[c]	45
Central and South America	
All countries[a,d]	116
Population in the tropical forest region[e]	22
Southeast Asia	
All countries[a]	685
Population living by shifting cultivation in the tropical forest region[f]	49

Agricultural populations for individual countries were taken from *Food and Agricultural Organization* [1977].

[a]All countries between 22½°N and 22½°S.

[b]This is based on maps showing the extent of shifting cultivation in Africa [*Grigg*, 1974] and discussions of agricultural practices in Africa [*Stamp and Morgan*, 1972] and is the total agricultural population in these regions.

[c]Total agricultural population of countries where the major form of vegetation is tropical forest [*Persson*, 1974; *World Atlas of Agriculture*, 1969; *Phillips*, 1959; *Stamp and Morgan*, 1972].

[d]Includes all of Mexico.

[e]It is assumed that shifting cultivation is practiced primarily by inhabitants of the tropical forest regions. In Brazil, less than 10% of the agricultural population live in the tropical forest [*World Atlas of Agriculture*, 1969; *Camargo*, 1958], while in Peru the fraction is 13% [*Watters*, 1971]. The fractions of the agricultural populations in regions where shifting cultivation is dominant in Mexico and Venezuela are 20 and 50%, respectively. Estimates for other countries are based on maps showing the extent of shifting cultivation [*Whittlesey*, 1939] and descriptions of vegetation zones [*World Atlas of Agriculture*, 1969; *Persson*, 1974].

[f]Taken from *Spencer* [1966]. Shifting cultivation is not significant outside the tropical forest region.

a harvested area of 7×10^{11} m^2, distributed as shown in Table 17. Our analysis implies that as much as 5% of the total area of tropical forest is cleared annually for agriculture in Africa and in the Far East. Land is used for a relatively brief period. It is reclaimed partially by forest, though it may be returned to cultivation after a delay of some 10–20 years [*Nye and Greenland*, 1960].

Tropical forests, according to *Whittaker and Likens* [1975], contain approximately 40 kg dry matter m^{-2}, producing 2 kg dry matter m^{-2} yr^{-1}. We assume that 30% of the mean standing biomass is consumed during clearing. This allows for the tendency to reuse land before the regenerating forest reaches maturity. It accounts also for the practice of leaving the largest trees in place during preparation of land. Tropical woodland contains 5–20 kg dry matter m^{-2}, savanna about 4 kg m^{-2} [*Persson*, 1974; *Whittaker and Likens*, 1975], and we assume that 4 kg m^{-2} of dry matter is burned during clearance of woodland and wooded savanna for cropland. We assume that the quantity of dry matter consumed by fire during maintenance of pasture, 0.4 kg m^{-2} yr^{-1}, corresponds to 50% of annual productivity as given by *Bourlière and Hadley* [1970] and *Murphy* [1975]. This value is consistent with measurements by *Hopkins* [1965] of savanna burning for experimental grasslands in Nigeria. Our estimate for CO sources due to clearance of forests and grassland is given in Table 16, 3.8 and 2.0 $\times 10^8$ tons CO yr^{-1}, and assumes an emission factor of 100 kg CO per ton of fuel as discussed earlier. These estimates, based on considerations outlined above, should be considered uncertain to at least a factor of 3. Our value for the total source of CO due to combustion of biomass carbon is similar to that given by *Crutzen et al.* [1979], though individual sources differ by as much as a factor of 2.

It appears that green plants may represent both sources and sinks for CO [*Wilks*, 1959; *Bidwell and Fraser*, 1972]. Recent laboratory and field experiments demonstrate that higher plants provide a net source at ambient concentrations of CO [*Seiler and Geihl*, 1977; *Bauer et al.*, 1979]. The production rate for CO per unit leaf surface area was measured as a function of light intensity and season for four plant species and reached a maximum of 4.4 $\times 10^{-12}$ gm cm^{-2} s^{-1} at noon in summer. *Bauer et al.* [1979] used these results, in combination with average values for global leaf surface area and light intensity, to estimate a global source of CO from plants of 7.0×10^7 tons yr^{-1}. This estimate is uncertain to at least a factor of 2. Oxidation of hydrocarbons emitted by plants may provide a significantly larger source of CO.

Oxidation of isoprene should lead to production of at least

TABLE 16. CO Emissions From Biomass Burning

	Area, 10^{10} m^2 yr^{-1}	Fuel Loading, kg m^{-2}	Total Fuel, 10^{14} gm yr^{-1}	CO Emitted, 10^6 tons yr^{-1}
Forest wildfires[a]	11 (5–22)	0.6–3.3	2.5	25 (8–75)
Clearing of forests for crops	24 (8–36)	13 (9–26)	32	320 (70–940)
Clearing of woodland for crops	16 (5–32)	4 (2–8)	6.4	64 (10–250)
Burning of pasture land	500 (250–750)	0.4 (0.2–0.8)	20	200 (50–600)
Wood used as fuel	—	—	8.5	51 (7–150)
Total[b]			70	660

Fuel loading is the amount of dry matter per unit area that is consumed by fire. Dry matter is taken to be 45% carbon. All categories except wood fuel assumed a CO emission factor of 100 kg CO per ton of fuel. For wood fuel a value of 60 kg CO per ton of wood was used.

[a]*Persson* [1974] gives the total area of the world's forests as 2.8×10^{13} m^2. We assumed that 0.4% of this area is affected by forest wildfires annually, and we used *Yamate*'s [1974] estimates of the amount of fuel burned per unit area, which range from 0.6 kg m^{-2} for tropical forests to 3.3 kg m^{-2} for temperate forests.

[b]This total does not include an estimate of CO emissions from the burning of agricultural waste. CO emissions from this source in the United States, prior to regulation, amounted to 1.5×10^6 tons yr^{-1} [*U.S. Environmental Protection Agency*, 1978c]. Since the total area of land harvested in the United States is about 10% of the total in the world [*Food and Agricultural Organization*, 1978], this suggests that burning of these wastes should not provide a large source of CO.

TABLE 17. Land Use in the Tropics (10^{10} m^2)

Region	Land Area (1)	Closed Forest (2)	Forest and Woodland (3)	Permanent Pasture (4)	Arable Land (5)	Total area Harvested (6)	Shifting Cultivation: Forest Cleared Per Year (7)	Shifting Cultivation: Area Harvested (8)
Africa	2291	190	627	660	174	75	7	45
Central and South America	1654	570	924	340	102	50	3	7
Far East	777	290	360	28	247	186	14	18
Total	4722	1050	1911	1028	523	311	24	70

Areas given are for countries located between 22½°N and 22½°S. Information in columns 1 and 3–6 is taken from *Food and Agricultural Organization* [1978] and column 2 is from *Persson* [1974]. The areas in columns 7 and 8 for the Far East are taken from *Spencer* [1966]. The areas for Africa and Central and South America are estimated from the populations given in Table 12, and the asumptions that 0.15 ha of land is cleared annually per shifting cultivator and that the land is harvested for 2 years.

one, and to perhaps as many as three, molecules of CO [*Zimmerman et al.*, 1978]. A recent laboratory study of oxidation initiated by reaction with OH [*Cox et al.*, 1979] found evidence for production of formaldehyde, methyl vinyl ketone ($CH_3COCH = CH_2$) and methyl acrolein ($CH_2 = C(CH_3)CHO$) in the presence of NO. Production of such compounds is consistent with the oxidation mechanism postulated by *Niki et al.* [1978*b*] for reaction of OH with unsaturated hydrocarbons. One would expect that product carbonyl compounds should be photooxidized readily in the atmosphere with consequent production of CO. Oxidation of isoprene initiated by reaction with ozone should also lead to production of CO. Studies investigating the mechanism for reaction of O_3 with simpler alkenes [*Herron and Huie*, 1977, 1978] show significant production of formaldehyde and other carbonyl compounds, and there is reason to believe that these species should be formed during photodecomposition of isoprene. It is probable that at least two molecules of CO should be produced during oxidation of isoprene even at very low ambient concentrations of NO, with uncertainty imposed largely by lack of knowledge of the possible role of heterogeneous chemistry for reactive intermediates.

Formation of particulate material may play an important role in the photodecomposition of terpenes such as α-pinene, β-pinene, 3-carene, and limonene [*Went*, 1960; *Schuetzle and Rasmussen*, 1978; *Graedel*, 1979]. These compounds are observed in forest environments with concentrations as high as 1 ppb [*Holdren et al.*, 1979]. It is difficult to make a reliable estimate for production of CO due to oxidation of isoprene and other terpenes. The difficulty may be attributed to uncertainties in the atmospheric photochemistry of these species and lack of global data for the magnitude of the relevant biospheric source. We assumed for purposes of Table 8 a source for isoprene of magnitude 4×10^8 tons yr^{-1}, with a similar source for other reactive hydrocarbons, and we adopted a yield of two molecules of CO per hydrocarbon precursor. The source strength for CO obtained in this manner could be uncertain to at least a factor of 5. The upper limit for the corresponding source in Table 8 was obtained by imposing a constraint that production from all processes should not exceed

TABLE 18. Global Budgets for Trace Gases

Species	Mixing Ratio[a]	$k(OH + X)$[a]	Global loss rate[b]: Molecules cm^{-2} s^{-1}	Global loss rate[b]: Tons year^{-1}	Lifetime[c] (Years)
H_2[d]	5.5–7	1.2–11 exp(−2200/T)[e]	3.9×10^{10}	2.1×10^7	9.4
CH_4	1.65–6	2.4–12 exp(−1710/T)[e]	1.4×10^{11}	5.8×10^8	7.9
CH_3Cl	6.0–10	2.20–12 exp(−1142/T)[e]	3.8×10^8	5.2×10^6	1.0
CH_3Br	2.0–11	7.90–13 exp(−889/T)[e]	1.2×10^7	3.0×10^5	1.1
C_2H_6	1.0–9	1.86–11 exp(−1232/T)[f]	3.9×10^9	3.1×10^7	0.17
C_2H_2	2.0–11	1.91–12 exp(−312/T)[f]	...	...	0.06
C_2H_4	...	2.18–12 exp(338/T)[f]	...	...	2 days
C_5H_8	1.0–9	7.40–11[g]	...	...	0.2 days

[a] Mixing ratios for H_2, CH_4, C_2H_6, CH_3Cl, and CH_3Br were assumed to be uniform throughout the troposphere. Mixing ratios for C_2H_2, C_2H_4, and C_5H_8 were assumed to be uniform below 1 km. The notation 1.0–11 should be read as 1.0×10^{-11}.

[b] Photochemical loss rates were calculated from the OH profiles of Figure 27. Loss rates are given in tons of H_2, CH_4, etc.

[c] Average tropospheric lifetimes towards reaction with OH are given. For C_2H_2, C_2H_4, and C_5H_8 lifetimes are given for the boundary layer.

[d] The photochemical source of H_2 from photolysis of CH_2O is approximately equal to the photochemical sink by reaction with OH.

[e] Rate constant from *NASA* [1979].

[f] Rate constant from *Atkinson et al.* [1979].

[g] Rate constant from *Cox et al.* [1979].

the magnitude of the global removal rate for CO given earlier. The upper limit for CO production due to burning of biospheric material is similarly constrained.

It would appear that greatest uncertainty is attached to the combined roles of biospheric burning and hydrocarbon oxidation. One might attempt to use overall budget constraints to refine estimates for these terms. It is clear, for example, that the quantity of CO removed photochemically from the atmosphere in the northern hemisphere exceeds that removed by this mechanism in the southern hemisphere by about 6×10^8 tons CO yr^{-1}. Net transport of CO-rich air from north to south removes an additional 1.2×10^8 tons CO yr^{-1} from the northern hemisphere. Uptake of CO by soils in the northern hemisphere exceeds that in the southern hemisphere by 1.7×10^8 tons CO yr^{-1}. This suggests that the source of CO in the northern hemisphere should exceed that in the southern hemisphere by about 1.0×10^9 tons CO yr^{-1}. A portion of this differential (4.8×10^8 tons CO yr^{-1}) is provided by combustion of fossil fuels and oxidation of anthropogenic hydrocarbons. The remainder, 5.4×10^8 tons CO yr^{-1}, must be produced largely by burning of biomass for purposes of agriculture and by oxidation of volatile biospheric hydrocarbons. Consideration of the geographical distribution of lands involved in shifting agriculture suggests that the agricultural source can account for at most a small part of the interhemispheric bias, about 1.4×10^8 tons CO yr^{-1}. It appears that most of the deficit should be attributed to a differentially larger source of CO in the northern hemisphere due to oxidation of isoprene and other hydrocarbons. Literal interpretation of the data in Table 8 suggests that the hemispheric and global budgets of CO would be balanced if we were to assume sources of CO from oxidation of hydrocarbons equal to 7.9×10^8 and 4.6×10^8 tons CO yr^{-1} in the northern and southern hemispheres, respectively. A bias in favor of the northern hemisphere would not be unreasonable in that 67% of the total land area of the earth is located in the northern hemisphere, with similar concentration of the land-based biosphere. The accuracy of various data in Table 8, in particular the interhemispheric distribution of the photochemical sink and the source from fossil fuel, however, is probably insufficient to justify such fine tuning of estimates for other components of the budget. It is clear that atmospheric considerations may be used to place valuable constraints on the magnitude of otherwise uncertain contributions to CO and that they may be employed to refine our understanding of the role of the biosphere.

A number of other gases are removed primarily by reaction with OH. A summary of computed rates for removal of CH_4, H_2, C_2H_6, CH_3Cl, and CH_3Br is given in Table 18, which includes data and assumptions made regarding abundances and distributions of these species.

6. Discussion

Concentrations of OH obtained here are similar to those derived almost a decade ago by *Levy* [1971] and *McConnell et al.* [1971]. However, models for the troposphere have evolved considerably in the interim. Recent progress may be attributed to refinement in our understanding of rates for certain key reactions and to advances in instrumentation allowing measurement of a number of important tropospheric gases, notably NO. It is clear that the rate at which CO is oxidized by OH is sensitive to pressure [*Bierman*, 1978]. It appears that reaction of OH with H_2O_2 is the major mechanism for removal of odd hydrogen. Previously, this rate was thought to be slow throughout the troposphere. The rate constant for reaction of NO with HO_2 is 40 times larger than values used in models prior to 1976 [*Howard*, 1979]. The faster rate for (7) ensures more efficient cycling of OH from HO_2, maintaining a higher concentration of OH for any given concentration of NO. The impact of the change in rate for (7) on models for OH is offset in part by the observations of NO and NO_2 [*McFarland et al.*, 1979; *Noxon*, 1978] that imply concentrations for NO much lower than values reported earlier by *Robinson and Robbins* [1969].

Early analyses of observational data for CH_3CCl_3 [*Lovelock*, 1977; *Singh*, 1977*a*, *b*; *Derwent and Eggleton*, 1978; *McConnell and Schiff*, 1978; *Neely and Plonka*, 1978; *Chang and Penner*, 1978] suggested lifetimes for CH_3CCl_3 in the range 3 –11 years implying mean values for OH between 2.5 $\times 10^5$ cm^{-3} and 10^6 cm^{-3}. Concentrations of OH obtained in this manner must be revised upward by a factor of about 1.3 to account for more recent measurements of the rate constant for reaction of OH with CH_3CCl_3 [*Kurylo et al.*, 1978; *Jeong and Kaufman*, 1979]. It is difficult, however, to relate the single number derived for OH in these studies to the complex distribution which must apply for the real atmosphere.

Analysis of CH_3CCl_3 in the present study involves comparison of observed and computed concentrations for the gas. The model indicates that about 70% of CH_3CCl_3 is removed in the tropics. The global lifetime, obtained by integrating loss over latitude and altitude, is 5 years, and it should be emphasized that one-dimensional models are inappropriate in this case for calculation of the lifetime. In what follows we emphasize comparison of present results with two-dimensional studies. The model for OH given by *Wofsy* [1976] predates recent measurements for (3) and (7) and used concentrations for NO from *Robinson and Robbins* [1969]. Assumptions and choice of data made by *Crutzen and Fishman* [1977] and by *Fishman et al.* [1979] are more directly comparable to those employed in the present work.

Crutzen and Fishman [1977] reported a mean value of 2.5×10^5 cm^{-3} for the concentration of OH in the northern hemisphere. Their model included an average over latitude, altitude, and season in the troposphere. Our model, on a similar basis, gives a mean value for the northern hemisphere of 1×10^6 cm^{-3}. The models are similar in their choice of quantum yields for $O(^1D)$ and in the selection of data for other key parameters such as the rate constant for reaction of CO with OH and concentrations for O_3, CO and CH_4. *Crutzen and Fishman* [1977] used higher values for the concentrations of NO in the boundary layer, a choice that should result in larger, rather than smaller, values for OH as shown in Figure 3. Part of the discrepancy may be attributed to differences in the choice of rate constants for the reactions of $O(^1D)$ with H_2O, N_2, and O_2. Crutzen and Fishman took rate constants from *NASA* [1977]. Use of more recent data for these reactions leads to upward revision in the source of odd hydrogen by a factor of 1.8 but is not in itself sufficient to account for the discrepancy. Differences in the choice for H_2O_2 lifetime in the two models also fail to account for the discrepancy (see Figure 24*c* and Table 7). Results could be reconciled if we were to assume that *Crutzen and Fishman* [1977] used concentrations for H_2O lower than values adopted here by a factor of about 3. The discrepancy might also reflect differences in the treatment of solar radiation (cf. Appendix 3).

Values for OH quoted by *Fishman et al.* [1979] are larger than those of *Crutzen and Fishman* [1977]. *Fishman et al.*

[1979] studied the functional dependence of OH on (NO + NO_2) and considered a range of models characterized by constant values for the mixing ratio for (NO + NO_2). Their model gave 3.8×10^5 cm^{-3} for the mean concentration of OH in the northern hemisphere in the limit where NO was set equal to zero. Our results agree to within a factor of 2 with this more recent study. Detailed comparison is impossible, however, since *Fishman et al.*, [1979] give only a partial summary of values used for rate constants and concentrations of background gases.

We argued that photochemistry should account for consumption of 3×10^9 tons CO yr^{-1}, with approximately 60% of the loss in the northern hemisphere. Loss of CO due to uptake by soil could provide additional removal of about 2.5×10^8 tons CO yr^{-1}, of which 80% might be expected in the northern hemisphere. We concluded that production of CO in the northern hemisphere should exceed production in the southern hemisphere by 1.0×10^9 tons CO yr^{-1}. Burning of fossil fuel accounts for part of the excess. There must be additional sources biased in favor of the northern hemisphere. These sources are attributed tentatively to oxidation of isoprene and other volatile biospheric hydrocarbons. Our budget for CO implies that approximately 60% of the global source is natural (biospheric hydrocarbons, wild fires, methane), while the remainder (fossil and wood fuels, agricultural burning) is directly or indirectly under the influence of man. If OH were a factor of 2 smaller than obtained here, as suggested by analysis of the budget for CH_3CCl_3, the estimates in Table 8 for CO sources from natural hydrocarbons and from biomass burning would be correspondingly reduced. In this case, 60% of the global source for CO would be attributed to human activities.

The distribution of odd nitrogen in clean air is an important component of current models for tropospheric photochemistry. We used calculated values for OH and observed distributions for HNO_3 to derive profiles for (NO + NO_2) consistent with the few available observations of these species in clean air. Concentrations derived for (NO + NO_2) are directly proportional to an uncertain parameter, the rate for heterogeneous loss of HNO_3. Loss rates adopted here correspond to a mean lifetime of 10 days for HNO_3, somewhat shorter than the lifetime implied by a recent study using a general circulation model [*Mahlman and Moxim*, 1978; *Levy et al.*, 1980]. If removal rates for HNO_3 were reduced to agree with *Levy et al.* [1980], we would predict (NO + NO_2) concentrations equal to about 1/4 of those shown in Figure 12.

Our model implies a source strength for (NO + NO_2) in the remote troposphere of about 10^7 tons N yr^{-1}. The source would be smaller if the lifetime for heterogeneous removal of HNO_3 were longer than we assumed. It appears that the magnitude of the source of odd N from lightning must be significantly smaller than some recent estimates, which range from $0.4\text{–}9 \times 10^7$ tons N yr^{-1}. A source in excess of 10^7 tons N yr^{-1} could be accomodated only if the mean residence time for HNO_3 were very short (less than 10 days) or if odd N produced by lightning were removed efficiently in the rain cloud.

The model indicates consumption of O_3 by gas phase tropospheric chemistry at an average rate of 2×10^{11} molecules cm^{-2} s^{-1}. About two thirds of the loss occurs in the tropics. Heterogeneous chemistry provides an additional, more distributed sink, about 7×10^{10} molecules cm^{-2} s^{-1} [*Fabian and Junge*, 1970; *Galbally and Roy*, 1980]. The total removal rate is significantly higher than the source from the stratosphere, $5\text{–}8 \times 10^{10}$ molecules cm^{-2} s^{-1} [*Danielson and Mohnen*, 1977; *Mahlman et al.*, 1980; *Gidel and Shapiro*, 1980]. It is balanced in the present model by photochemical production associated with oxidation of CO and CH_4. The magnitude of the photochemical source is proportional to NO but less sensitive to CO. The balance obtained for O_3 provides indirect support for the distribution calculated for NO.

A well-calibrated and reliable model for OH places important constraints on global budgets for a variety of gases including CH_4, H_2, and CH_3Cl in addition to CO. Accurate measurements of species such as CH_3CCl_3 can provide valuable checks on global models that must integrate over a variety of atmospheric conditions (cloudiness, moisture, etc.). However, emission rates for the relevant gases must be adequately quantified. Kinetic features of models are best tested by selected local measurements of OH, with simultaneous definition of radiation, H_2O, O_3, CO, CH_4, and NO. Local measurements, however, cannot substitute for more inclusive tests attended by measurement of globally dispersed gases such as CH_3CCl_3. Such tests are hampered at present by discrepancies in concentrations measured by different observers and by uncertainties in estimates of global emission rates. We believe that present results for the global distribution of OH are accurate to about a factor of 2. Similar accuracy may be attached to the global source strengths quoted for a number of gases in Table 18. These gases reflect the complex metabolism of the biosphere. Studies of tropospheric chemistry can provide important, indeed invaluable, information on the overall function of the global ecosystem. Further observational and theoretical work is required to realize this potential.

Appendix 1. Role of Aerosols in Chemistry of Peroxides

Hydrogen peroxide and organic peroxides (CH_3OOH, ROOR') may be removed from the atmosphere by heterogeneous reactions involving aerosols. Observations of aerosols in the marine boundary layer imply a volume of particles per unit volume of air ('specific volume') in the range $5\text{–}20 \times 10^{-12}$ cm^3 cm^{-3}. The surface area of the particles lies typically between 1×10^{-7} and 8×10^{-7} cm^2 cm^{-3} [*Jaenicke et al.*, 1971; *Junge*, 1963, 1972; *Mesaroz and Vissy*, 1974; *Jaenicke*, 1978; *Parungo et al.*, 1979]. Somewhat larger concentrations of aerosols are observed in clean continental areas (specific volumes of $5\text{–}30 \times 10^{-12}$ cm^3 cm^{-3} and specific areas of about 2×10^{-6} cm^2 cm^{-3} [*Junge*, 1963; *Jaenicke et al.*, 1978; *Whitby*, 1978]) while aerosol concentrations in the upper troposphere are at least a factor of 10 lower than those in the marine boundary layer [*Toba*, 1965; *Blifford and Ringer*, 1969; *Blifford*, 1970; *Elterman*, 1969; *Bigg*, 1977; *Gras and Michael*, 1979]. Values adopted for the aerosol size distribution are given in Table 1.

It seems reasonable to assume that the physical properties of aerosols should be similar to those of liquid water droplets or of solid particles coated with liquid water [cf. *Ho et al.*, 1974]. In this case, partitioning of ambient H_2O_2 between gas and aerosol phases may be estimated from solubility data for H_2O_2 in water [*Scatchard et al.*, 1952]. We find at equilibrium that the fraction of peroxide molecules contained in or on aerosols should be quite small, about $5\text{–}30 \times 10^{-6}$ for the marine boundary layer or upper troposphere. Furthermore, the time required to achieve equilibrium should be less than 10 s. This estimate is based on the observed aerosol size distribution and on a sticking probability of 10^{-3} for H_2O_2 colliding with an aerosol [*Baldwin and Golden*, 1979].

Since only a small fraction of ambient H_2O_2 resides in the aerosol phase, destruction in aerosols would be negligible compared to homogeneous loss (5×10^{-6} s^{-1}) unless the loss frequency for absorbed molecules was quite large (>0.2 s^{-1}). Aqueous peroxide can be photolyzed, or it can react with oxidizeable species, but loss frequencies associated with these reactions are likely to be much slower than 0.2 s^{-1}. Photolysis rates for dissolved H_2O_2 are less than 10^{-5} s^{-1} [*Molina et al.*, 1977; *Lin et al.*, 1978]. Reactions of aqueous H_2O_2 with I^-, SO_3^{-2}, or Fe^{+2} are slow even at 25°C, with rate constants of 1.2×10^{-2}, 0.2, and 63 l mole^{-1} s^{-1}, respectively, and these reactions have large activation energies [*Edwards*, 1962; *Behrman and Edwards*, 1967; *Bamford and Tipper*, 1972.]. Thus the concentration of ferrous iron (Fe^{+2}) in natural aerosols would have to exceed 2 mmol l^{-1} in order for oxidation of this species to represent a significant sink for atmospheric H_2O_2. The concentration of sulfite (SO_3^{-2}) would have to exceed 1000 mmol l^{-1}. Marine and background aerosols appear to contain much smaller concentrations of such species [*Junge*, 1963]. However, air parcels influenced by urban pollution have considerably higher concentrations of aerosols [*Whitby*, 1978] and might contain sufficient quantities of reduced material to provide an efficient sink for atmospheric H_2O_2. Note that if rapid chemical destruction of H_2O_2 were to occur in natural aerosols, the loss rate would be limited by supply of H_2O_2 to particle surfaces. For a sticking probability of 10^{-3}, this limit corresponds to an effective removal frequency of about 5×10^{-6} s^{-1} in the boundary layer.

In summary, the limited data available for aerosol distributions and for solution chemistry of H_2O_2 suggest that aerosol processes do not represent a significant sink for H_2O_2 in clean air. Similar arguments may be advanced for CH_3OOH, OH, and HO_2. Aerosol losses could be marginally important for HO_2 if the sticking probability were anomalously high ($\gtrsim$0.1) and if destruction of adsorbed HO_2 were instantaneous [*Warneck*, 1974]. In this case, OH concentrations would be reduced slightly (1–5%). It is possible, however, that aerosols could play an important role in removal of peroxides (including HO_2) from the polluted atmosphere, and in clouds these species would be significantly depleted by solution in liquid droplets.

APPENDIX 2. MODEL DESCRIPTION

The photochemical model discussed here is similar to the stratospheric model described by *Wofsy* [1978] and *Logan et al.* [1978]. Numerical methods are the same as those of the earlier work. Distributions for the long-lived gases (H_2O, O_3, CO, CH_4, and H_2) are prescribed as functions of latitude and season using observational data (see Table 4). The vertical resolution of the model is 2 km except near the ground where computations are carried out at 0, 0.5, 1, and 2 km. The latitudinal resolution is 15° from 0° to 60° latitude. Atmospheric structure (*T*, *P*) [*U.S. Standard Atmosphere Supplements*, 1966] and stratospheric ozone profiles [*Hering and Borden*, 1975] are specified.

Distributions for NO_x could not be specified from available data and were derived therefore from a series of one-dimensional eddy diffusion calculations. Nitric acid and NO_x (= NO + NO_2 + NO_3 + 2 · N_2O_5 + $ClNO_3$ + HNO_2 + HO_2NO_2) were allowed to diffuse separately. Partitioning among NO_x species and rates of chemical interchange between HNO_3 and NO_x were calculated by using the photochemical model discussed in the text. The vertical transport coefficient was taken as constant (10^5 cm^2 s^{-1}) from the ground to 2 km below the tropopause. A somewhat smaller value (3×10^4 cm^2 s^{-1}) was adopted in the upper 2 km of the troposphere. (Concentrations of NO_x are insensitive to the vertical transport coefficient except near the boundaries.) The transport parameterization did not attempt to simulate in detail the boundary layer near the surface. The lowest 100 m may be shown to have little influence on the global budgets of interest here.

The NO_x model was run for four seasons in each hemisphere at latitudes of 15° and 45°. The following boundary conditions were adopted:

1. A downward flux of (HNO_3 + NO_x) was assumed across the tropopause, with magnitude 1.4×10^8 cm^{-2} s^{-1}. This value was calculated in two-dimensional and three-dimensional model studies [*Wofsy*, 1978; *Logan et al.*, 1978; *Levy et al.*, 1980] as the net flux resulting from photooxidation of stratospheric N_2O (2×10^8 cm^{-2} s^{-1}), less recombination of NO with N (6×10^7 cm^{-2} s^{-1}). The relative abundances of HNO_3 and NO_x at the upper boundary were fixed at a global mean value (7:1) derived from model calculations.
2. A relatively large deposition velocity (0.5 cm s^{-1}) was adopted for HNO_3 at the surface, reflecting the high reactivity and solubility of the gas.
3. Rainout and washout of HNO_3 were parameterized as given in Table 1, consistent with the recent discussion of *Levine and Schwartz* [1981]. The lifetime for tropospheric HNO_3 in the model had a mean value of 10 days.
4. The surface flux of NO_x was set equal to zero over the oceans (model A). The concentration of odd nitrogen was prescribed over the continents (model B) to have a value of 100 ppt at the ground.
5. Oxidation of NH_3, lightning, and other processes were assumed to produce an in situ source of NO_x distributed through the troposphere as shown in Figure 12. The height-integrated magnitude of this source was set equal to 3×10^9 cm^{-2} s^{-1}.

The budget studies of CH_3CCl_3, $CFCl_3$, CF_2Cl_2, and CO employed the box model for tropospheric transport described in section 5. Profiles for OH were calculated in each box at an appropriate mean latitude (45°N, 15°N, 15°S, and 45°S) for four seasons. Separate calculations were performed for marine and continental distributions of NO_x (models A and B, respectively) weighted by appropriate ocean/land coverage in each box. More detailed latitude resolution produced insignificant changes (<5%) in global budgets. Production and loss rates for various species (CO, CH_4, CH_3CCl_3, etc.) were calculated by suitably weighting these 32 calculations.

Since completion of the calculations presented here, revised rate constant data have been reported for reactions involving HNO_3 and HO_2NO_2 [*NASA*, 1981]. Incorporation of these data in the model leads to slight reduction (<5%) in calculated concentrations of OH. The model indicates significant concentrations of HO_2NO_2 in the colder regions of the middle and upper troposphere, ($[HO_2NO_2] \approx [HNO_3]$). The new rates reduce photochemical production of O_3 by as much as 20% at midlatitudes, by ~5% in the tropics, but have only minor influence on budgets for CH_4, CO, CH_3CCl_3, etc.

APPENDIX 3. INFLUENCE OF AEROSOLS AND CLOUDS ON THE MEAN INSOLATION

Estimates of rates for photolysis of O_3 and NO_2 require accurate computation of the ultraviolet radiation field. The intensity of light in the troposphere is determined by the extra-

TABLE A1. Ultraviolet Fluxes and Cross Sections

λ(Å)	$F\lambda$(photon cm^{-2} s^{-1}) in 50 Å Interval	σ_{O_3}(cm^2)	O(^1D) Quantum Yield 220°K	O(^1D) Quantum Yield 300°K
2825	2.00×10^{14}	27×10^{-19}	1.00	1.00
2875	2.70	16	1.00	1.00
2925	3.63	10	1.00	1.00
2975	3.88	4.7	1.00	1.00
3025	3.97	2.6	0.98	1.00
3075	4.64	1.4	0.63	0.86
3125	5.43	0.68	0.09	0.30
3175	6.18	0.36	0.00	0.03
3225	6.99	0.18		0.00
3275	7.79	0.077		
3325	8.09	0.041		
3375	8.33	0.020		
3425	8.59	0.007		
3475	8.85	0.004		
3525	9.13	0.002		
3575	9.56			
3625	10.05			
3675	10.25			
3725	10.15			
3775	10.05			
3825	10.3			
3875	11.4			
3925	13.6			
3975	16.3			
4025	17.1			

terrestrial solar flux, transmission through the stratosphere, absorption and scattering by tropospheric gases and aerosols, and reflection from clouds and the earth's surface.

The flux of solar radiation was taken from recent observations [*Vernazza et al.*, 1976], averaged over 50 Å intervals, as given in Table A1. Absorption cross sections were averaged over the same intervals. The influence of attenuation, molecular scattering, and reflection was modeled in each wavelength interval by the equation of radiative transfer for an inhomogeneous, plane-parallel atmosphere [*Chankdresekhar*, 1960]. A second-order finite difference scheme [*Prather*, 1974] was used to solve for the intensity of radiation at three quadrature angles. The angular distribution of light scattered by air molecules was approximated by Rayleigh's phase function.

The influence of wavelength resolution was examined by carrying out calculations for wavelength intervals of 10 Å. Rates for important photolytic processes, for example production of O(^1D), changed by less than 2%. We conclude that negligible error is introduced by averaging solar flux and absorption cross sections over the wavelength intervals adopted here.

The influence of aerosols and clouds must be included in a realistic calculation of the tropospheric radiation field. Data collected by the *World Meteorological Organization* (WMO) [1972–1976] show that the contribution of aerosols to the optical depth at 3100 Å is about 0.4, on average, for tropical sites, and also for mid-latitude locations during summer. Extinction by aerosols is less important in winter at middle and high latitudes. Observations of turbidity by *McCartney and Unsworth* [1978] and *Elterman et al.* [1969] indicate aerosol extinction similar to that derived from the WMO network. More than half of the aerosol extinction occurs in the lowest 2 km of the atmosphere, although as much as 20% may be distributed through the middle and upper troposphere [*Elterman et al.*, 1969].

Optical depths associated with extinction by aerosols are comparable to the optical depth due to Rayleigh scattering, about 1.2 at 3100Å [*Edlen*, 1953; *Penndorf*, 1957]. Extinction by natural aerosols results from both scattering and absorption. *Fischer* [1973], *Hanel* [1976], *Levin and Lindberg* [1979], and *Gerber* [1979] report absorption amounting to 11–37% of scattering for a variety of marine and continental aerosols collected at unpolluted sites. We adopt a single scattering albedo of 0.75 for tropospheric aerosols, consistent with these observations [*Livshits*, 1977; *Hanel*, 1976; *Gerber*, 1979].

Figure 30 compares calculated extinction with data obtained by *Stair et al.* [1952, 1954, 1958] at several clean mountain locations. Daily minimum values for the optical depth at

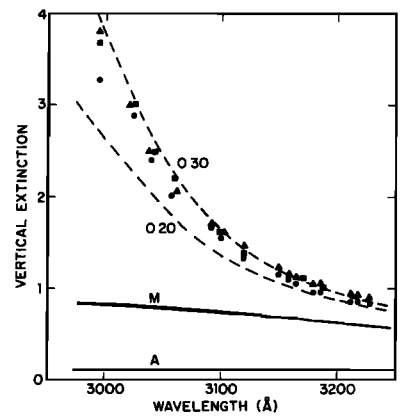

Fig. 30. Atmospheric extinction in the ultraviolet. Observations of the vertical opacity at Climax, Colorado (September 1951, solid circle), Sac Peak, New Mexico (July, 1953, solid triangle), and Mauna Loa, Hawaii (May, 1957, solid square) are from *Stair* [1952, 1956, 1958]. The model calculations are shown by the dashed lines and include absorption by ozone (0.2 and 0.3 cm-atm STP), Rayleigh scattering by molecules, and extinction by aerosols. Contribution to the total extinction from the molecular (M) and aerosol (A) components are shown separately. The aerosol extinction is based on the lowest quartile of the turbidity observations at Mauna Loa during May [*World Meteorological Organization*, 1973–1976].

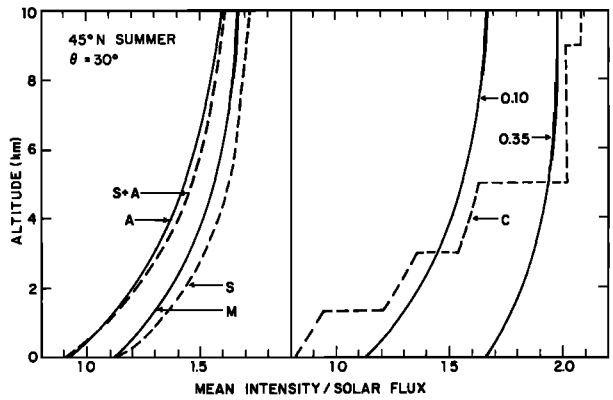

Fig. 31. Mean intensity of radiation at 3500 Å in the troposphere. The calculations were made with a 45°N summer atmosphere and a solar zenith angle of 30°. The right panel shows results for a clear, molecular atmosphere with Lambertian ground albedos of 0.10 and 0.35. This panel also shows the effects of the mean mid-latitude cloud model that has a planetary albedo of 0.35 and a ground albedo of 0.10 (curve C, see also Table 6). The left panel shows the effect of including aerosol scattering (S) and absorption (A) in the model, which has a ground albedo of 0.1. Curve M includes only molecular scattering. Curve S includes an aerosol extinction of 0.4, with a single scattering albedo of $\tilde{\omega} = 1.00$. Curve S+A includes the same aerosol extinction with $\tilde{\omega} = 0.75$. Curve A includes only the aerosol absorption component of S+A (i.e., total extinction of 0.1 with $\tilde{\omega} = 0.0$). In these calculations, aerosols are assumed to have a 2-km scale height and a scattering phase function described by *Deirmendjian* [1969] (haze L at 4500 Å).

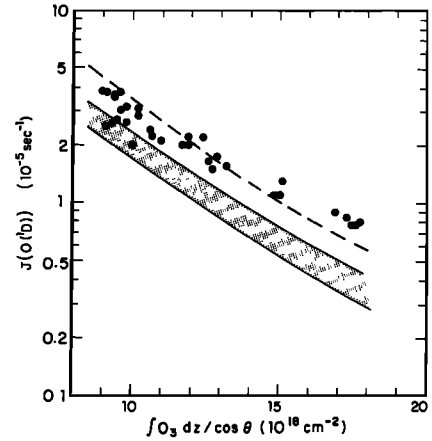

Fig. 32. Rate for production of $O(^1D)$ from O_3 photolysis as a function of the slant path column of ozone. The corrected $J(O^1D)$ values of *Dickerson et al.* [1979, 1980] are shown as a function of the overhead ozone column and the solar zenith angle (θ). The theoretical calculations are described in Appendix 3 and used the 45°N July atmosphere with a lower boundary of 300°K at 1.8 km. The shape of the ozone profile was taken from *Krueger and Minzner* [1976] with a column abundance of 8.5×10^{18} cm^{-2}. A ground albedo of 0.15 was adopted to simulate the mean radiation field. Since the actinometer measurements were made over a black surface, the upward component of the radiation field was omitted in this estimate of the photolysis rate for ozone. The shaded area corresponds to a range of aerosol extinctions observed during the summer months at Boulder, Colorado. If we assume a single scattering albedo of 0.75, the aerosol absorption optical depth at Boulder ranges from 0.03 to 0.14 [*World Meteorological Organization*, 1975–1976]. The dashed line corresponds to no aerosol absorption and a ground albedo of 0.30, without a localized black surface.

3100 Å due to aerosols is observed to be in excess of 0.08 on 75% of clear days at Mauna Loa [*WMO*, 1972–1976, statistics for May], and the figure suggests that similar values may apply at other mountain sites. Thus, aerosols may contribute to extinction of sunlight even under very clear conditions.

The omnidirectional intensity at 3500 Å and the production rate of $O(^1D)$ are shown in Figure 31. The calculations were performed with a variety of models for scattering and absorption by aerosols, with conditions appropriate for summer at mid-latitudes. The angular dependence of scattering by aerosols was represented by *Deirmendjian*'s [1969] haze L, H, or M (4500Å). These haze models span the range of size distributions observed for natural aerosols [*Junge*, 1972; *Meszaros and Vissy*, 1974; *Hanel and Bullrich*, 1978; *Jaenicke*, 1978]. The radiative transfer equation was solved in a manner similar to that described above but with 20 quadrature angles. The figure shows that scattering by aerosols is unimportant for optical depths typical of clean conditions. This result follows from the forward-peaked scattering that characterizes natural hazes. On the other hand, absorption by aerosols leads to significant reduction in the intensity of UV light, with a corresponding decrease in production of $O(^1D)$. The marked difference between these results and *Fiocco et al.* [1979] reflects their choice of single-scattering albedo (0.99) and their selection of a size distribution for aerosols dominated by very small (Rayleigh) particles.

Model calculations for production of $O(^1D)$ at Boulder, Colorado, are compared in Figure 32 with observations by *Dickerson* [1980]. Model and observations agree fairly well at small solar zenith angles. Observations are significantly higher (~70%) than calculations, however, when the sun is low in the sky. Specular reflection of sunlight might increase the effective ground albedo at low sun angles, with corresponding enhancement of $J(O(^1D))$ (see dashed curve in Figure 32). It appears that the observed variability of $O(^1D)$ production [*Dickerson et al.*, 1979; *Dickerson*, 1980] may be mediated largely by fluctuations in atmospheric aerosols.

Cloudiness plays a major role in determining the intensity of solar radiation in the troposphere, and the mean concentration of OH is sensitive to the global distribution of clouds. We calculated the net effects of clear, cloudy, and partly cloudy conditions by averaging radiation fields for cloudy and cloud-free atmospheres. Cloud layers were represented by totally reflecting Lambertian surfaces with cloud coverage adjusted to give the observed mean albedo of the earth, about 0.25 in the tropics and 0.35 at mid-latitudes [*Raschke et al.*, 1973; *Jacobowitz et al.*, 1979]. Cloud heights were chosen to reflect the distribution reported by *London* [1952]. The model reproduces the mean insolation observed at ground stations [*Burt and Quinn*, 1967].

TABLE A2. Global Mean Cloud Distribution

	Albedo[a]	Altitude, km[b]	Cloud Cover[b]	
			Tropics	Mid-latitudes
Cloud Type				
Cirrus	0.20	9	0.081	0.107
Cumulonimbus, nimbostratus	0.90	5	0.069	0.125
Cumulus	0.70	3	0.087	0.095
Stratus	0.50	1.5	0.055	0.156
Average surface	0.10			
Land	0.14			
Ocean	0.08			

[a] *Conover* [1965].

[b] The distribution of cloud cover given by *London* [1952] has been scaled to give an albedo of 0.25 in the tropics and 0.35 at mid-latitudes [*Raeschke et al.*, 1973].

Table A2 gives a summary of parameters used to calculate the radiation field for global-average conditions. The standard model incorporates absorption and scattering by molecules and absorption due to aerosols (curve A in Figure 31). Scattering by aerosols is neglected.

Acknowledgments. The authors would like to thank H. J. Mastenbrook and A. B. Pittock for generously providing unpublished measurements of tropospheric H_2O and O_3 and for permitting us to analyze and present these data. A. H. Oort kindly supplied analyses of the NOAA specific humidity data. J. Mill of the U.S. Air Force (ETAC) went to considerable effort to locate computer tapes of Mastenbrook's data. We would like to acknowledge useful discussions with D. Kley and H. Levy II. We are indebted to many colleagues who made data available prior to publication. C. Spivakovsky assisted in the analysis of the water vapor and halocarbon data. Special thanks are due to F. Forrestel Zingale for expert editorial assistance. This work was supported by the National Science Foundation and the National Aeronautics and Space Administration under grants ATM79-13251 and NSG-2031, respectively. Acknowledgment is made to both the National Center for Atmospheric Research, which is sponsored by the National Science Foundation, and the Ames Research Center of NASA for computer time.

REFERENCES

Amimoto, S. T., A. P. Force, and J. R. Wiesenfeld, Ozone photochemistry: Production and deactivation of $O(2^1D_2)$ following photolysis at 248 nm, *Chem. Phys. Lett., 60,* 40–43, 1978.

Amimoto, S. T., A. P. Force, R. G. Gulotty, and J. R. Weisenfeld, Collisional deactivation of $O(2^1D_2)$ by the atmospheric gases, *J. Chem. Phys., 71,* 3640–3647, 1979.

Angell, J. K., and J. Korshover, Global ozone variations: An update into 1976, *Mon. Weather Rev., 106,* 725–737, 1978.

Apling, A. J., G. J. Potter, and M. L. Williams, Air pollution from oxides of nitrogen, carbon monoxide and hydrocarbons, *Rep. LR306,* Warren Spring Lab., Stevenage, England, 1979.

Arnold, J. E. M., and J. Jongma, Fuelwood and charcoal in developing countries, *Unasylva, 29,* 2–9, 1978.

Atkinson, R., K. R. Darnall, A. C. Lloyd, A. M. Winer, and J. N. Pitts, Jr., Kinetics and mechanisms of the reactions of the hydroxyl radical with organic compounds in the gas phase, *Advan. Environ. Sci. Tech., 11,* 375–488, 1979.

Attmannspacher, W., and R. Hartmannsgruber, Some results of 6 years (1967–1972) of regular ozone soundings at the Meteorological Observatory Hohenpeissenberg, FRG, *Beit. Phys. Atmos., 49,* 18–33, 1976.

Ayers, G. P., and J. L. Gras, Ammonia gas concentrations over the Southern Ocean, *Nature, 284,* 539–540, 1980.

Baldwin, A. C., and D. M. Golden, Heterogeneous atmospheric reactions: Sulfuric acid aerosols as tropospheric sinks, *Science, 206,* 562–563, 1979.

Bamford, C. H., and C. F. H. Tipper, *Chemical Kinetics,* vol. 6 and 7, Elsevier New York, 1972.

Barrett, R. E., S. E. Miller, and D. W. Locklin, Field investigation of emissions from combustion equipment for space heating, *EPA-R2-73-084a,* U.S. Environ. Prot. Agency, Washington, D. C., 1973.

Bass, A. M., L. C. Glasgow, C. Miller, J. P. Jesson, and D. L. Filkin, Temperature dependent absorption cross sections for formaldehyde: The effect of formaldehyde on stratospheric chlorine chemistry, *Planet. Space Sci., 28,* 675–679, 1980.

Bauer, E., A catalog of perturbing influences on stratospheric ozone, 1955–1975, *J. Geophys. Res., 84,* 6926–6940, 1979.

Bauer, K., W. Seiler, and H. Giehl, CO production by higher plants, *Zeit. Pflanzenphys., 94,* 219–230, 1979.

Baulch, D. L., R. A. Cox, R. F. Hampson, J. A. Kerr, J. Troe, R. T. Watson, Evaluated kinetic and photochemical data for atmospheric chemistry, *J. Phys. Chem. Ref. Data, 9,* 295–472, 1980.

Becker, K., D. Jost, K. U. Martin, and H. Neidhard, Recommendations to reduce the emission of pollutants. Motor vehicle exhaust emissions, *Rep. 7/76,* Fed. Environ. Agency, Berlin, Fed. Rep. of Germany, 1976.

Behrman, E. J., and J. O. Edwards, Nucleophilic displacements on peroxide oxygen and related reactions, in *Progress in Physical Organic Chemistry,* vol. 4, edited by A. Streitweiser and R. W. Taft, Interscience, New York, 1967.

Bidwell, R. G. S., and D. E. Fraser, Carbon monoxide uptake and metabolism by leaves, *Can. J. Bot., 50,* 1435–1439, 1972.

Biermann, H. W., C. Zetzsch, and F. Stuhl, On the pressure dependence of the reaction of HO and CO, *Ber. Bunsenges. Phys. Chem., 82,* 633–639, 1978.

Bigg, E. K., Some properties of the aerosol at Mauna Loa Observatory, *J. Appl. Meteorol., 16,* 262–267, 1977.

Bleichrodt, J. F., Mean tropospheric residence time of cosmic-ray-produced beryllium fat north temperate latitudes, *J. Geophys. Res., 83,* 3058–3062, 1978.

Blifford, I. H., Tropospheric aerosols, *J. Geophys. Res., 75,* 3099–3103, 1970.

Blifford, I. H., and L. D. Ringer, The size and number distribution of aerosols in the continental troposphere, *J. Atmos. Sci., 26,* 716–726, 1969.

Bourliere, F., and M. Hadley, The ecology of tropical savannas, *Ann. Rev. Ecol. Syst., 1,* 125–152, 1970.

Brock, J. C., and R. T. Watson, Laser flash photolysis of ozone: $O(^1D)$ quantum yields in the fall-off region 297–325 nm, *Chem. Phys., 46,* 477–484, 1980.

Bush, Y. A., D. Parrish, and F. C. Fehsenfeld, Measurements of trace gases in the troposphere, Paper presented at CACGP symposium on the Budgets and Cycles of Trace Gases in the Atmosphere, Boulder, Colo., Aug. 12–18, 1979, Colorado.

Camargo, F. C., Report on the Amazon Region in, *Problems of the Humid Tropical Regions,* UNESCO, Paris, 1958.

Campbell, M. J., J. C. Sheppard, and B. F. Au, Measurement of hydroxyl concentration in boundary layer air by monitoring CO oxidation, *Geophys. Res. Lett., 6,* 175–178, 1979.

Cato, G. A., L. J. Muzio, and D. E. Shore, Field testing: Application of combustion modifications to control pollutant emissions from industrial boilers, Phase II, *EPA-600/2-76-086a,* U.S. Environ. Prot. Agency, Washington, D. C., 1976.

Chameides, W. L., Effect of variable energy input on nitrogen fixation in instantaneous linear discharges, *Nature, 277,* 123–125, 1979.

Chameides, W. L., and R. L. Cicerone, Effects of nonmethane hydrocarbons in the atmosphere, *J. Geophys. Res., 83,* 947–952, 1978.

Chameides, W., and J. C. G. Walker, A photochemical theory of tropospheric ozone, *J. Geophys. Res., 78,* 8751–8760, 1973.

Chandrasekhar, S., *Radiative Transfer,* Dover, New York, 1960.

Chang, J. S., and J. E. Penner, Analysis of global budgets of halocarbons, *Atmos. Environ., 12,* 1867–1873, 1978.

Chatfield, R., and H. Harrison, Tropospheric ozone, 2, Variations along a meridional band, *J. Geophys. Res., 82,* 5969–5976, 1977*a*.

Chatfield, R., and H. Harrison, Tropospheric ozone, 1, Evidence for higher background values, *J. Geophys. Res., 82,* 5965–5968, 1977*b*.

Chodes, N., J. Warner, and A. Gagin, A determination of the condensation coefficient of water from the growth rate of small cloud droplets, *J. Atmos. Sci., 31,* 1351–1357, 1974.

Conover, J. H., Cloud and terrestrial albedo determinations from TIROS satellite pictures, *J. Appl. Meteorol., 4,* 378–386, 1965.

Cox, R. A., and J. P. Burrows, Kinetics and mechanism of the disproportionation of HO_2 in the gas phase, *J. Phys. Chem., 83,* 2560–2568, 1979.

Cox, R. A., and M. J. Roffey, Thermal decomposition of peroxyacetyl nitrate in the presence of NO, *Environ. Sci. Tech., 11,* 900–906, 1977.

Cox, R. A., and G. S. Tyndall, Rate constants for the reactions of CH_3O_2 with HO_2, NO and NO_2 using molecular modulation spectrometry, *J. Chem. Soc. Faraday II, 76,* 153–163, 1980.

Cox, R. A., R. G. Derwent, and P. M. Holt, Relative rate constants for the reactions of OH radicals with H_2, CH_4, CO, NO, and HONO at atmospheric pressure and 296°K, *J. Chem. Soc. Faraday I, 72,* 2031–2043, 1976.

Cox, R. A., R. G. Derwent, and M. R. Williams, Atmospheric photooxidation reactions: Rates, reactivity, and mechanism for reaction of organic compounds with hydroxyl radicals, *Environ. Sci. Tech., 14,* 57–61, 1979.

Crawford, A. R., E. H. Manny, and W. Bartok, Control of utility boiler and gas turbine pollutants emissions by combustion modification—Phase 1, *EPA-600/7-78-036a,* U. S. Environ. Prot. Agency, Washington, D. C., 1978.

Cronn, D., and E. Robinson, Tropospheric and lower stratospheric vertical profiles of ethane and acetylene, *Geophys. Res. Lett., 6,* 641–644, 1979.

Cronn, D. R., R. A. Rasmussen, E. Robinson, and D. E. Harsch, Hal-

ogenated compound identification and measurement in the troposphere and lower stratosphere, *J. Geophys. Res., 82,* 5935–5944, 1977.

Crutzen, P., A discussion of the chemistry of some minor constituents in the stratosphere and troposphere, *Pure Appl. Geophys., 106–108,* 1385–1399, 1973.

Crutzen, P., Photochemical reactions initiated by and influencing ozone in unpolluted tropospheric air, *Tellus, 26,* 47–57, 1974.

Crutzen, P., The role of NO and NO_2 in the chemistry of the troposphere and stratosphere, *Ann. Rev. Earth. Planet. Sci., 7,* 443–472, 1979.

Crutzen, P. J., and J. Fishman, Average concentrations of OH in the troposphere and the budgets of CH_4, CO, H_2, and CH_3CCl_3, *Geophys. Res. Lett., 4,* 321–324, 1977.

Crutzen, P. J., L. E. Heidt, J. P. Krasnec, W. H. Pollack, and W. Seiler, Biomass burning as a source of atmospheric gases CO, H_2, N_2O, NO, CH_3Cl, and COS, *Nature, 282,* 253–256, 1979.

Danielson, E., and V. Mohnen, Project Duststorm: Ozone transport, in situ measurements and meteorological analysis of tropopause folding, *J. Geophys. Res., 82,* 5867–5877, 1977.

Davis, D. D., W. Heaps, and T. McGee, Direct measurements of natural tropospheric levels of OH via an aircraft borne tunable dye laser, *Geophys. Res. Lett., 3,* 331–333, 1976.

Davis, D. D., M. O. Rodgers, S. D. Fischer, and K. Asai, An experimental assessment of the O_3/H_2O interference problem in the detection of natural levels of OH via laser induced fluorescence, *Geophys. Res. Lett., 8,* 69–72, 1981*a*.

Davis, D. D., M. O. Rodgers, S. D. Fischer, and W. S. Heaps, A theoretical assessment of the O_3/H_2O interference problem in the detection of natural levels of OH via laser induced fluorescence, *Geophys. Res. Lett., 8,* 73–76, 1981*b*.

Dawson, G. A., Nitrogen fixation by lightning, *J. Atmos. Sci., 37,* 174–178, 1980.

DeAngelis, D. G., and R. B. Reznik, Source assessment: Residential combustion of coal, *EPA-600/2-79-019a,* U.S. Environ. Prot. Agency, Washington, D. C., 1979.

Deirmendjian, D., *Electromagnetic Scattering on Spherical Polydispersions,* Elsevier, New York, 1969.

Derwent, R. G., and A. E. J. Eggleton, Halocarbon lifetimes and concentrations distributions calculated using a two-dimensional tropospheric model, *Atmos. Environ., 12,* 1261–1269, 1978.

Dickerson, R. R., Direct measurements of ozone and nitrogen dioxide photolysis rates in the atmosphere, Ph.D. thesis, Univ of Mich., Ann Arbor, 1980.

Dickerson, R. R., D. H. Stedman, W. L. Chameides, P. J. Crutzen, and J. Fishman, Actinometric measurements and theoretical calculations of $j(O_3)$, the rate of photolysis of ozone to $O(^1D)$, *Geophys. Res. Lett., 6,* 833–835, 1979 (correction, *Geophys. Res. Lett., 7,* 112, 1980).

Drummond, J. W., Atmospheric measurements of nitric oxide using a chemiluminescent detector, Ph.D. thesis, Univ. of Wyoming, Laramie, 1977.

Dütsch, H., The ozone distribution in the atmosphere, *Can. J. Chem., 52,* 1491–1504, 1974.

Dütsch, H., and C. C. Ling, Six years of regular ozone soundings over Switzerland, *Pure Appl. Geophys., 106–108,* 1151–1168, 1973.

Eckholm, E., Planting for the future: Forestry for human needs, *Pap. 26,* Worldwatch Inst., Washington, D. C., 1979.

Edlen, B., The dispersion of standard air, *J. Opt. Soc. Am., 43,* 339–344, 1953.

Edwards, J. O., *Peroxide Reaction Mechanisms,* Interscience, New York, 1962.

Ehhalt, D. H., The CH_4 concentration over the ocean and its possible variation with latitude, *Tellus, 30,* 169–176, 1978.

Ehhalt, D. H., and U. Schmidt, Sources and sinks of atmospheric methane, *Pure Appl. Geophys., 116,* 452–464, 1978.

Elterman, L., R. Wexler, and D. T. Chang, Features of tropospheric and stratospheric dust, *Appl. Opt., 8,* 893–903, 1969.

Fabian, P., and C. E., Junge, Global rate of O_3 destruction at the earth's surface, *Arch. Meteorol. Geoph. Biokl. Ser. A, 19,* 161–172, 1970.

Fabian, P., and P. G. Pruchniewicz, Meridional distribution of ozone in the troposphere and its seasonal variations, *J. Geophys. Res., 82,* 2063–2073, 1977.

Fabian, P., R. Borchers, K. H. Weiler, U. Schmidt, A. Volz, D. H. Ehhalt, W. Seiler, and F. Muller, Simultaneously measured vertical profiles of H_2, CH_4, CO, N_2O, $CFCl_3$, and CF_2Cl_2 in the mid-latitude stratosphere and troposphere, *J. Geophys. Res., 84,* 3149–3154, 1979.

Fairchild, C. E., E. J. Stone, and G. M. Lawrence, Photofragment spectroscopy of ozone in the UV region 270–310 nm and at 600 nm, *J. Chem. Phys., 69,* 3632–3638, 1978.

Fiocco, G., A. Mugnai, and W. Forlizzi, Effects of radiation scattered by aerosols on the photodissociation of ozone, *J. Atmos. Terr. Phys., 40,* 949–961, 1978.

Fischer, K., Mass absorption coefficient of natural aerosol particles in the 0.4-2.4 μm wavelength interval, *Beit. Phys. Atmos., 46,* 89–100, 1973.

Fishman, J., and P. J. Crutzen, The origin of ozone in the troposphere, *Nature, 274,* 855–857, 1978.

Fishman, J., and W. Seiler, The implication of some recent findings on the global distribution of the OH radical, *Eos Trans., AGU, 61,* 966, 1980.

Fishman, J., S. Solomon, and P. J. Crutzen, Observational and theoretical evidence in support of a significant in situ photochemical source of tropospheric ozone, *Tellus, 31,* 432–446, 1979.

Food and Agricultural Organization, Shifting cultivation, *Unasylva, 11,* 9–11, 1957 (reprinted in *Tropical Agriculture, 34,* 159–164, 1958).

Food and Agricultural Organization, *Production Yearbook 1977,* United Nations, New York, 1978.

Food and Agricultural Organization, Yearbook of forest production statistics 1966–1977, United Nations, Rome, 1979.

Fraser, P. J. B., and G. I. Pearman, Atmospheric halocarbons in the southern hemisphere, *Atmos. Environ., 12,* 839–844, 1978.

Galbally, I. E., and C. R. Roy, Loss of fixed nitrogen from soils by nitric oxide exhalation, *Nature 275,* 734–735, 1978.

Galbally, I. E., and C. R. Roy, Destruction of ozone at the earth's surface, *Q. J. R. Meteorol. Soc., 106,* 599–620, 1980.

Gebhart, R., R. Bojkov, and J. London, Stratospheric ozone: A comparison of observed and computed models, *Beit. Phys. Atmos., 43,* 209–227, 1970.

Georgii, H. W., and G. Gravenhorst, The ocean as source or sink of reactive trace gases, *Pure Appl. Geophys., 115,* 503–511, 1977.

Gerber, H. E., Absorption of 632.8 nm radiation by maritime aerosols near Europe, *J. Atmos. Sci., 36,* 2502–2512, 1979.

Gidel, L. T., and M. A. Shapiro, General circulation model estimates of the net vertical flux of ozone in the lower stratosphere and the implications for the tropospheric ozone budget, *J. Geophys. Res., 85,* 4049–4058, 1980.

Goldan, P., W. C. Custer, D. L. Albritton, and A. L. Schmeltekopf, Stratospheric $CFCl_3$, CF_2Cl_2, and N_2O height profile measurements at several latitudes, *J. Geophys. Res., 85,* 413–423, 1980.

Goreau, T. J., W. A. Kaplan, S. C. Wofsy, M. B. McElroy, F. W. Valois, and S. W. Watson, Production of NO^-_2 and N_2O by nitrifying bacteria at reduced concentrations of oxygen, *Appl. Environ. Microbiol., 40,* 526–532, 1980.

Gourou, P., *The Tropical World,* 4th ed., John Wiley, New York, 1966.

Graedel, T. E., Terpenoids in the atmosphere, *Rev. Geophys. Space Phys., 17,* 937–947, 1979.

Graham, R. A., and H. S. Johnson, Photochemistry of NO_3 and the kinetics of the N_2O_5-O_3 system, *J. Phys. Chem., 82,* 254–268, 1978.

Graham, R. A., A. M. Winer, and J. N. Pitts, Temperature dependence of the unimolecular decomposition of pernitric acid and its atmospheric implications, *Chem. Phys. Lett., 51,* 215–220, 1977.

Gras, J. L., and C. G. Michael, Measurement of the stratospheric aerosol particle size distribution, *J. Appl. Meteorol., 18,* 855–860, 1979.

Grigg, D. B., *The Agricultural Systems of the World,* Cambridge University Press, New York, 1974.

Griggs, M., Absorption coefficients of ozone in the ultraviolet and visible regions, *J. Chem. Phys., 49,* 857–859, 1968.

Grimsrud, E. P., and R. A. Rasmussen, The analysis of chlorofluorocarbons in the troposphere by gas chromatography mass spectrometry, *Atmos. Environ., 9,* 1010–1013, 1975.

Grimsrud, E. P., H. H. Westberg, and R. A. Rasmussen, Atmospheric reactivity of monoterpene hydrocarbons, NO_x photo-oxidation and ozonolysis, *Int. J. Chem. Kin. Symp., 1,* 183–195, 1975.

Hameed, S., J. P. Pinto, and R. W. Stewart, Sensitivity of the predicted CO-OH-CH_4 perturbation to tropospheric NO_x concentrations, *J. Geophys. Res., 84,* 763–768, 1979.

Hamilton, E. J., and R. R. Lii, The dependence on H_2O and on NH_3 of the kinetics of the self-reaction of HO_2 in the gas-phase: Formation of HO_2-H_2O and HO_2-NH_3 complexes, *Int. J. Chem. Kin., 9,* 875–885, 1977.

Hampson, R. F., and D. Garvin, Reaction rate and photochemical data for atmospheric chemistry—1977, *Spec. Publ. 513,* Natl. Bur. Stand., Washington, D. C., 1978.

Hancock, G., W. Lange, M. Lenzi, and K. H. Welge, Laser fluorescence of NH_2 and rate constant measurement of NH_2 + NO, *Chem. Phys. Lett., 33,* 168–172, 1977.

Hanel, G., The properties of atmospheric aerosol particles as functions of the relative humidity at thermodynamic equilibrium with the surrounding moist air, *Advan. Geophys., 19,* 73–188, 1976.

Hanel, G., and K. Bullrich, Physico-chemical property models of tropospheric aerosol particles, *Beit. Phys. Atmos., 51,* 129–138, 1978.

Heidner, R. F., D. Husain, and J. R. Weisenfeld, Kinetic investigation of electronically excited oxygen atoms $O(2^1D_2)$ by time resolved attenuation of atomic resonance radiation in the vacuum ultraviolet, 2, Collisional quenching by the atmospheric gases N_2, O_2, CO, CO_2, H_2O, and O_3, *J. Chem. Soc. Faraday II, 69,* 927–937, 1973.

Heidt, L. E., and D. H. Ehhalt, Corrections of CH_4 concentrations measured prior to 1974, *Geophys. Res. Lett., 7,* 1023, 1980.

Heidt, L. E., J. P. Krasnec, R. A. Lueb, W. H. Pollock, B. E. Henry, and P. J. Crutzen, Latitudinal distributions of CO and CH_4 over the Pacific, *J. Geophys. Res., 85,* 7329–7336, 1980.

Heidt, L. E., R. Lueb, W. Pollock, and D. H. Ehhalt, Stratospheric profiles for CCl_3F and CCl_2F_2, *Geophys. Res. Lett., 2,* 445–447, 1975.

Hendry, D. G., and R. A. Kenley, Atmospheric chemistry of peroxynitrates, in *Nitrogeneous Air Pollutants: Chemical and Biological Implications,* edited by D. Grosjean, Ann Arbor Science, Michigan, 1979.

Hering, W. S., and T. R. Borden, Ozonesonde observations over North America, vol. 2, *Environ. Res. Pap. 38, AFCRL-64-30(II),* Air Force Cambridge Res. Labs., Cambridge, Mass., 1964.

Hering, W. S., and T. R. Borden, Ozonesonde observations over North America, Vol. 4., *Environ. Res. Pap. 279, AFCRL-64-30(IV),* Air Force Cambridge Res. Labs., Cambridge, Mass., 1967.

Hering, W. S., and T. R. Borden, Ozonesonde observations over North America 1967–1969, report, Air Force Cambridge Res. Lab., Cambridge, Mass., 1975.

Herron, J. T., and R. E. Huie, Stopped flow studies of the mechanisms of ozone-alkene reactions in the gas phase: Ethylene, *J. Am. Chem. Soc., 99,* 5430–5435, 1977.

Herron, J. T., and R. E. Huie, Stopped flow studies of the mechanisms of ozone-alkene reactions in the gas phase: Propene and isobutene, *Int. J. Chem. Kin., 10,* 1019–1041, 1978.

Hester, N. E., E. R. Stephens, and O. C. Taylor, Fluorocarbon air pollutants, Measurements in the lower stratosphere, *Environ. Sci. Tech., 9,* 875–876, 1975.

Hiatt, R., *Organic Peroxides,* vol. 2, *Hydroperoxides,* edited by D. Swern, pp. 1–151, Interscience, New York, 1971.

Hill, R. D., R. G. Rinker, and H. D. Wilson, Atmospheric nitrogen fixation by lightning, *J. Atmos. Sci., 37,* 179–192, 1980.

Ho, W., G. M. Hidy, and R. M. Govan, Microwave measurements of the liquid water content of atmospheric aerosols, *J. Appl. Meteorol, 13,* 871–879, 1974.

Holdren, M. W., H. H. Westberg, and P. R. Zimmerman, Analysis of monoterpene hydrocarbons in rural atmospheres, *J. Geophys. Res., 84,* 5083–5088, 1979.

Hopkins, B., Observations on savanna burning in the Olokemeji Forest Reserve, Nigeria, *J. Appl. Ecol., 2,* 367–381, 1965.

Howard, C. J., Kinetics of the reaction of HO_2 with NO_2, *J. Chem. Phys., 67,* 5258–5263, 1977.

Howard, C. J., Temperature dependence of the reaction HO_2 + NO $\rightarrow$OH + NO_2, *J. Chem. Phys., 71,* 2352–2359, 1979.

Huebert, B. J., Nitric acid and aerosol nitrate measurements in the equatorial Pacific region, *Geophys. Res. Lett., 7,* 325–328, 1980.

Huebert, B. J., and A. L. Lazrus, Global tropospheric measurements of nitric acid vapor and particulate nitrates, *Geophys. Res. Lett., 5,* 577–580, 1978.

Huebert, B. J., and A. L. Lazrus, Tropospheric gas phase and particulate nitrate measurements, *J. Geophys. Res., 85,* 7322–7328, 1980.

International Petroleum Encyclopedia, Petroleum Publishing, Tulsa, Okla., 1979.

Jacobowitz, H., W. L. Smith, H. B. Howell, F. W. Nagle, and J. R. Hickey, The first 18 months of planetary radiation budget measurements from the Nimbus-6 ERB experiment, *J. Atmos. Sci., 36,* 501–507, 1979.

Jaenicke, R., Aitken particle size distribution in the Atlantic North East trade winds, *Meteor. Forsch. Ergebnisse, B13,* 1–9, 1978.

Jaenicke, R., C. Junge, and H. J. Kanter, Messungen der Aerosolgrossenverteilung uber dem Atlantik, *Meteorol. Forsch. Ergebnisse, B7,* 1–54, 1971.

Jaffe, L. S., Carbon monoxide in the biosphere: Sources, distribution and concentration, *J. Geophys. Res., 78,* 5293–5305, 1973.

Japar, S. M., C. H. Wu, and H. Niki, Rate constants for the reaction of ozone with olefins in the gas phase, *J. Phys. Chem., 78,* 2318–2320, 1974.

Jeong, K.-M., and F. Kaufman, Rates of the reactions of 1,1,1-trichloroethane and 1,1,2-trichloroethane with OH, *Geophys. Res. Lett., 6,* 757–759, 1979.

Junge, C., *Air Chemistry and Radioactivity,* Academic, New York, 1963.

Junge, C., Our knowledge of the physico-chemistry of aerosols in the undisturbed marine environment, *J. Geophys. Res., 77,* 5183–5200, 1972.

Junge, C., W. Seiler, and P. Warneck, The atmospheric ^{12}CO and ^{14}CO budget, *J. Geophys. Res., 76,* 2866–2879, 1971.

Kajimoto, O., and R. J. Cvetanovic, Absolute quantum yield of $O(^1D_2)$ in the photolysis of ozone in the Hartley band, *Int. J. Chem. Kin., 11,* 605–612, 1979.

Kan, C. S., and J. G. Calvert, Water vapor dependence of the kinetics of the CH_3O_2-CH_3O_2 reaction, *Chem. Phys. Lett., 63,* 111–114, 1979.

Keeling, C. D., Industrial production of carbon dioxide from fossil fuels and limestone, *Tellus, 25,* 174–198, 1973.

Kelly, T. J., D. H. Stedman, J. A. Ritter, and R. B. Harvey, Measurements of oxides of nitrogen and nitric acid in clean air, *J. Geophys. Res., 85,* 7417–7425, 1980.

Kemp, V. E., and O. W. Dykema, Inventory of combustion related emissions from stationary sources (second update), *EPA-600/7-78-100,* U.S. Environ. Prot. Agency, Washington, D. C., 1978.

Keyser, L. F., Absolute rate constant of the reaction OH $+H_2O_2 \rightarrow HO_2 + H_2O$ from 245 to 423 K, *J. Phys. Chem., 84,* 1659–1663, 1980.

Kley, D., J. W. Drummond, M. McFarland, and S. C. Liu, Tropospheric profiles of NO_x, *J. Geophys. Res.,* 86, 3153–3161, 1981.

Klippel, W., and P. Warneck, Formaldehyde in rain water and on the atmospheric aerosol, *Geophys. Res. Lett., 5,* 177–179, 1978.

Klippel, W., and P. Warneck, The formaldehyde content of the atmospheric aerosol, *Atmos. Environ., 14,* 809–818, 1980.

Krey, P. W., R. J. Lagomarsino, and L. E. Toonkel, Gaseous halogens in the atmosphere in 1975, *J. Geophys. Res., 82,* 1753–1766, 1977.

Kurasawa, H., and R. Lesclaux, Kinetics of the reaction of NH_2 with NO, *Chem. Phys. Lett., 66,* 602–607, 1979.

Kurasawa, H., and R. Lesclaux, Rate constant for the reaction of NH_3 with ozone in relation with atmospheric processes, *Chem. Phys. Lett., 72,* 437–442, 1980.

Kurylo, M. J., P. C. Anderson, and O. Klais, A flash photolysis, resonance fluorescence investigation of the reaction OH + CH_3CCl_3 $\rightarrow H_2O$ + CH_2CCl_3, *Geophys. Res. Lett., 6,* 760–762, 1979.

Lee, L. C., and T. G. Slanger, Atmospheric OH production: The $O(^1D)$ + H_2O reaction rate, *Geophys. Res. Lett., 6,* 165–166, 1979.

Lesclaux, R., and M. DeMissy, On the reaction of NH_2 radical with oxygen, *Nouv. J. Chim., 1,* 443–444, 1977.

Levin, Z., and J. D. Lindberg, Size distribution, chemical composition, and optical properties of urban and desert aerosols in Israel, *J. Geophys. Res., 84,* 6941–6950, 1979.

Levine, S. Z., and S. E. Schwartz, In-cloud and below cloud scavenging of nitric acid vapor, *Atmos. Environ.,* in press, 1981.

Levy, H., II, Normal atmosphere: Large radical and formaldehyde concentrations predicted, *Science, 173,* 141–143, 1971.

Levy, H., II, Photochemistry of the lower troposphere, *Planet. Space Sci., 20,* 919–935, 1972.

Levy, H., II, Photochemistry of the troposphere, *Advan. Photochem., 9,* 369–524, 1974.

Levy, H., II, J. D. Mahlman, and W. J. Moxim, A stratospheric source of reactive nitrogen in the unpolluted troposphere, *Geophys. Res. Lett., 7,* 441–444, 1980 (correction, *Geophys. Res. Lett., 7,* 854, 1980).

Liebl, K. H., and W. Seiler, CO and H_2 destruction at the soil surface,

in *Microbial Production and Utilization of Gases*, edited by H. G. Schlegel, G. Gottschalk, and N. Pfennig, Göttingen Akademie der Wissenschaften, 1976.

Lin, C. L., and W. B. DeMore, $O(^1D)$ production in ozone photolysis near 3100A, *J. Photochem., 2*, 161–164, 1973.

Lin, C. L., N. K. Rohotgi, and W. B. DeMore, Ultraviolet absorption cross sections of hydrogen peroxide, *Geophys. Res. Lett., 5*, 113–115, 1978.

Linnenbom, V. J., J. W. Swinnerton, and R. A. Lamontagne, The ocean as a source of atmospheric CO, *J. Geophys. Res., 78*, 5833–5840, 1973.

Liu, S. C., D. Kley, M. McFarland, J. D. Mahlman, and H. Levy, On the origin of tropospheric ozone, *J. Geophys. Res., 85*, 7546–7552, 1980.

Livshits, G. S., Atmospheric aerosol absorption in the ultraviolet, *Izv. Atmos. Oceanic Phys., 13*, 839–840, 1977.

Logan, J. A., M. J. Prather, S. C. Wofsy, and M. B. McElroy, Atmospheric chemistry: Response to human influence, *Phil. Trans. R. Soc. London, Ser. A., 290*, 187–234, 1978.

London, J., The distribution of radiational temperature change in the northern hemisphere during March, *J. Meteorol., 9*, 145–151, 1952.

Lovelock, J. E., Atmospheric fluorine compounds as indicators of air movement, *Nature, 230*, 379, 1971.

Lovelock, J. E., Atmospheric turbidity and CCl_3F concentrations in rural southern England and southern Ireland, *Atmos. Environ., 6*, 917–925, 1972.

Lovelock, J. E., Atmospheric halocarbons and stratospheric ozone, *Nature, 252*, 292–294, 1974.

Lovelock, J. E., Methyl chloroform in the troposhere as an indicator of OH radical abundance, *Nature, 267*, 32, 1977.

Lovelock, J. E., R. J. Maggs, and R. J. Wade, Halogenated hydrocarbons in and over the Atlantic, *Nature, 241*, 194–196, 1973.

Lowe, D. C., U. Schmidt, and D. H. Ehhalt, A new technique for measuring tropospheric formaldehyde, *Geophys. Res. Lett., 7*, 825–828, 1980.

Lydolph, P. E., *Geography of the U.S.S.R.*, John Wiley, New York, 1970.

Mahlman, J. D., and W. J. Moxim, Tracer simulation using a global general circulation model: Results from a mid-latitude instantaneous source experiment, *J. Atmos. Sci., 35*, 1340–1374, 1978.

Mahlman, J. D., H. Levy, and W. J. Moxim, Three-dimensional tracer structure and behavior as simulated in two ozone precursor experiments, *J. Atmos. Sci., 37*, 655–685, 1980.

Mastenbrook, H. J., Water vapor observations at low, middle and high latitudes during 1964 and 1965, *Rep. 6447*, Naval Res. Lab., Washington, D. C., 1966.

Mastenbrook, H. J., Water vapor distribution in the stratosphere and high troposphere, *J. Atmos. Sci., 25*, 299–311, 1968.

McCarthy, R. L., F. A. Bower, and J. P. Jesson, The fluorocarbon-ozone theory, I, World Production and release of CCl_3F and CCl_2F_2 through 1975, *Atmos. Environ., 11*, 491–497, 1977.

McCartney, H. A., and M. H. Unsworth, Spectral distribution of solar radiation, I, Direct radiation, *Q. J. R. Meteorol. Soc., 104*, 699–718, 1978.

McConnell, J. C., Atmospheric ammonia, *J. Geophys. Res., 78*, 7812–7821, 1973.

McConnell, J. C., and H. I. Schiff, Methyl chloroform: Impact on stratospheric ozone, *Science, 199*, 174–177, 1978.

McConnell, J. C., M. B. McElroy, and S. C. Wofsy, Natural sources of atmospheric CO, *Nature, 233*, 187–188, 1971.

McFarland, M., D. Kley, J. W. Drummond, A. L. Schmeltekopf, and R. J. Winkler, Nitric oxide measurements in the equatorial Pacific region, *Geophys. Res. Lett., 6*, 605–608, 1979.

Meszaros, A., and K. Vissy, Concentration, size distribution and chemical nature of atmospheric aerosol particles in remote oceanic areas, *J. Aerosol Sci., 5*, 101–109, 1974.

Molina, L. T., S. C. Schinke, and M. J. Molina, Ultraviolet absorption spectrum of hydrogen peroxide vapor, *Geophys. Res. Lett., 4*, 580–582, 1977.

Molina, M. J., and G. Arguello, Ultraviolet absorption spectrum of methyl hydroperoxide vapor, *Geophys. Res. Lett., 6*, 953–955, 1979.

Moore, H. E., S. G. Poet, and E. A. Martell, ^{222}Rn, ^{210}Bi, and ^{210}Po profiles and aerosol residence times versus altitude, *J. Geophys. Res., 78*, 7065–7075, 1973.

Moortgat, G. K., and E. Kudszus, Mathematical expression for the $O(^1D)$ quantum yields from the O_3 photolysis as a function of temperature (230–320 K) and wavelength (295–320 nm), *Geophys. Res. Lett., 5*, 191–194, 1978.

Murphy, P. G., Net primary productivity in tropical terrestrial ecosystems, in *Primary Productivity of the Biosphere*, edited by H. Lieth and R. H. Whittaker, Springer-Verlag, New York, 1975.

NASA, Chlorofluoromethanes and the stratosphere, edited by R. D. Hudson, *Ref. Publ. 1010*, 1977.

NASA, The Stratosphere: Present and Future, *Ref. Publ. 1049*, 1979.

NASA, Chemical kinetic and photochemical data for use in stratospheric modelling, Evaluation Number 4: NASA Panel for Data Evaluation, *Publ. 81-3*, Jet. Propul. Lab., Pasadena, Calif., 1981.

Neely, W. B., and J. H. Plonka, Estimation of the time-averaged hydroxyl radical concentration in the troposphere, *Environ. Sci. Tech., 12*, 317–321, 1978.

Neitzert, V., and W. Seiler, Measurements of formaldehyde in clean air, *Geophys. Res. Lett., 8*, 79–82, 1981.

Newell, R., G. Boer, and J. Kidsen, An estimate of the interhemispheric transfer of carbon-monozide from tropical general circulation data, *Tellus, 26*, 103–107, 1974.

Niki, H., P. D. Maker, C. M. Savage, and L. P. Breitenbach, FTIR spectroscopic observation of peroxyalkyl nitrates formed via ROO + $NO_2 \rightarrow ROONO_2$, *Chem. Phys. Lett., 55*, 289–292, 1978*a*.

Niki, H., P. D. Makar, C. M. Savage, and L. P. Breitenbach, Mechanism for hydroxyl radical initiated oxidation of olefin-nitric oxide mixtures in parts per million concentrations, *J. Phys. Chem., 82*, 135–137, 1978*b*.

Noxon, J. F., Atomic nitrogen fixation by lightning, *Geophys. Res. Lett., 3*, 463–465, 1976.

Noxon, J. F., Tropospheric NO_2, *J. Geophys. Res., 83*, 3051–3057, 1978 (correction, *J. Geophys. Res., 85*, 4560–4561, 1980).

Noxon, J. F., R. B. Norton, and E. Marovich, NO_3 in the troposphere, *Geophys. Res. Lett., 7*, 125–128, 1980.

Nye, P. H., and D. J. Greenland, The soil under shifting cultivation, *Tech. Comm. 51*, Commonwealth Bureau of Soils, Commonwealth Agricultural Bureau, Farnham Royal, England, 1960.

Oltmans, S. J., Surface ozone measurements in clean air, *J. Geophys. Res., 86*, 1174–1180, 1981.

Openshaw, K., Wood fuels the developing world, *New Sci., 61*, 271–272, 1974.

Oort, A. H., and E. M. Rasmusson, Atmospheric circulation statistics, *NOAA Prof. Pap., 5*, 1971.

Organization for Economic Cooperation and Development, Energy statistics 1973–1975, Paris, 1976.

Ortgies, G., K.-H. Gericke, and F. J. Comes, Is UV laser induced fluorescence a method to monitor tropospheric OH?, *Geophys. Res. Lett., 7*, 905–908, 1980.

Pack, D. H., J. E. Lovelock, G. Cotton, and C. Curthoys, Halocarbon behavior from a long time series, *Atmos. Environ., 11*, 329–344, 1977.

Parkes, D. A., The oxidation of methyl radicals at room temperature, *Int. J. Chem. Kin., 9*, 451–469, 1977.

Parungo, F., E. Ackerman, W. Caldwell, and H. K. Weickmann, Individual particle analysis of Antarctic aerosols, *Tellus, 31*, 521–529, 1979.

Penndorf, R., Tables of the refractive index for standard air and the Rayleigh scattering coefficient for the spectral region between 0.2 and 20.0 μm and their application to atmospheric optics, *J. Opt. Soc. Am., 47*, 176–182, 1957.

Perner, D., D. H. Ehhalt, H. W. Patz, U. Platt, E. P. Roth, and A. Volz, OH radicals in the lower troposphere, *Geophys. Res. Lett., 3*, 466–468, 1976.

Persson, R., World forest resources, *Res. Notes 17*, Dep. of Forestry Surv., Royal Coll. of Forestry, Stockholm, 1974.

Philen, D., W. Heaps, and D. D. Davis, Boundary layer and free tropospheric OH measurements at tropical and subtropical latitudes in the northern and southern hemispheres, *EOS Trans. AGU, 59*, 1079, 1978.

Phillips, J., *Agriculture and Ecology in Africa*, Faber and Faber, London, 1959.

Pierotti, D., L. E. Rasmussen, and R. A. Rasmussen, The Sahara as a possible sink for trace gases, *Geophys. Res. Lett., 5*, 1001–1004, 1978.

Pittock, A. B., Climatology of the vertical distribution of ozone over Aspendale (38°S, 145°E), *Q. J. R. Meteorol. Soc., 103*, 575–584, 1977.

Platt, U., D. Perner, and H. W. Patz, Simultaneous measurement of

atmospheric CH_2O, O_3, and NO_2 by differential optical absorption, *J. Geophys. Res., 84,* 6329–6335, 1979.

Platt, U., and D. Perner, Direct measurements of atmospheric CH_2O, HNO_2, O_3, NO_2, and SO_2 by differential optical absorption in the near UV, *J. Geophys. Res., 85,* 7453–7458, 1980.

Platt, U., D. Perner, A. M. Winer, G. W. Harris, and J. N. Pitts, Detection of NO_3 in the polluted troposphere by differential optical absorption, *Geophys. Res. Lett., 7,* 89–92, 1980.

Prather, M. J., Solution of the inhomogeneous Rayleigh scattering atmosphere, *Astrophys. J., 192,* 787–792, 1974.

Pratt, R., and P. Falconer, Circumpolar measurements of ozone particles and carbon monoxide from a commercial airliner, *J. Geophys. Res., 84,* 7876–7882, 1979.

Prior, E. J., and B. J. Oza, First comparison of simultaneous IRIS, BUV, and ground-based measurements of total ozone, *Geophys. Res. Lett., 5,* 547–550, 1978.

Quinn, W. H., and W. V. Burt, Weather and solar radiation in the equatorial trough, *J. Appl. Meteorol., 6,* 988–993, 1967.

Raeschke, G., T. H. Vonder Haar, W. R. Bandeen, and M. Pasternak, The annual radiation balance of the earth-atmosphere system during 1969–1970 from Nimbus-3 measurements, *J. Atmos. Sci., 30,* 341–364, 1973.

Rasmussen, R. A., Isoprene: Identified as a forest-type emission to the atmosphere, *Env. Sci. Tech., 4,* 667–671, 1970.

Rasmussen, R. A., What do hydrocarbons from trees contribute to air pollution, *J. Air Pollut. Control Assoc., 22,* 537–543, 1972.

Rasmussen, R. A., Interlaboratory comparison of fluorocarbon measurements, *Atmos. Environ., 12,* 2505–2508, 1978.

Rasmussen, R. A., and M. A. K. Khalil, Atmospheric halocarbons: Measurements and analyses of selected trace gases, in *Proceedings of NATO Advanced Study Institute on Atmospheric Ozone: Its Variation and Human Influences,* edited by M. Nicolet and A. C. Aiken, *FAA-EE-80-20,* U.S. Dep. of Transp., Washington, D. C., 1980.

Rasmussen, R. A., D. Pierotti, J. Krasnec, and B. Halter, Trip report on the cruise of the *Alpha Helix* research vessel from San Diego, California to San Martin, Peru, March 5–20, 1976, Wash. State Univ., Pullman, Wash., 1976.

Rasmussen, R. A., M. A. K. Khalil, and R. W. Dalluge, Atmospheric trace gases in Antarctica, *Science, 211,* 285–287, 1981.

Reichle, H. G., and E. P. Condon, Vertical profiles of CO and CH_4 in the lower and middle troposphere over the eastern United States, January 1978, *Geophys. Res. Lett., 6,* 949–952, 1979.

Revelle, R., and W. Munk, The carbon dioxide cycle and the biosphere, in *Energy and Climate,* National Academy of Sciences, Washington, D. C., 1977.

Ripperton, L. A., H. E. Jeffries, and O. White, Formation of aerosols by reaction of ozone with selected hydrocarbons, *Advan. Chem. Ser., 113,* 219–231, 1972.

Robinson, E., Hydrocarbons in the atmosphere, *Pure Appl. Geophys., 116,* 372–384, 1978.

Robinson, E., and R. C. Robbins, Sources, abundance and fate of gaseous atmospheric pollutants, *Res. Proj. PR-6755,* Suppl. rep., Stanford Res. Inst., Menlo Park, Calif., 1969.

Robinson, E., R. Rasmussen, J. Krasnec, D. Pierotti, and M. Jakubovic, Detailed halocarbon measurements across the Alaskan tropopause, *Geophys. Res. Lett., 3,* 323, 1976.

Routhier, F., and D. D. Davis, Free tropospheric/boundary layer airborne measurements of H_2O over the latitude range of 58°S to 70°N: Comparison with simultaneous ozone and carbon monoxide measurements, *J. Geophys. Res., 85,* 7293–7306, 1980.

Routhier, F., R. Dennett, D. D. Davis, A. Wartburg, P. Haagenson, and A. C. Delany, Free tropospheric and boundary-layer airborne measurements of ozone over the latitude range of 58°S to 70°N, *J. Geophys. Res., 85,* 7307–7321, 1980.

Rowland, F. S., S. C. Tyler, and D. C. Montague, Global distributions of CH_3CCl_3, CCl_3F, and CCl_2F_2 in July 1979, Paper presented at the IAMAP Quadrennial Ozone Symposium, Boulder, Colo., Aug. 4–9, 1980.

Roy, C. R., I. E. Galbally, and B. A. Ridley, Measurements of nitric oxide in the stratosphere of the southern hemisphere, *Q. J. R. Meteorol. Soc., 106,* 887–894, 1980.

Rudolph, J., D. H. Ehhalt, and G. Gravenhorst, Recent measurements of light hydrocarbons in remote areas, in *Proceedings of First European Symposium on Physico-Chemical Behavior of Atmospheric Pollutants,* pp. 41–51, Commission of European Communities, 1979.

Ruthenberg, H., *Farming Systems in the Tropics,* Clarendon, Oxford, 1976.

Salveson, K. G., K. J. Wolfe, E. Chu, and M. A. Herther, Emission characterization of stationary NO_x sources, vol. 1 results, *EPA-600/7/78-120a,* U.S. Environ. Prot. Agency, Washington, D. C., 1978.

Sanadze, G. A., On the condition of evolution of the diene C_5H_8 (isoprene) from leaves, *Fiziol. Rast., 11,* 42–45, 1963.

Sander, S. P., and R. T. Watson, Kinetic studies of the reactions of CH_3O_2 with NO, NO_2, and CH_3O_2 at 298 K, *J. Phys. Chem., 84,* 1664–1674, 1980.

Scatchard, G., G. M. Kavanagh, and L. B. Ticknor, Vapor-liquid equilibrium, 8, Hydrogen peroxide-water mixtures, *J. Am. Chem. Soc., 74,* 3715–3720, 1952.

Schiff, H. I., A. Pepper, and B. A. Ridley, Tropospheric NO measurements up to 7 km, *J. Geophys. Res., 84,* 7895–7897, 1979.

Schmidt, U., The latitudinal and vertical distribution of molecular hydrogen in the troposphere, *J. Geophys. Res., 83,* 941–946, 1978.

Schuetzle, D., and R. A. Rasmussen, The molecular composition of secondary aerosol particles formed from terpenes, *J. Air Pollut. Control Assoc., 28,* 236–240, 1978.

Seiler, W., The cycle of atmospheric CO, *Tellus, 26,* 118–135, 1974.

Seiler, W., The cycle of carbon monoxide in the atmosphere, in *Proceedings of the ICESA Conference,* vol. 2, I.E.E.E., New York, 1976.

Seiler, W., and H. Giehl, Influence of plants on the atmospheric carbon monoxide, *Geophys. Res. Lett., 4,* 329–332, 1977.

Seiler, W., H. Giehl, and H. Ellis, A method for monitoring of background CO and first results of continuous CO registrations on Mauna Loa Observatory, *Spec. Environ. Rep. 10,* p.p. 31–39, World Meteorol. Organ., Geneva, 1976.

Seiler, W., F. Muller, and H. Oeser, Vertical distribution of chlorofluoromethanes in the upper troposphere and lower stratosphere, *Pure Appl. Geophys., 116,* 554–566, 1978.

Seiler, W., and U. Schmidt, New aspects of CO and H_2 cycles in the atmosphere, in *Proceedings of the International Conference on the Structure, Composition, and General Circulation of the Upper and Lower Atmospheres and Possible Anthropogenic perturbations,* pp. 192–222, IAMAP, Melbourne, 1974.

Selzer, P. M., and C. C. Wang, Quenching rates and fluorescence efficiency in the A $^2\Sigma^+$ state of OH, *J. Chem. Phys., 71,* 3786–3791, 1979.

Simanaitis, D. J., Emission test cycles around the world, *Automot. Eng., 85,* 34–43, 1977.

Singh, H. B., Atmospheric halocarbons: Evidence in favor of reduced average hydroxyl radical concentration in the troposphere, *Geophys. Res. Lett., 4,* 101–104, 1977*a*.

Singh, H. B., Preliminary estimates of average tropospheric OH concentrations in the northern and southern hemispheres, *Geophys. Res. Lett., 4,* 453–456, 1977*b*.

Singh, H. B., L. J. Salas, and L. A. Cavanagh, Distribution, sources and sinks of atmospheric halogenated compounds, *J. Air Pollut. Contr. Assoc., 27,* 332–336, 1977*a*.

Singh, H. B., L. Salas, H. Shiegeshi, and A. Crawford, Urban-nonurban relationships of halocarbons, SF_6, N_2O and other atmospheric trace constituents, *Atmos. Environ., 11,* 819–828, 1977*b*.

Singh, H. B., L. J. Salas, H. Shigeishi, and E. Scribner, Atmospheric halocarbons hydrocarbons, and sulphur hexafluoride: global distributions, sources, and sinks, *Science, 203,* 899–903, 1979.

Slinn, W. G. N., L. Hasse, B. B. Hicks, A. W. Hogan, D. Lal, P. S. Liss, K. O. Munnich, G. A. Sehmel, and O. Vittori, Some aspects of the transfer of atmospheric trace constituents past the air-sea interface, *Atmos. Environ., 12,* 2055–2087, 1978.

Soderlund, R., and B. H. Svensson, The global nitrogen cycle, in Nitrogen, Phosphorus and Sulphur—Global Cycles, SCOPE *Rep. 7, Ecol. Bull., 22,* 23–74, 1976.

Somner, A., Attempt at an assessment of the worlds tropical forests, *Unasylva, 28,* 5–25, 1976.

Sparks, R. K., L. R. Carlson, K. Shobatake, M. L. Kowalczyk, and Y. T. Lee, Ozone photolysis: A determination of the electronic and vibrational state distributions of primary products, *J. Chem. Phys., 72,* 1401–1402, 1980.

Spencer, J. E., Shifting cultivation in southeastern Asia, *Univ. of Calif. Publ. in Geogr.,* vol. 19, University of California Press, Berkeley, 1966.

Spicer, C. W., The fate of nitrogen oxides in the atmosphere, *Advan. Environ. Sci. Tech., 7,* 163–261, 1977.

Sridharan, U. C., B. Reiman, and F. Kaufman, Kinetics of the reac-

tion OH + $H_2O_2 \rightarrow HO_2 + H_2O$, *J. Chem. Phys., 73,* 1286–1293, 1980.
Stair, R., Ultraviolet radiant energy from the sun observed at 11,190 feet, *J. Res. Natl. Bur. Stand., 49,* 227–234, 1952.
Stair, R., and R. G. Johnston, Some studies of atmospheric transmittance on Mauna Loa, *J. Res. Natl. Bur. Stand., 61,* 419–428, 1958.
Stair, R., R. G. Johnston, and T. C. Bagg, Spectral distribution of energy from the sun, *J. Res. Natl. Bur. Stand., 53,* 113–119, 1954.
Stamp, L. D., and W. T. W. Morgan, *Africa: A Study in Tropical Development,* John Wiley, New York, 1972.
Stevens, C. M., L. Krout, D. Walling, A. Vanters, A. Engelkemeir, and L. Gross, The isotopic composition of atmospheric carbon monoxide, *Earth and Planet. Sci. Lett., 16,* 147–165, 1972.
Streit, G. E., C. J. Howard, A. L. Schmeltekopf, J. A. Davidson, and H. I. Schiff, Temperature dependence of $O(^1D)$ rate constants for reactions with O_2, N_2, CO_2, O_3 and H_2O, *J. Chem. Phys., 65,* 4761–4764, 1976.
Stuhl, F., Absolute rate constant for the reaction OH + $NH_3 \rightarrow NH_2$ + H_2O, *J. Phys. Chem., 59,* 535–537, 1978.
Sze, N. D., Anthropogenic CO emissions: Implications for atmospheric CO-OH-CH_4 cycle, *Science, 195,* 673–675, 1977.
Thompson, A. M., Wet and dry removal of formaldehyde at a coastal site, *Tellus, 32,* 376–383, 1980.
Thrush, B. A., and J. P. T. Wilkinson, Pressure dependence of the rate of reaction between HO_2 radicals, *Chem. Phys. Lett., 66,* 441–443, 1979.
Toba, Y., On the giant sea-salt particles in the atmosphere, 1, General features of the distribution, *Tellus, 17,* 131–145, 1965.
Tsunogai, S., Ammonia in the oceanic atmosphere and the cycle of nitrogen compounds through the atmosphere and the hydrosphere, *Geochem. J., 5,* 57–67, 1971.
Tuck, A. F., Production of nitrogen oxides by lightning discharges, *Q. J. R. Meteorol. Soc., 102,* 749–755, 1976.
Tyson, B. J., J. F. Vedder, J. C. Arveson, and R. B. Brewer, Stratospheric measurements of CF_2Cl_2 and N_2O, *Geophys. Res. Lett., 5,* 369–372, 1978.
United Nations, *Annual Bulletin of Transport Statistics for Europe,* vol. 24, New York, 1973.
United Nations, *Annual Bulletin of General Energy Statistics for Europe, 1972,* New York, 1974.
United Nations, *World Energy Supplies, 1950–1974, Stat. Pap., 19, Ser. J,* New York, 1976*a*.
United Nations, *Annual Bulletin of Transport Statistics for Europe,* Vol. 27, New York, 1976*b*.
United Nations, *World Energy Supplies, 1973–1976, Stat. Pap. 21, Ser. J,* New York, 1978*a*.
United Nations, *Yearbook of Industrial Statistics, 1976,* New York, 1978*b*.
U.S. Department of Transportation, Highway Statistics, 1977, *Rep. FHWA-HP-HS-77,* Washington, D. C., 1977.
U.S. Environmental Protection Agency, 1973 National emissions report: National emissions data system of the aerometric and emissions reporting system, *EPA-450/2-76-007,* Washington, D. C., 1976.
U. S. Environmental Protection Agency, Compilation of air pollution emission factors, *Publ. AP-42,* Wasington, D. C., 1977.
U.S. Environmental Protection Agency, Mobile source emission factors, *EPA-400/9-78-006,* Washington, D. C., 1978*a*.
U.S. Environmental Protection Agency, 1974 national emissions report: National emissions data system of the aeormetric and emissions reporting system, *EPA 450/2-78-026,* Washington, D. C., 1978*b*.
U.S. Environmental Protection Agency, National air quality, monitoring and emissions trends report, *EPA-450/2-78-052,* Washington, D. C., 1978*c*.
U.S. Standard Atmosphere Supplement, U.S. Government Printing Office, Washington, D. C., 1966.
Uselman, W. M., S. Z. Levine, W. H. Chan, J. G. Calvert, and J. H. Shaw, The kinetics of the decay of gaseous peroxynitric acid, *Chem. Phys. Lett., 58,* 437–440, 1978.
Vernazza, J. E., E. H. Avrett, and R. Loeser, Structure of the solar chromosphere, II, The underlying photosphere and temperature-minimum region, *Astrophys. J. Suppl., 30,* 1, 1976.
Volz, A., D. H. Ehhalt, and R. G. Derwent, Seasonal and latitudinal variation of ^{14}CO and the tropospheric concentration of OH radicals, *J. Geophys. Res.,* in press, 1981.
Wang, C. C., L. Davis, C. H. Wu, S. Japar, H. Niki, and B. Weinstock, Hydroxyl radical concentrations measured in ambient air, *Science, 189,* 797–800, 1975.
Wang, C. C., L. I. Davis, Jr., P. M. Zelzer, and R. Munoz, Improved airborne measurements of OH in the atmosphere using the technique of laser induced fluorescence, *J. Geophys. Res., 86,* 1181–1186, 1981.
Warneck, P., On the role of OH and HO_2 radicals in the troposphere, *Tellus, 26,* 39–46, 1974.
Watters, R. F., Shifting cultivation in Latin America, *Forestry Devlop. Pap. 17,* Food and Agricultural Organ., Rome, 1971.
Webster, C. C., and P. N. Wilson, *Agriculture in the Tropics,* Longmans, New York, 1967.
Weinstock, B., Carbon monoxide: Residence time in the atmosphere, *Science, 166,* 224–225, 1969.
Weinstock, B., H. Niki, and T. Y. Chang, Chemical factors affecting the hydroxyl radical concentration in the troposphere, *Advan. Environ. Sci. Tech., 10,* 221–258, 1980.
Welzel, K., and P. Davids, *Die Kohlenmonoxide Emissionen in der Bundes Republik Deutschland in den Jahren 1965, 1970, 1973, and 1974,* A. Bernecker, Melsungen, 1975.
Went, F. W., Organic matter in the atmosphere, and its possible relation to petroleum formation, *Proc. Nat. Acad. Sci., 46,* 212–221, 1960.
Whitby, K. T., The physical characteristics of sulfur aerosols, *Atmos. Environ., 12,* 135–159, 1978.
Whittaker, R. H., and G. E. Likens, The biospere and man, in *Primary Productivity of the Biosphere,* edited by H. Lieth and R. H. Whittaker, pp. 305–331, Springer-Verlag, New York, 1975.
Whittlesey, D., Fixation of shifting cultivation, *Econ. Geog., 13,* 139–154, 1937.
Wilbert, J. (Ed.), The evolution of horticultural systems in native South America, Causes and consequences, A symposium, *Antropoligica, Suppl. Publ. 2,* 1961.
Wilcox, R. W., Comments on 'Tropospheric ozone, 1, evidence for higher background values' by R. Chatfield and H. Harrison, *J. Geophys. Res., 83,* 6263–6264, 1978.
Wilkniss, P. E., R. A. Lamontagne, R. E. Larson, J. W. Swinnerton, C. R. Dickson, and T. Thompson, Atmospheric trace gases in the southern hemisphere, *Nature, 245,* 45–47, 1973.
Wilkniss, P. E., J. W. Swinnerton, D. J. Bressan, R. A. Lamontagne, and R. E. Larson, CO, CCl_4, Freon-11, CH_4 and Rn-222 concentrations at low altitude over the Arctic Ocean in January 1974, *J. Atmos. Sci., 32,* 158–162, 1975*a*.
Wilkniss, P. E., J. W. Swinnerton, R. A. Lamontagne, and D. J. Bressan, Trichlorofluoromethane in the troposphere, distribution and increase, 1971 to 1974, *Science, 187,* 832–834, 1975*b*.
Wilkniss, P. E., R. A. Lamontagne, R. E. Larsen, and J. W. Swinnerton, Atmospheric trace gases and land and sea breezes at the Sepik River Coast of Papua New Guinea, *J. Geophys. Res., 83,* 3672–3674, 1978.
Wilks, S. S., Carbon monoxide in green plants, *Science, 129,* 964–966, 1959.
Winer, A. M., A. C. Lloyd, K. R. Darnall, R. Atkinson, and J. N. Pitts, Rate constants for the reaction of OH radicals with n-propyl acetate, sec-butyl acetate, tetrahydroturan and peroxyacetyl nitrate, *Chem. Phys. Lett., 51,* 221–226, 1977.
Wofsy, S. C., Interactions of CH_4 and CO in the earth's atmosphere, *Ann. Rev. Earth Planet. Sci., 4,* 441–469, 1976.
Wofsy, S. C., Temporal and latitudinal variations of stratospheric trace gases: A critical comparison between theory and experiment, *J. Geophys. Res., 83,* 364–378, 1978.
Wofsy, S. C., J. C. McConnell, and M. B. McElroy, Atmospheric CH_4, CO, and CO_2, *J. Geophys. Res., 77,* 4477–4493, 1972.
World Atlas of Agriculture, 1969, Instituto Geographico de Agostini, S.P.A. Novara, Italy, 1969.
World Meterological Organization, Atmospheric turbidity and precipitation chemistry data for the world 1972, 1973, 1974, National Climate Center, Ashville, North Carolina, 1972–1974.
World Meteorological Organization, Global monitoring of the environment for selected atmospheric constituents, 1975, 1976, National Climate Center, Ashville, North Carolina, 1975–1976.
Yamate, G., State of the art report on atmospheric aspects of forest fires, *Rep. C8269-2,* ITT Res. Inst., Chicago, Ill., 1975.
Zafiriou, O. C., and M. B. True, Nitrite photolysis as a source of free

radicals in productive surface waters, *Geophys. Res. Lett., 6,* 81–84, 1979.

Zafiriou, O. C., J. Alford, M. Herrerra, G. Peltzer, A. M. Thompson, R. B. Gagosian, and S. C. Liu, Formaldehyde in remote marine air and rain: Flux measurements and estimates, *Geophys. Res. Lett., 7,* 341–344, 1980.

Zafonte, L., N. E. Hester, E. R. Stephens, and O. C. Taylor, Background and vertical atmospheric measurements of fluorocarbon 11 and fluorocarbon 12 over Southern California, *Atmos. Environ., 9,* 1007–1009, 1975.

Zimmerman, P. R., R. B. Chatfield, J. Fishman, P. J. Crutzen, and P. L. Hanst, Estimates on the production of CO and H_2 from the oxidation of hydrocarbon emissions from vegetation, *Geophys. Res. Lett., 5,* 679–682, 1978.

(Received November 14, 1980;
revised April 7, 1981;
accepted April 10, 1981.)